INTERFEROMETRIC STUDIES

ON

CRYSTALS OF QUARTZ

Thesis submitted to the
University of London
for the Degree of
Doctor of Philosophy

by

William Bardsley

October 1951

CONTENTS

PART I

INTRODUCTION

CHAPTER I

PIEZO-ELECTRICITY

The production of electrical effects by mechanical forces has been known since the time of the ancient Greeks, who observed the attractive power of amber when rubbed. In Europe, in the eighteenth century, it was known that tourmaline when heated displayed a similar property showing opposite polarities at the two ends of the crystal. In 1824 Brewster, who investigated this effect in several crystals, named it pyro-electricity.

In 1880, in France, the brothers P. and J. Curie (1880) found a new method of producing polar electricity in crystals. They showed that some crystals when compressed in certain directions showed positive and negative charges on certain parts of their surfaces, the charges being proportional to the pressure and disappearing when the pressure was withdrawn. They recognised that the phenomenon was closely related to the crystal symmetry, investigating many crystals and making quantitative measurements on quartz and tourmaline. Piezo-electricity was the name proposed for the phenomenon by Hankel to distinguish it from pyro-electricity.

It may be defined as the electric polarisation produced by mechanical strain in crystals belonging to certain classes, the polarization being proportional to the strain and changing sign with it (Cady 1946). It covers

a wide field of crystal physics and has been dealt with in a comprehensive bibliography by Cady (1946). In addition to the direct piezo-electric effect, as defined above, there exists also a converse piezo-electric effect predicted by Lippman who applied thermodynamic principles to reversible processes which involved electrical quantities. This converse effect was verified later by the Curies.

Voigt rigorously carried out the classical piezo-electric formulation in 1894 when he combined the elements of symmetry of elastic tensors and electric vectors with the geometrical symmetry elements of the crystal. This is published in his Lehrbuch der Kristallphysik (1910).

An atomic theory of piezo-electricity was discussed later by M.Born in his general theory of crystal lattice dynamics.

In the period 1914-1918 Langevin and others used quartz plates, excited electrically, to emit ultrasonic vibrations in liquids and gases. In 1918, Cady examined the mechanical resonances and the electrical behavior at resonance of Rochelle salt plates used for the same purpose. As a result of this work he evolved the concept of the piezo-electric resonator. His work, and subsequent developments, showed that piezo-electric crystals could be used as oscillators, stabilizers and filters, their operation involving

a combination of the direct and converse piezo-electric effects. Their technical uses are enormous and on the purely scientific side they have been used to gain information on the nature of the elastic vibrations in crystal substances and on the dynamic values of the elastic and piezo-electric constants.

Amongst the large number of crystals in the classes showing piezo-electric properties, quartz is outstanding in its technical importance owing to its physical properties. A survey of these properties forms the subject matter of the next chapter.

CHAPTER 2

THE PROPERTIES OF QUARTZ

The general properties of quartz have been described in detail by Sosman (1927), Cady (1946), Heising (1947) and Booth and Vigoureux (1950). A brief description of the more important physical properties follows.

Quartz (silicon dioxide, SiO_2) crystallises in hard, brittle, glass-like six sided prisms often with pyramidal terminations. Its melting point is 1750°C, density 2.65 and hardness on the Mohr scale 7. It transforms from alpha to beta quartz at 573°C. Alpha quartz is insoluble in all acids except hydrofluoric acid but dissolves in hot alkalies.

A perfect crystal of quartz may be considered to consist of a central hexagonal prismatic block terminated by hexagonal pyramids Fig. 1.1. The pyramidal surfaces are not all similar but alternate ones are, thus the quartz has a threefold symmetry around the optic axis, the Z axis, which joins the apexes of the pyramids. The atomic structure is of a spiral nature (Bragg and Gibbs 1925) which may be left handed or right handed along the Z axis and determines the direction of rotation of the plane of polarization of light travelling along the optic axis. The two types of crystal are shown, (a) being left hand and (b) right hand. There are three similar

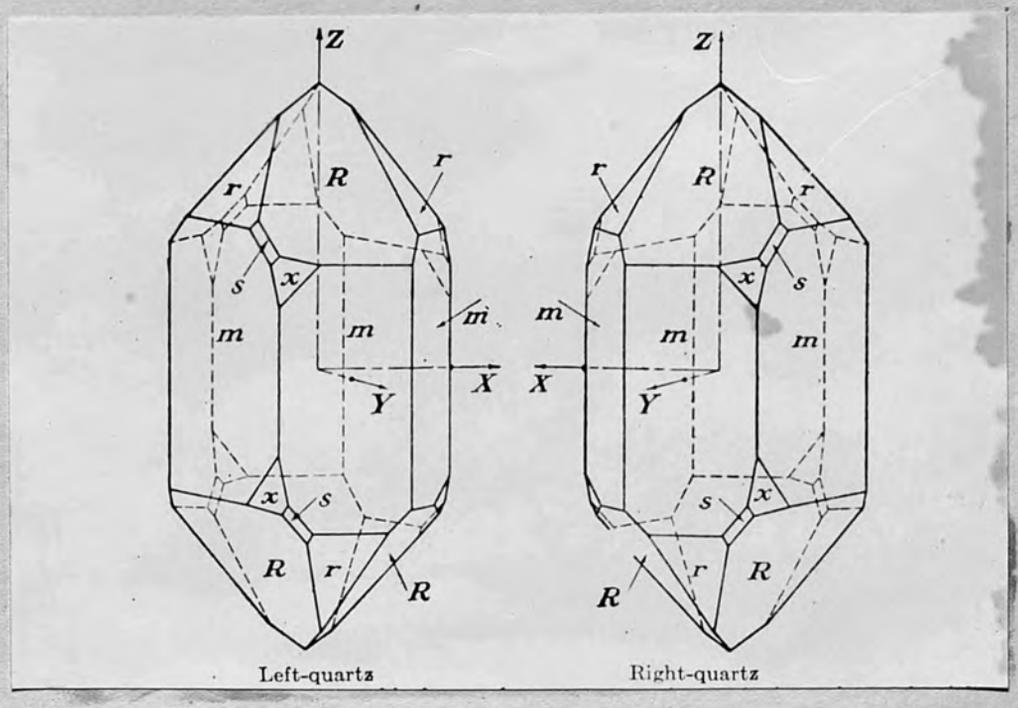
Z
r
R
r
s
x
m
m
m
X
Y
x
s
R
r
R
Left-quartz
Z
r
R
r
x
s
m
m
m
X
Y
s
x
r
R
R
Right-quartz

a b

FIG. I.1.

electric axes, the X axes, possessing two fold symmetry at right angles to the optic axis. They intersect the angles of the prism faces. The positive direction of the X axis is taken towards the end which shows positive electrification on the application of a positive stress (tension) along the axis. The third direction, which forms an orthogonal axial system with the optic and electric axes, is known as the Y axis and it is chosen to form a right handed co-ordinate system for right handed crystals and a left handed system for left handed crystals.

At 573°C the crystal changes its symmetry from trigonal to hexagonal and is no longer piezo-electric.

As mentioned in Chapter I, Voigt formulated a mathematical relation between the stresses, strains, polarisations and electric fields existing in a crystal. The relations in the case of quartz and the experimental values of the constants relating the mechanical and electrical parameters have been given by many authors. Their results have been summarised by Cady (1946).

The change in dimensions of a quartz element in an electric field is very small, a gradient of 300 volts per cm. along the X direction of a bar 1 cm. long in the Y direction, will alter the length of the bar by approx-

imately 6 x 10^{-8} cm. If the field is an alternating one and its frequency coincides with a natural mechanical resonance of the bar, then the bar vibrates at that frequency and the amplitude of the deformation increases to thousands of times the static value. The inertia forces become so great that the elements are easily shattered. In virtue of the direct piezoelectric effect, this considerable motion produces on the electrodes large alternating quantities of electricity which react on the circuit supplying the alternating potential. The frequency of vibration is practically independent of the electrical circuit, being almost entirely controlled by the elastic constants of the quartz and the dimensions of the vibrator.

Dye (1926) translated the mechanical mass, stiffness and friction of a crystal vibrator into the analogous electrical quantities of inductance, inverse of capacitance and resistance respectively and proved that the experimental results agreed with the calculations resulting from this transformation. This idea allows the electromechanically resonant system to be discussed in terms of familiar electrical theory. In particular, a figure of merit, the Q value, or the ratio of inductive reactance to resistance may be used to describe the performance of a quartz vibrator. Q values of up to 2 x 10^{6} can be achieved whereas the Q of a normal tuned circuit may be of the order of 2 x 10^{2}.

Quartz possesses a crystal form which is very stable under normal conditions and combines a very low damping with sufficient piezo-electric power to react on and control the frequency of valve oscillators more accurately than is possible with electrical tuning alone. This precision reaches its culmination in the use of a quartz plate or ring in a quartz clock which can be used as a very constant timepiece.

Quartz is both doubly refracting and optically active. As quartz is a uniaxial crystal it is doubly refracting or birefringent along all directions other than the optic axis, whilst it is optically active in the direction of the optic axis.

The optical constants are changed under mechanical strain (piezo-optic effect) and under electrical stress (linear electro-optic effect). The theoretical and experimental investigation of these effects was made by Pockels (1889, 1890, 1894). More recently Ny Tsi Ze (1927, 1928) and Gunther (1932) have investigated the electro-optic effect for quartz. The rotary polarisation is unaffected by mechanical stress but as quartz can become biaxial under stress then there is double refraction along the optic axis which changes the apparent rotary power.

The properties of quartz briefly enumerated in this chapter form a background for the experimental work discussed in this thesis.

CHAPTER 3

QUARTZ VIBRATORS

The study of raw quartz, its imperfections and its economical use are described by Heising (1947) and Booth and Vigoureux (1950).

The tolerances which are allowed in the manufacture of vibrators from the raw quartz are of importance, for it is on such finished vibrators that experimental investigations are carried out. The precision of orientation and the mechanical processes involved in the production of vibrators help to determine their behaviour as circuit elements.

The terminology describing the form of the vibrator and the direction of the crystal axes in relation to its physical form is that used by Booth and Vigoureux (1950). The vibrator can be in the form of a bar, a rectangular plate, a circular disc or a ring of rectangular cross section. Its direction in relation to the crystal axes is determined by the particular use for which the vibrator is designed. Fig. 12. shows some of the cuts used in the experiments described in this thesis.

The exciting field is applied by suitable electrodes in a variety of ways according to the type of vibrator, the desired mode of motion and the particular exciting circuit. They may be external metal conductors or metal films coated on the surface of the vibrator. The exciting

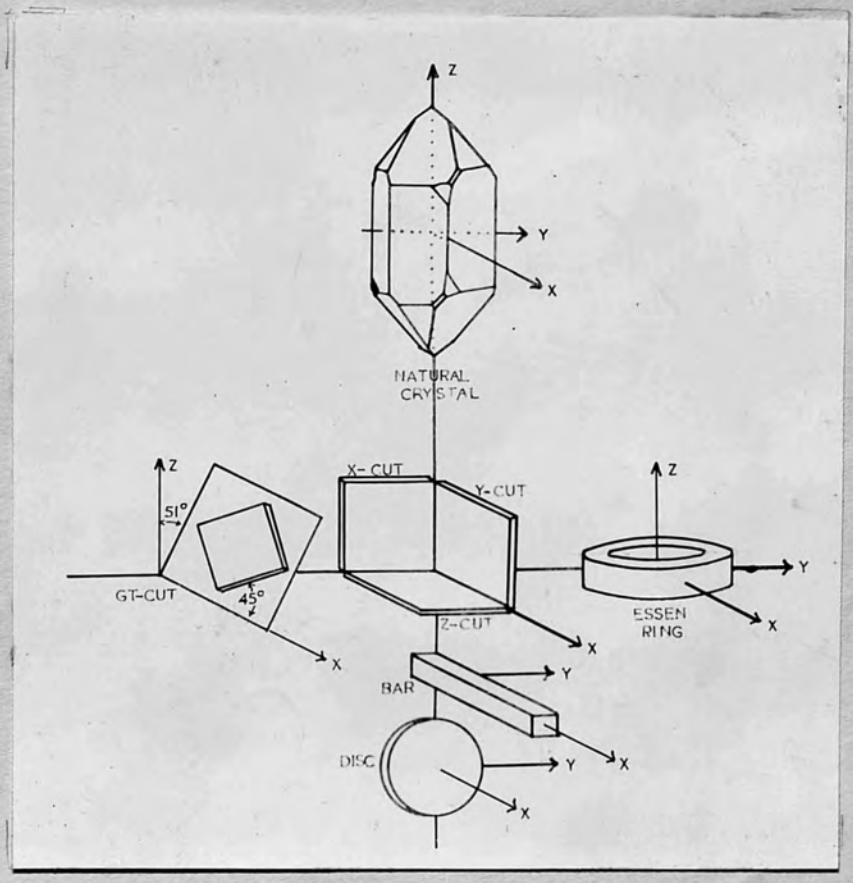
Z
Y
X
NATURAL
CRYSTAL
Z
51°
X-CUT
Y-CUT
Z
Y
GT-CUT
45°
X
Z-CUT
X
ESSEN
RING
X
Y
BAR
Y
X
DISC
Y
X

FIG.I.2.

circuit may be in the form of an oscillator similar to the Hartley or in the form of a maintaining circuit such as the Pierce. In the first case the vibrator is said to run as a resonator; in the second as an oscillator.

All quartz vibrators are affected by ageing (Booth and Vigoureux (1950)). Activity ageing is a fall in piezo-electric activity after manufacture and can be eliminated effectively by care in the processing of the vibrator. Frequency ageing is a change of the resonant frequency with lapse of time, the rate of frequency drift being quite rapid at first then gradually falling off. It can be reduced by various technical expedients but the residual ageing is thought to be due to the quartz itself, and is important when long period tolerances of a few parts in 10^6 are required in frequency standards.

Basically four types of motion can be considered, namely flexural, extensional or compressional, shear and torsion, these types and their combinations being considered to represent most cases observed in quartz vibrators (Cady 1946).

The motion of a vibrator is dependent almost wholly on its dimensions and the particular type of wave generated or frequency applied and very little on

the driving system employed provided that the coupling is small. In quartz the electromechanical coupling is small (Heising 1947)

Apart from the low order flexures it is difficult to obtain isolated modes of motion. For vibrations of higher frequencies, because of the elastic coupling between the various modes of motion, the resultant motion is often complex.

The general mathematical solution to the problem of the motion in terms of the displacement at the boundaries even for an isotropic body has not yet been achieved. The problem is generally formulated along classical lines after Rayleigh (1926) and Love (1934) and the results are limited to isotropic bodies. They provide, however, considerable guidance to the modes of motion existing in an aeotropic body such as quartz. A single theory that would relate all the known resonances in quartz vibrators together with the effects of coupling between the modes would be prodigious indeed.

A knowledge of the displacement at the boundaries and thus the position of any nodal regions enables the vibrator to be mounted with the minimum of external damping. The absence of a mathematical theory capable of predicting

the distribution of the nodal regions has necessitated an experimental approach to the problem.

The investigation of the modes of motion of quartz vibrators forms the subject of a wide literature.

The methods of investigation may be classified under two headings. In the first the frequencies of vibration of the different modes, predicted by existing mathematical theory, are experimentally examined and empirical rules governing the frequency are evolved. In the second, the physical form of the vibration at the different resonant frequencies is observed. This is done either by observing the position of the nodal and antinodal regions on the vibrator surface or by investigating the distribution of stress inside the body of the vibrator. It is to the second type of experiment that Chapter 4 is devoted.

CHAPTER 4

INVESTIGATION OF THE MODES OF VIBRATION

The use of light interference to measure small amplitudes of vibration dates back to Thomas and Warren (1928), Fujimoto (1927) and Paasche (1928). The application of the method to the study of the vibrations of quartz plates was made in 1927 by Dye in this country when, from his experimental work on quartz and partly as a result of a visit to America in that year, he formed the opinion that the method might give some information on the nature of the vibrations (Rayner 1933).

In a posthumous paper (prepared for publication by Vigoureux) Dye (1932) described the application of Fizeau fringes to the study of the vibrational patterns on the surface of several rectangular plates and circular discs of quartz. The fringes, which were of the localised two beam type, were formed in reflection between the flat polished upper surface of the quartz and the lower surface of an optically flat glass reference plate, using unfiltered monochromatic light from a mercury source. When the reference plate was tilted with respect to the quartz surface to form a wedge, black, equidistant straight line fringes were formed parallel to the direction of the wedge apex.

By means of a suitable oscillatory circuit and electrodes, the quartz vibrators could be resonated at many of their natural frequencies. When the quartz vibrated, the fringes became blurred wherever there was an up and down motion of the surface since this motion caused a to and fro motion of the fringes, but the fringes remained undisturbed where the surface was at rest. The pattern thus revealed the nodal and antinodal regions of the vibration.

Fig.I.3., taken from Booth and Vigoureux (1950) shows the appearance of the fringes, (a) at rest and (b) in motion for a fifth order flexural vibration. In order to overcome the blurring of the fringes, light from a helium discharge tube, driven by the oscillator at the same frequency as the vibrating quartz, was used to provide stroboscopic illumination. Fig.I.3, (c), shows the appearance of the fringes under stroboscopic illumination.

Dye investigated the nodal patterns obtained at different frequencies for X cut crystals of various dimensions, identifying types of vibration such as compressional, flexural, torsional and complex combinations of these. Simultaneous observations on the opposite parallel surfaces of a quartz disc were made for compressional vibrations along the direction of the thickness. Dye declined to measure the amplitude of

a

b

c

FIG. I.3.

vibration on the grounds of uncertainty about the light intensity distribution in the fringe system. He noted the regularity of the low frequency flexural vibrations and the complex irregularity of the higher frequency compressional vibrations.

About the same time in America Osterberg (1929) used two beam interference fringes for the same purpose, obtaining localised fringes, using the filtered green mercury line (5461 A), on the quartz surface by making it one of the two fully silvered mirrors in a Michelson interferometer. The silver coating was conveniently used as one of the exciting electrodes. On resonating the quartz vibrator the fringes behaved as in Dyes' experiment. Osterberg gave an equation relating the amplitude of vibration to the visibility of the fringe system. He observed that the nodal patterns were not geometric for the compressional modes and that the motion of opposite surfaces was not the same. The amplitude was plotted against the applied crystal voltage. Only a few points were plotted and the graph was non linear.

Later Osterberg (1932) gave the derivation of the equation quoted in his 1929 paper and extended it to include the case of a fundamental displacement and its first two harmonics, showing how the harmonics could vary the observed fringe pattern.

The following year (1933) he published details of

a triple interferometer to observe the relative motion of opposite faces of a vibrator and in a further paper (1933b) extended the idea in a multiple interferometer which made possible the examination of the relative motion of adjacent faces. He thus distinguished between flexural and compressional wave trains and observed the motion of the wave trains in certain X cut plates.

Subsequently he gave details (1934) of a refracting interferometer for the examination of longitudinal modes in vibrators of bar form by observing the change in optical path presented to a beam of light traversing the quartz in a direction normal to the direction of the wave motion. This was effected by placing the bar in one arm of a Michelson interferometer and using polarised light. For a compressional vibration along the length, nodes of motion along the length were antinodes of stress. As the major surfaces were free these pressure antinodes coincided in position with the antinodes of outward or lateral motion of the major surfaces. He demonstrated that the lateral motion was too small to be observed with the usual fringe system, but that the stress caused a change of refractive index sufficient to change the optical path by a visible amount. The change in the refractive index was complex being different for the ordinary and the extraordinary ray and depending on the

direction of the light beam and the direction of the wave motion in the X and Y cut plates investigated. He hoped at some future date to calibrate this method by correlating the changes in refractive index with the amplitude of crystal vibration so that the results could be compared with those obtained for the static case(by applying a high D.C. potential to the quartz) by Hy Tsi Ze (1928). That this was not done was due,no doubt,to the difficulty of producing lateral motions large enough to be observed by the two beam fringe system without shattering the quartz vibrator.

Straubel (1933) modified Osterberg's method by arranging the Michelson interferometer so that the field of view over the quartz vibrator surface was dark when the latter was stationary. Any regions of vibration were shown as bright areas on a dark background. Later Straubel (1934) applied the technique to the study of shear vibration in Y cut quartz plates. He obtained two values of amplitude using Osterberg's original equation and measured the crystal voltage at these amplitudes,concluding that the amplitude/voltage relation was non linear.

Schumacher (1937) referred to Osterberg (1929) but used Dye's (1932) method to investigate compressional waves in Y cut quartz plates. He showed that the wave

motion in a disc depended on the shape of the edge and observed that the complexity of wave motion of compressional waves was probably due to the reflection of wave trains at the bounderies of the crystal. Of interest is the use he made of the technique to investigate mounting problems, showing that if the quartz were clamped along a nodal line the pattern was unchanged, but that if it was clamped in an antinodalregion the pattern was badly distorted.

Kotlyarevski and Pumper (1941), in a rather long paper, gave a critical resume of the work of Dye (1932), Osterberg (1929 et seq.) and Straubel (1933, 1934). They used Dye's method to examine the vibrations of three similar resonator discs and a rectangular plate over a considerable frequency spectrum. Comparing the results for each of the three discs they found that the frequency spectrum was completely regulated by the crystal structure and the boundary conditions of the discs, but that chance inhomogenities in the crystal structure could destroy this regulation. Also that the symmetry of the vibrational pattern was a measure of the homogenity of the quartz discs. The pattern was little affected by temperature or pressure changes, the electrodes on which the crystal was resting, or non uniformity of the electrical field. They summarized the difficulties inherent in the theoretical

approach to the vibrations of anisotropic bodies as revealed by Bechmann (1934). They discussed the practical approach also, stating that the practical solution would require an immense amount of material. Attention was drawn to the fact that in all previous papers no account was taken of the chance factors distorting the vibration pattern and that no serious attempt had been made to measure the amplitude of oscillation. No measurements of amplitude were, however, presented in this paper.

During the same period as the interferometric investigations, attempts were made by other workers to use different optical techniques on the same problem. In particular polarised light was used to examine the distribution of stress in the body of the vibrator.

Tawil (1926), in France, was the first experimenter to use polarised white light to investigate the vibratory motion of X cut plates of quartz. The plate was placed between crossed nicols with an optical compensator to give extinction over the field when the vibrator was at rest. When the plate was resonated, a change of refractive index was produced at regions of stress in the quartz and hence the stress pattern in the body of the crystal was revealed as a black arabesque on a bright background.

In later papers Tawil (1928,1929) applied the technique to further cases.

Boens and Verschaffeldt (1927) used polarised light in a similar manner to Tawil,but analysed the light with a spectroscope producing a channelled spectrum. They showed that the vibrations produced a birefringence alon g the optic axis,and a change of birefringence in directions other than the optic axis.

Wachsmuth and Auer (1928) examined X cut bars with polarised light and the glow discharge as well as lycopodium powder to investigate the variation of the propagation speed of flexural waves with frequency.

Petrzilka (1931) repeated Tawil's experiments with parallel plane-polarised light and extended the observations to include the use of convergent polarised light. He discussed the effect of the electrical field and the vibrational motion on the optical properties of quartz.

Wy Tsi Ze and Tsien (1934) used polarised ligh t to examine th e vibrations of hollow quartz cylinders cut with the optic axis running parallel to their length and in a later paper (1935) and with Sung Hung (1936) used the same technique in further investigations on this type of resonator.

Kao (1935) noted that the patterns formed in

the polarised light method should, by revealing any lack of symmetry in the vibrational pattern, show flaws in the quartz element which would otherwise not be detected. He commented that this method did not easily give quantitative results.

The Schlieren method of Toepler has also been adapted to the study of quartz vibrators by Strong (1932), Petrzilka and Zachoval (1934) and Schaffs (1937) but no quantitative measurements were made.

In the above mentioned papers and in Cady (1946) references will be found to other methods of investigating the motion of quartz vibrators. In particular the glow discharge method of Giebe and Schiebe (1925) deserved mention. If a quartz vibrator is resonated in an atmosphere of mercury vapour at a pressure of a few mm. then a glow discharge appears at regions of stress due to the liberation of electrical charges at those regions. The areas of discharge indicate approximately the nodal regions but are a sensitive indication of resonance.

Lycopodium powder was first used to reveal the nodal regions by Cady (1922) and later by other workers including Petrzilka (1935). Schumacher (1937) observed that both the discharge and the powder methods could only

give approximate information on the form of the vibration. In particular Osterberg (1934) has shown that lycopodium powder is unreliable at large amplitudes or for high frequencies.

It is worth noting, in conclusion, that only with the light interference method does it seem possible to measure the amplitude and phase of the surface motion of a vibrating quartz element. The polarised light technique gives qualitative information on the stress inside the element but a quantitative approach is difficult. No calibration of the stress, as revealed by the change of refractive index, in terms of the strain, as revealed by the surface displacement, has been made in the dynamic case.

As many patterns on quartz resonators have a certain symmetry, of interest is the recent verification and extension of Chladni's (1802) famous work by Waller (1937 et seq.) who has investigated the wave patterns of isotropic materials of various geometric shapes when resonated.

PART II

THEORETICAL DISCUSSION

CHAPTER I

TWO BEAM INTERFERENCE SYSTEMS

Interference of light is produced by combining two or more separate beams that originate from the same source. An interferometer is an instrument which separates a beam of light into two or more parts which are then reunited to produce interference. The interference may be localised in space or non localised.

In 1862 Fizeau devised an interferometer to produce localised interference fringes. Fig.II.1 shows the usual optical arrangement for producing Fizeau fringes. Monochromatic light from a pin hole A is formed into a parallel beam by a well corrected lens L. This parallel beam falls on to the interferometer wedge formed by the two inclined plane surfaces DC and EC. Interference takes place between the light reflected from the bottom surface of DC and the top surface of EC and may be observed in reflection at B. Straight line fringes are formed in the wedge at values of t given by the formula

$$n\lambda = 2\mu t \cos\phi$$

λ = wavelength of light

n = order of interference

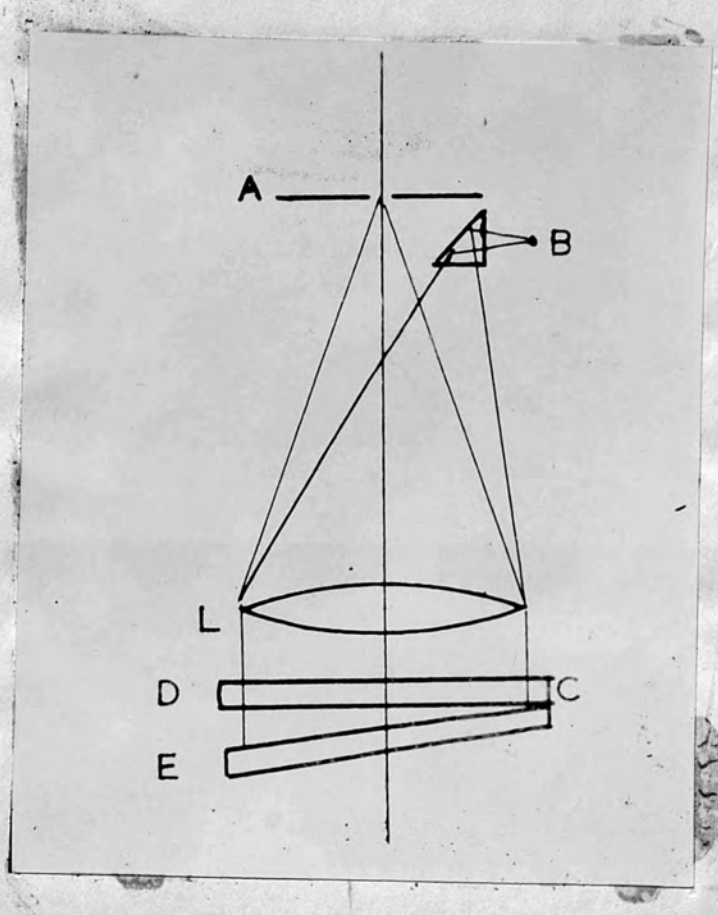

FIG. II.1.

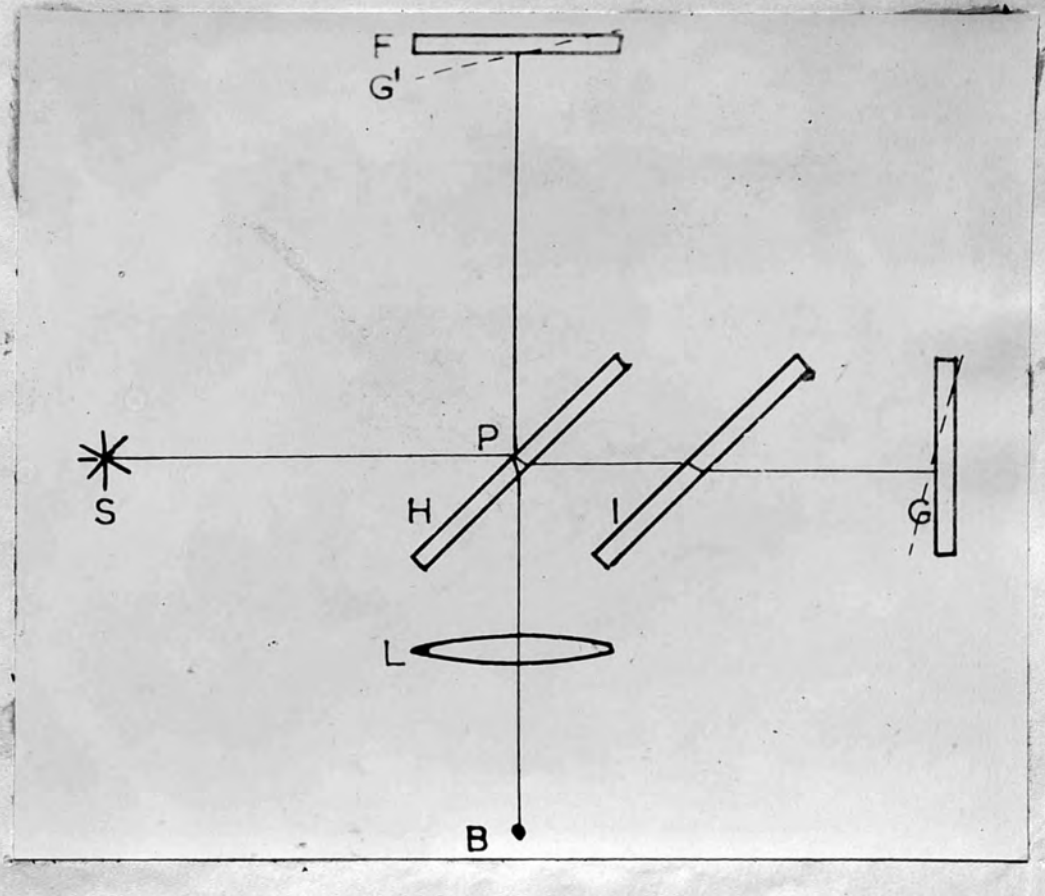

FIG. II.2.

μ = refractive index of the wedge

ϕ = angle of incidence of light

The fringes are normally observed in reflection when the amplitudes of the two interfering beams are nearly the same and the visibility of the fringes is very good. The fringe system is practically a $\cos^2$ distribution if the reflectivities of the two wedge surfaces are the same. In transmission the fringes which are complementary to the reflected fringes, are superimposed on a bright background and the visibility of the system is poor.

In 1881 Michelson invented the celebrated interferometer which bears his name. It can be used to produce localised fringes and in this case the arrangement is as shown in Fig.II.2. The two arms FP and GP are at right angles to each other. F and G are fully silvered mirrors placed normally to FP and GP respectively. H is a half silvered mirror at 45° to both FP and GP and I is a compensating glass plate. When the optical paths FP and GP are identical and G is given a slight tilt with respect to F then the image of G in H is localised at G' and the localised interference fringes similar to Fizeau fringes may be observed at B . They are visible over small optical path differences

between F and G' and increase in visibility as the aperture of L is decreased. If the silvering on H is chosen so that the two interfering beams are of equal intensity the visibility of the fringes will be unity i.e. the minima will go down to zero intensity, and as there are only two beams interfering the fringes will have a $\cos^2$ intensity distribution. This is shown graphically in Fig.II.3. The light and dark areas are equal and the half width of the fringe, defined as the width at half the maximum intensity is equal to half the distance between orders, or successive fringes.

If one of the two surfaces forming the wedge is optically flat then these localised fringes will contour the other surface, following regions in the wedge of constant 't' value. From the fringe pattern the actual contour or shape of the other surface may be determined.

Practically then with both systems the two surfaces producing the interference system must be polished and flat. The reference surface must be optically flat and the other surface should not be less flat than the order of tens of wavelengths of the incident light.

If the two surfaces are both optically flat

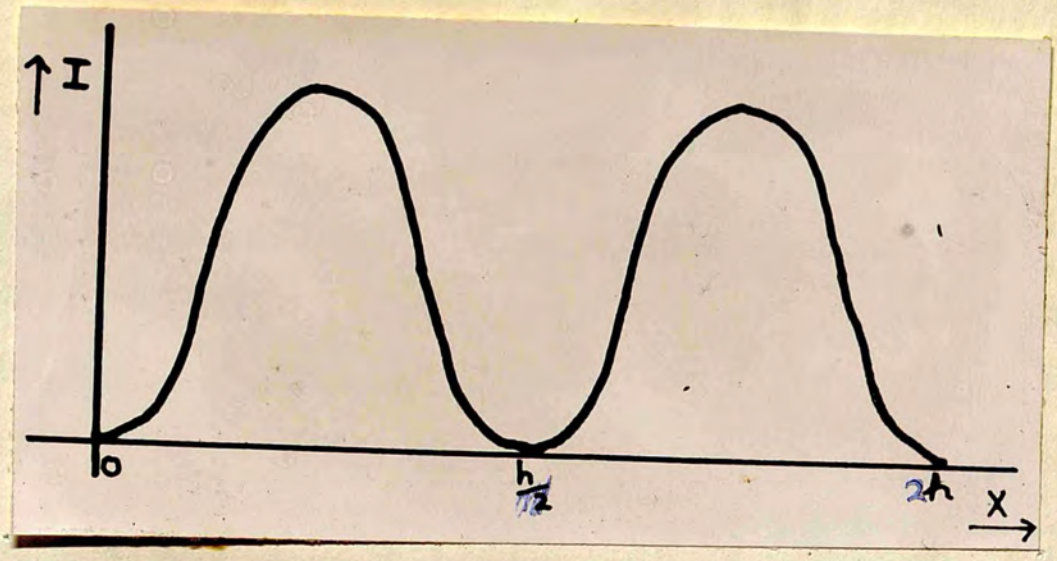

FIG. II. 3.

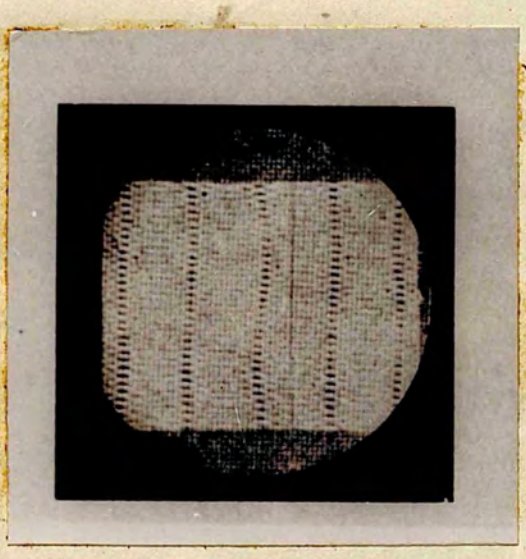

FIG. II. 4.

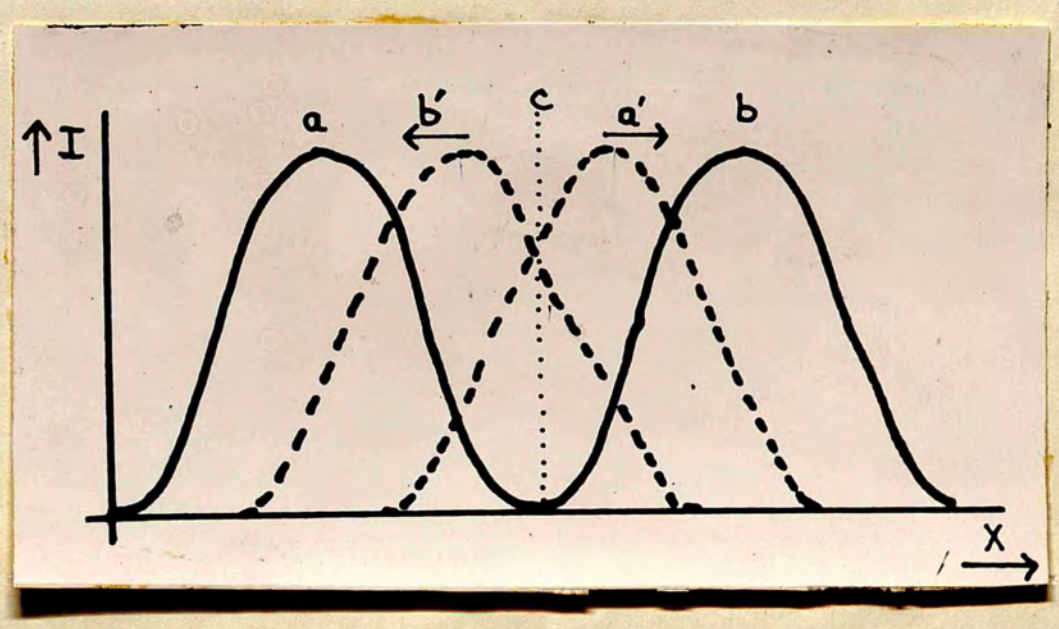

FIG. II. 5.

then the fringes will be straight lines parallel to the direction of the wedge apex. If now one of the surfaces remains fixed whilst the other is moved away from it the fringes will move laterally so that they remain at the same values of the wedge thickness. If the moving surface suffers a simple harmonic displacement about its normal position then the fringes will also suffer a simple harmonic displacement laterally with respect to their normal position, the amplitude of their displacement being proportional to the amplitude of the moving surface with respect to the fixed reference surface.

The resultant appearance of the fringe system for a simple harmonic motion of frequency greater than 25 cycles per second may be discussed both graphically and mathematically. This has been done, as was mentioned in Part I Chapter 4, by Osterberg (1932). His treatment will now be given.

For a fringe system as shown in Fig.II.3. with a $\cos^2$ intensity distribution the brightness of the fringes I_o may be written as

$$I_o = K\left(1 + \cos \frac{2\pi x}{h}\right)$$

where K = a constant

h = twice fringe width

x = perpendicular distance across the fringes

If the fringes move in a simple harmonic manner of amplitude R and frequency I/T then the instantaneous brightness at any point

$$I_i = K\left[1 + \cos\frac{2\pi}{h}\left(x - R\cos\frac{2\pi t}{T}\right)\right]$$

The resultant brightness

$$I = \frac{2K}{T}\int_0^{T/2} I_i \, dt.$$

If this expression is integrated, and the amplitude of the fringe displacement R related to the amplitude of the surface displacement r causing it, then the resultant brightness

$$I = K\left[1 + J_0\frac{4\pi r}{\lambda}\cos\frac{2\pi x}{h}\right]$$

in terms of the fringe parameters, the amplitude r and the Bessel function of zero order J_0.

The maxima of I and I_0 occur for the same value of x or are one half fringe width out of step according as $J_0\frac{4\pi r}{\lambda}$ is positive or negative. Maximum

contrast occurs for $J_0 \frac{4\pi r}{\lambda} = J_0(0) = 1$ when $I = I_0$ and the fringes are at rest.

When $J_0 \frac{4\pi r}{\lambda} = 0$, $I = K$ and no fringes are visible. As the amplitude r increases then the value of $J_0 \frac{4\pi r}{\lambda}$ will go through successive maxima and minima separated by zero values, the visibility of the fringes at each maxima or minima gradually decreasing . If the surface vibrates only in certain parts several sets of fringes will be visible simultaneously. The visual appearance is that of sets of fringes, each displaced by half an order from the neighbouring set and each set separated by blurred regions as seen in Fig.II.4. The presence of any harmonics in the vibration leads to more complex expressions for the intensity distribution .

A graphical treatment is instructive . Fig.II.5. shows the displacement of two fringes ab for a simple harmonic motion of amplitude $\lambda/2$ (total excursion) when the fringe displacement is h/2. The maxima of brightness is at c, for the velocity of motion of the fringes is a minimum there. This amplitude does not produce the best fringe contrast as earlier investigators considered, for a certain amount of overlapping of a and b to a' and b' will increase the brightness at C. This is shown in the mathematics. Thus the first minimum of $J_0 \frac{4\pi r}{\lambda}$

occurs for $r/\lambda = 0.304$ instead of 0.25. A similar treatment of the problem has been given by Smith (1945).

The amplitude of the moving surface is thus measured by estimating the fringe visibility and Osterberg quotes the accuracy to which the amplitude may be measured as being almost $\lambda/10$.

With the two beam system then it is not easy to see the precise form of the surface displacement by visual examination of the resultant fringe system and any attempt to measure the amplitude of this displacement involves difficult subjective visibility estimations. This may be overcome by using stroboscopic illumination. The smallest amplitude which can be detected is some 500 Å. In the next chapter the multiple beam interference system will be compared with the two beam interference system in these respects.

CHAPTER 2

MULTIPLE BEAM INTERFERENCE SYSTEMS

The discovery and development of multiple beam interferometry, its fundamental theory and relation to previous interferometric work, together with its subsequent application to many problems in physics have been described by Tolansky (1948) in a summary of his work in which reference to the original papers is made. Consequently a detailed dissertation on multiple beam theory will not be attempted, but a brief description of those principle parts which are of special interest to this thesis will be given.

Multiple beam interference between plane parallel surfaces was investigated theoretically by Airy (1831) and practically by Boulouch (1906) and Fabry and Perot (1897). It has been shown experimentally by Tolansky and his school that the same theoretical considerations can be applied to multiple beam interference between the inclined surfaces of a wedge.

Multiple beam interference is produced by coating the two surfaces of a wedge with a suitable transparent metal film of high reflecting coefficient. Then, provided that all the resultant beams are summed, the intensity

distribution within a fringe is the same as in the classical Airy distribution.

The expression controlling the transmission fringe shape in such a wedge interferometer may be written as follows, (Tolansky 1948)

$$I = \frac{I_{MAX}}{1 + F \sin^2 \delta/2}$$

where $\delta = \frac{2\pi}{\lambda}(2\mu t \cos\phi)$

I = intensity at any point

I_{MAX} = peak intensity of the fringe $= \frac{T^2}{(1-R)^2}$

$F = \frac{4R}{(1-R)^2}$ or the Fabry 'Coefficient of Finesse'

R = reflecting coefficient of the metal films

λ = wavelength of the incident light

μ = refractive index of the wedge

t = wedge thickness

ϕ = angle of incidence of the light

$T = 1-R$ (zero absorption)

The factor F controls the sharpness of the fringes. The effect of increasing R is shown in Fig.II.6 for R 0.70 and 0.90 (Tolansky 1948)

For sharp fringes $\sin\delta$ can be replaced by δ, then

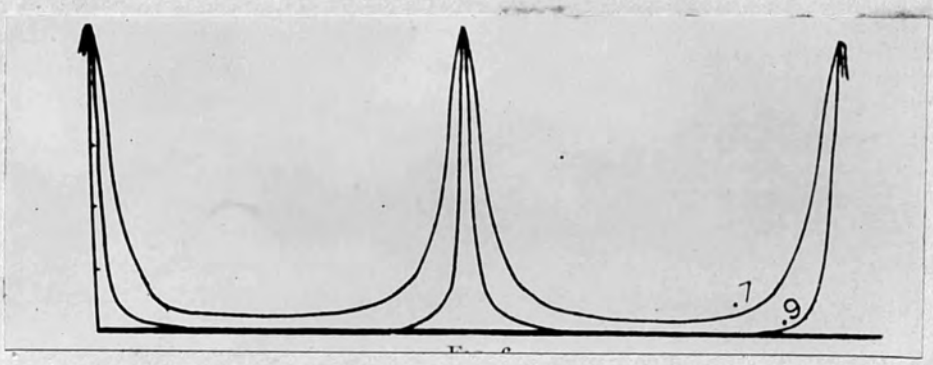

FIG. II. 6.

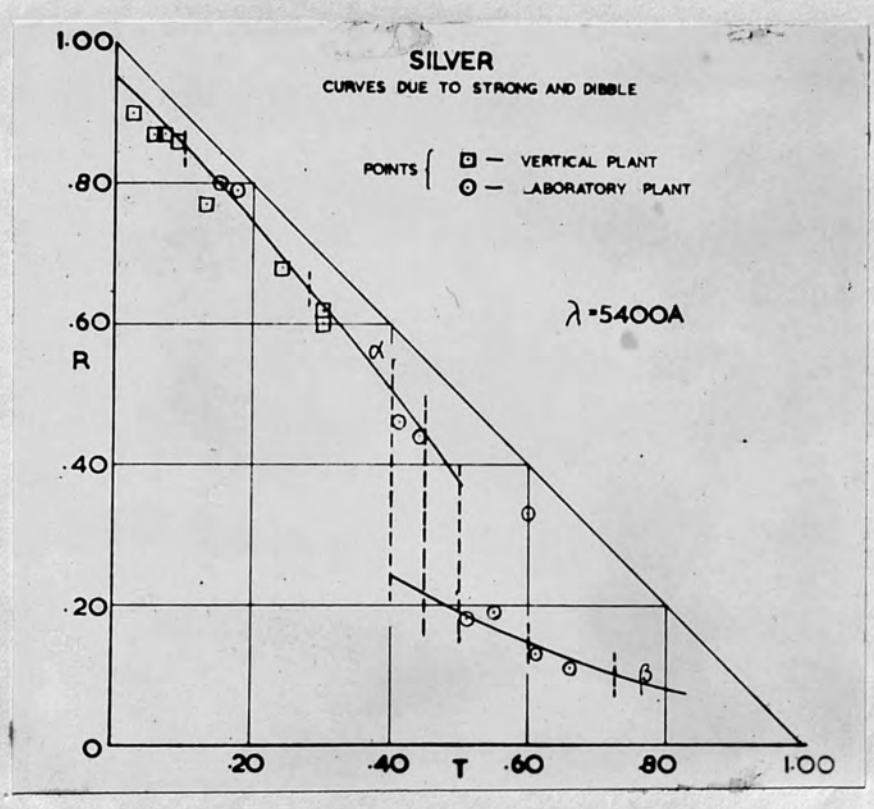

FIG. II. 7.

$$I = \frac{I_{max}}{1 + F\delta^2/4}$$
$$= \frac{I_{max}}{1 + \{R/(1-R)^2\}\delta^2}$$

At the half width

$$I = \frac{I_{max}}{2}$$

and so

$$\delta = \frac{1-R}{\sqrt{R}}$$

For symmetrical fringes, the phase angle corresponding to the fringe half width is

$$2 \cdot \frac{1-R}{\sqrt{R}}$$

and as the phase difference between successive orders is 2π the fringe half width, as a fraction of an order is

$$W = \frac{1-R}{\pi\sqrt{R}}$$

Table II.I gives the values of W for some values of R and is taken from Tolansky (1948)

Table II.I

R	0.04	0.7	0.8	0.85	0.9	0.925	0.94
W	I/3	I/9	I/14	I/19	I/30	I/40	I/50

The Airy treatment of multiple beam interference thus shows that the shape of the transmitted fringe depends only on the reflecting coefficient of the metal films. The reflection, transmission and absorption of an evaporated

film of silver vary with the thickness of the film and the wavelength of the radiation used. Typical values for green light are shown in Table II.2 (Tolansky 1946)

Table II.2

R(%)	60	70	75	80	85	90	94
T(%)	35.5	27	22	16.5	10.5	4.5	0.7
A(%)	4.5	3	3	3.5	4.5	5.5	5.3

An increase in the film thickness will increase the reflecting coefficient of the film and thus decrease the fringe width. However, a plot of the transmission against the reflection for a silver film using green light shows the practical limitation of increased fringe definition to be one of light transmission. Fig.II.7 (Avery 1950) shows this feature for some silver films produced in the laboratory by the Edwards plant described in Part III and a laboratory plant. They are compared with some films produced by Strong and Dibble (1940). The transmission depends critically on the absorption in the film at high reflecting coefficients.

In the reflected system the absorption is also important, as it reduces the fringe visibility in that the fringe minima no longer reach zero intensity.

Because of these considerations the process of depositing metal films of high reflecting coefficient

and low absorption is an important part of the practice of multiple beam interferometry. For work in the wavelength region 5-7000 Angstroms, silver when evaporated in a vacuum can give mirrors of sufficiently high reflecting coefficient (exceeding 0.95) and low absorption. (below 0.05) The precise value of the reflecting coefficient need not be known numerically since what is required is the highest reflectivity consistent with the thickness permitted by the light source available.

The measurement of a fringe displacement depends on the accuracy with which a setting can be made on the fringe and this depends on the intensity distribution within the fringe. The critical conditions for the use of multiple beam Fizeau fringes have been discussed by Tolansky (1948), Brossel (1947) and for the reflected system by Holden (1949). The reflected fringes are not complementary to the transmitted fringes in the multiple beam system because of absorption in, and phase changes at, the reflecting metal films.

Briefly the multiple beam reflections impose restrictions on the value of t for a given fringe dispersion and a given accuracy of collimation of the incident light beam. Provided these restrictions are observed, the multiple beams can be summed by a suitable lens to give an Airy distribution in the back focal plane.

Table II.3 has been drawn up from values suggested by Tolansky (1948) showing the permissible values of stop size d, collimation error ϕ and fringe dispersion X for four values of t mm.

Table II.3

t mm	I	0.I	0.0I	0.00I
ϕ°	I/I0	I/3	I	3
d mm	0.2	0.6	2	6
X cm^{-1}	3.5	I0.I	35.5	I0I

In practice the important fact is that t should be as small as possible.

The lens must be capable of collecting all the beams from the wedge. It has been shown that the numerical aperture necessary is $2x\Theta$, where x no. of beams and Θ- wedge angle.

With low magnifications (less than x 5) and a low dispersion on the wedge (less than I fringe per mm.) the necessary numerical aperture is small (less than 0.I) and can be accomodated by any well corrected wide aperture camera lens.

The multiple beam Fizeau fringes are usually formed with monochromatic light. However the formula $n\lambda = 2\mu t\cos\phi$ shows the possibility of producing other multiple beam fringe systems by varying λ, t, and ϕ.

Usually μ is constant and table II.4 taken from Tolansky (1948) shows the systems obtained by varying one of the three quantities λ, t, ϕ and keeping the other two constant.

Table II.4

Fringe types

Nature of light	*Constant quantity*	*Fringe type*	*Name*	*Filter action*
Monochromatic (λ constant)	t	Equal inclination	Fabry-Perot	Angular
	ϕ	Equal thickness	Fizeau	Linear
White (λ variable)	ϕ	Equal t/λ	Equal chromatic order	Wave-length
	t	Equal $(t \cos \phi)/\lambda$	White-light Fabry-Perot	..

With parallel white light at normal incidence on a wedge interferometer fringes of equal t/λ, multiple beam fringes of equal chromatic order are formed when the light passing through the wedge is analysed by a spectrograph.

The same theoretical considerations as are applied to the multiple beam Fizeau fringes apply equally to the multiple beam fringes of equal chromatic order. However the fringe dispersion in the fringes of equal chromatic order is shown to be only a function of the interferometer gap and the spectrograph dispersion, and not of the wedge angle as in the Fizeau fringes. This

means that higher magnifications can be used with the fringes of equal chromatic order than with the Fizeau fringes without the reduction in the sharpness which occurs with the latter.

In the fringes of equal chromatic order the projecting lens is used to focus the multiple beams on to the slit of the spectrograph. It thus controls the dimensions of the line section of the wedge being observed.

The use of multiple beam fringes to measure topographical detail by measuring the fringe shift as a fraction of the order distance has been discussed by Tolansky (1948). The accuracy of measurement depends on the fringe width being as small a fraction of the order distance as possible.

The application of multiple beam techniques to the study of vibrating surfaces will now be discussed.

The formula for the intensity distribution in a multiple beam fringe has been given as

$$I = \frac{I_{max}}{1 + F \sin^2 \delta/2}$$

where

$$\delta = \frac{2\pi}{\lambda}(2\mu t \cos\phi)$$

If c is varied in a simple harmonic manner, following Osterberg's treatment, the resultant expression is cumbersome and does not admit of easy integration. A graphical treatment is more revealing.

In Fig.II.8. the full line shows an idealised microphotometer trace for a multiple beam fringe system in transmission. Fig. II.9 shows the intensity curve when the fringe system is given a simple harmonic motion of amplitude (total excursion) about $\lambda/4$, each fringe moving either side of its central position a, b, to the extreme positions indicated by a' and b'. It can be seen that if the half width is a small fraction of the distance between orders, each moving fringe will not be affected by the adjecent moving fringe. Fig.II.10 shows an X cut bar oscillating in a flexural overtone with a fringe amplitude of this order.

The position of the maxima of the resultant oscillating fringe pattern with respect to the actual amplitude of motion of the surface causing it must be examined. The sharp maxima at the extremes of the oscillating fringe pattern are characteristic of the multiple beam fringes used in this way and they are due to the simple harmonic nature of the fringe displacement. As the actual fringe sweeps across any ordinate of this curve, the blackening it

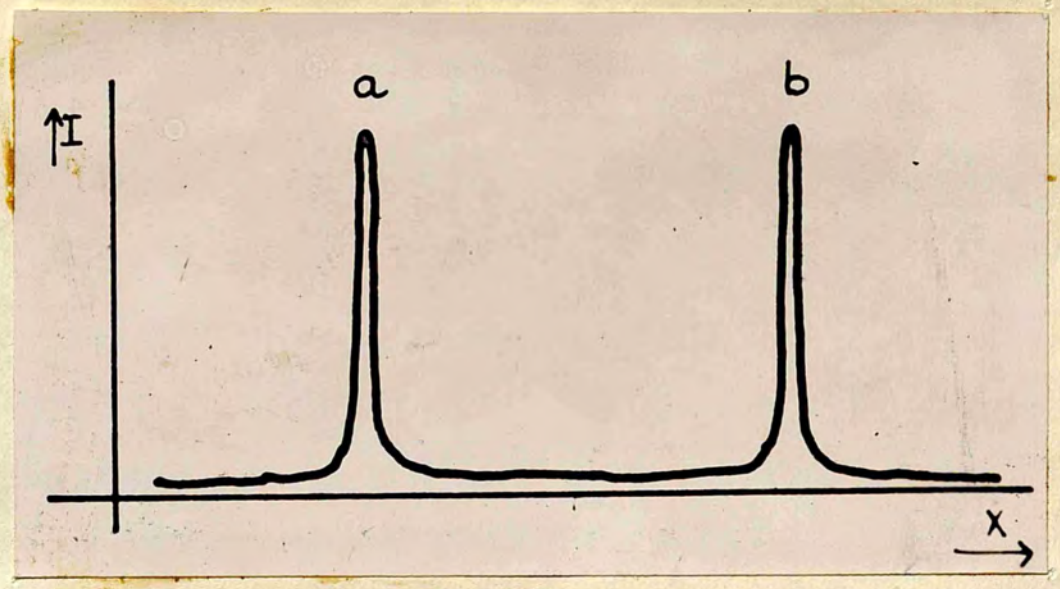

FIG. II.8

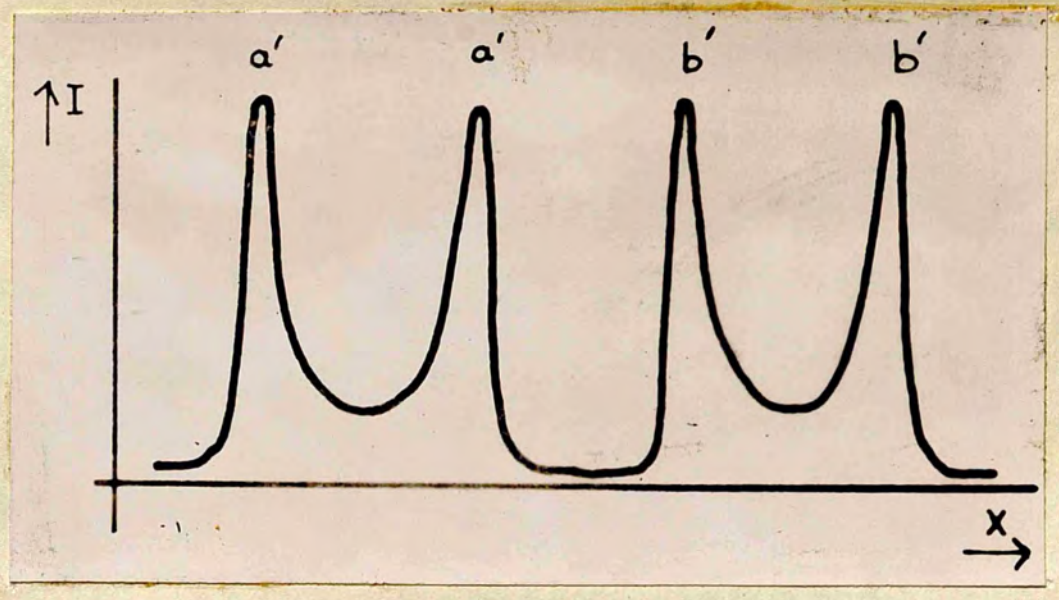

FIG. II.9.

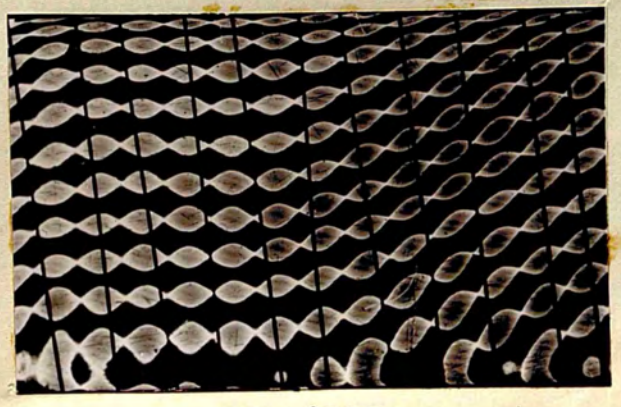

FIG. II.10.

produces on the photographic plate at that position will depend on the intensity distribution of the fringe and the velocity with which each part of this distribution crosses the ordinate. At the extreme positions of the fringe displacement the additional time factor may cause a displacement of the resultant maxima inwards from the positions reached by the fringe maximum.

As an illustration the fringe may be drawn in the successive positions reached in equal time intervals as in Fig.II.II. As the extreme positions are reached it may be seen that the fringes begin to overlap. Two positions a''' and a'''' are drawn which overlap at the half width position. The maxima of the resultant intensity distribution must lie between these two maxima at each side, for it cannot lie outside a'''', and a''' represents the last ordinate across which the whole of the fringe passes, and it moves more slowly towards a'''' than it does from a''.

This illustration may be used to provide an estimate of any errpr that may result when the amplitude is measured by observing the separation of the two maxima of the resultant intensity distribution. The error cannot exceed twice the half width of the stationary fringe.

In an actual case several microphotometer

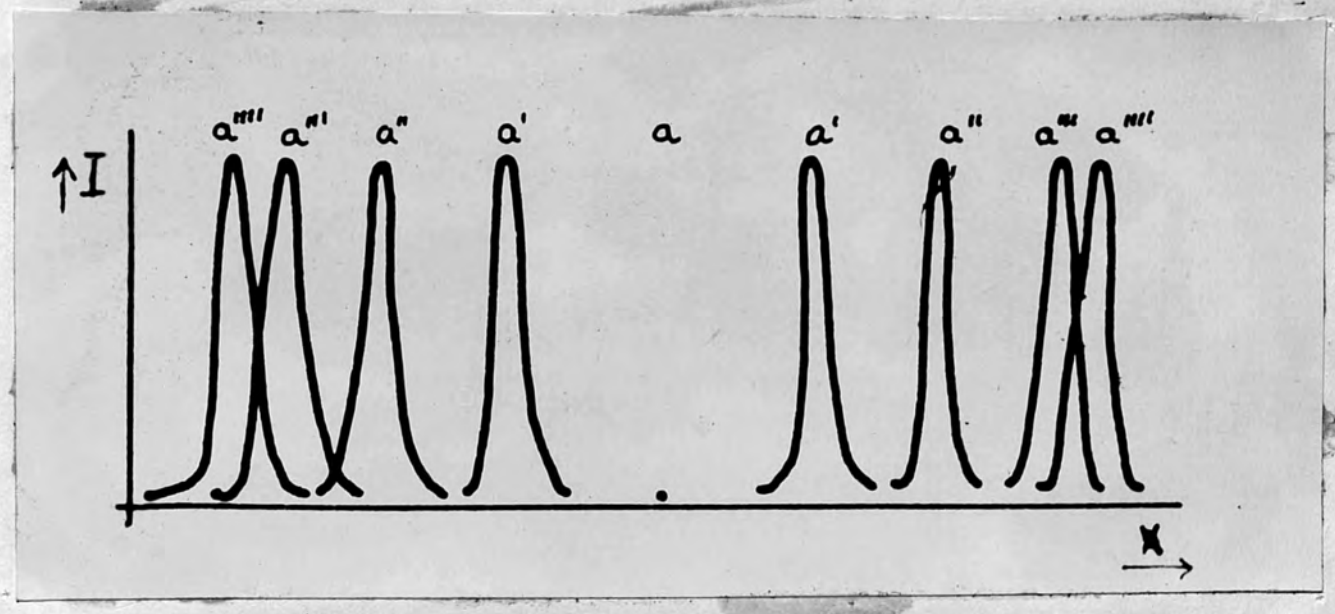

FIG.II.11.

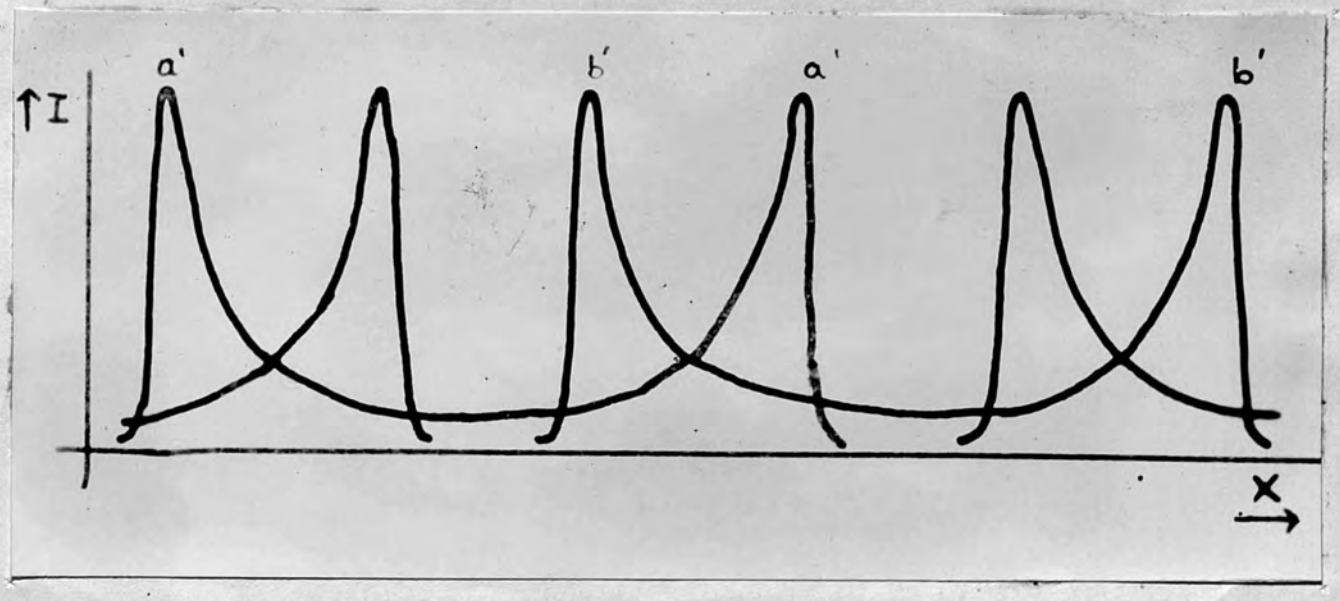

FIG.II.12.

traces were taken on oscillating fringes whose stationary half width could be estimated from the reflecting coefficient of the silver film used. The fringes and a typical microphotometer trace across one of the antinodal regions are shown in Plate II.1 and Fig.IV.2 (Page 77A) of Part IV. The silvering was 0.95 and the calculated half width $\lambda/100$. The amplitude obtained by measuring the separation of the maxima of the resultant intensity distribution was $\lambda/4$ across the middle of an antinodal region. The amplitude was therefore $\lambda/4 \pm \lambda/100$. The distance between the fringe envelope and the ordinate through the maxima of the resultant intensity distribution was found to be some 3 per cent of the amplitude of $\lambda/4$ or $\lambda/130$. The contour is thus not that of the stationary fringe but corresponds to one of half width $\lambda/65$. Allowing for small errors in the determination of the reflecting coefficient and the intensity distribution it appears that the maxima may suffer a slight shift.

In the case of an amplitude a',b', which is greater than $\lambda/2$ the resultant intensity distributions will overlap as shown in Fig.II.12 from which it can be seen that at amplitudes near to $\lambda/2$ the maxima of each distribution will be superimposed on a steep intensity

gradient from the adjacent distribution. This can cause a shift in the position of the maxima, the shift depen ding on the amount of overlap and the nature of the intensity distribution at the overlap. This problem has been discussed by Oldenburg (1922) for two adjacent fringes of identical shape whose shape is the Doppler distribution of the line. He evaluated the contraction as a percentage of the peak separation in terms of the relative percentage saddle height as shown below. (Tolansky 1947).

Table II.5

Rel. saddle ht.	85	75	65	55	49	47	45
Correction %	11.6	5.4	2.7	1.25	0.80	0.70	0.55

It can be seen that the effect is considerable for peaks which are just resolved and can be reasonably disregarded when the peaks are separated to the point where the base of the saddle portion has half the intensity it has at the limit of resolution.

The intensity distribution of Fig. II.12 is not a Doppler distribution and so Oldenburg's treatment is not exactly applicable. However the treatment shows that the effect is a maximum when the intensity gradient superimposed has the steepest gradient. The intensity distribution of Fig. II.12 falls off less rapidly than the Doppler distribution and therefore is less steep at

corresponding amounts of overlapping. Thus the Oldenburg correction may be used as a practical working index for the overlapping of uniformly spaced fringes oscillating with the same amplitude.

Although it has not been possible to investigate fully the theoretical intensity distribution across fringes of various half widths oscillating with different amplitudes the above considerations provide some guidance in the interpretation of the interferograms shown in Part IV. It should however be possible to investigate experimentally the nature of the resultant intensity distribution at different amplitudes in relation to the width of the stationary fringe.

In reflection there is an additional complication that the multiple beam fringes are superimposed on a bright background and therefore the visibility of the fringe system is decreased when it oscillates. From the data published by Holden (1949) the optimum conditions for using the reflected system may be realised. Fig.II.13 shows two graphs (reproduced from Holden's paper) based on the figures for the interferometric coatings given in the Table II.2. It can be seen that the maxima of the fringe visibility in the reflected system occurs for reflecting coefficients just over 0.80. At this value

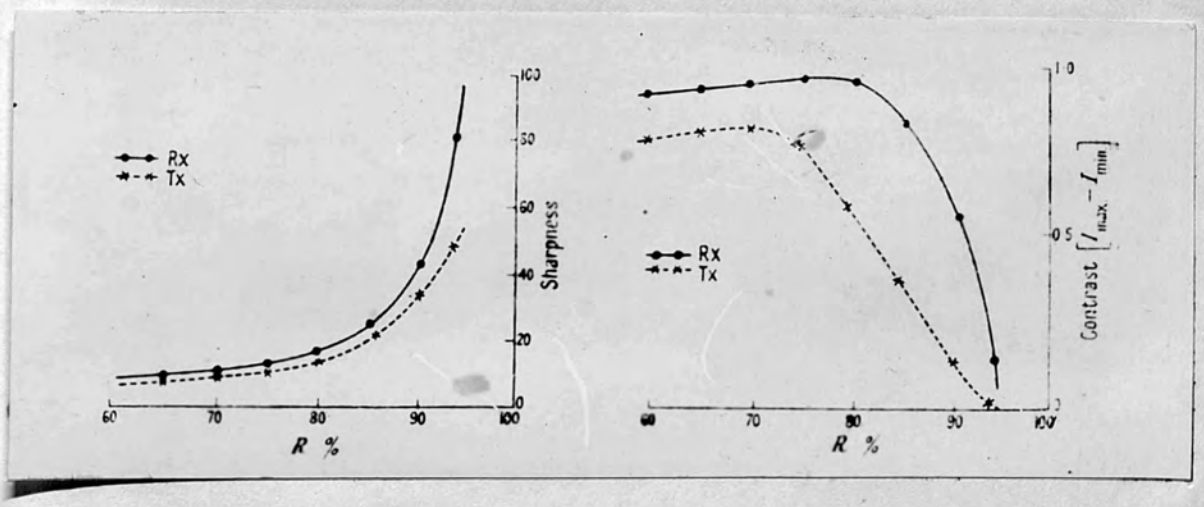
Rx
Tx
Sharpness
R %
Rx
Tx
Contrast $\left[\frac{I_{max.}-I_{min}}{I_{max.}+I_{min}}\right]$
R %

FIG. D.13.

the fringe sharpness begins to rise rapidly and is about I/20 of an order. That under these circumstances the reflected system may be used in oscillation can be seen in Plates I2 and I3 in Part IV. (Page 79A)

The above discussion applies equally for the multiple beam fringes of equal chromatic order.

Comparison of the multiple beam system with the two beam system shows that in the former a fringe motion of less than $\lambda/4$ can be accurately measured, the smallest amplitude observable and the accuracy depending on the fringe width, while with the two beam system amplitudes of less than $\lambda/4$ can only just be detected. For amplitudes greater than $\lambda/4$ the multiple beam system offers a direct measurement except at certain amplitudes while with the two beam system the measurement is based on subjective visibility estimations, unless stroboscopic illumination is used.

With stroboscopic illumination the multiple beam system is freed from some of its restrictions and the accuracy with which the amplitude can be measured is greater than in the two beam system because of the improved fringe sharpness.

The application of multiple beam systems to the observation of moving surfaces raises further

considerations.

The multiple beam system formed between a reference surface and another surface may be imagined to consist of plane parallel zones, distant at intervals of $\lambda/2$ from the reference surface, the thickness of the zones being only a few per cent of the distance between successive zones. In each zone there is a visible change of intensity between successive planes only a few Angstroms apart. Between these zones there is little light and no intensity gradient. If any part of the other surface moves with respect to the reference surface, that motion will only be seen if the area moving falls within a zone of maximum light. Therefore there must be a large number of zones of maximum light over the surface, or else the surface must fall completely with in one of these zones. That is, the fringe dispersion must either be very small or very large. The latter state is more sensitive but leads to restrictions on the surface finish. In the low dispersion case, the surface need only be flat to a wavelength over the whole surface. In the high dispersion case the flatness must be comparable with the fringe half width.

Comparison of the Fizeau system of multiple beam fringes with those of equal chromatic order shows

that with the former the amplitude at any point is only observed when that point is crossed by a fringe, that is, at some adjacent position to the undisplaced fringe, while with the latter, the actual amplitude of the moving surface at the line section selected by the projecting lens and the spectrograph slit is revealed.

In the fringes of equal chromatic order, the equation relating the change in interferometric gap dt to the fringe shift $d\lambda$ is

$$dt = \tfrac{1}{2} n \cdot d\lambda$$

neglecting any phase changes on reflection at the metallic films, and hence as the blue end of the spectrum is approached $d\lambda$ diminishes in order to maintain a constant dt.

Rewriting

$$dt = \frac{1}{2} n \frac{\lambda_{n+1}}{\lambda_n - \lambda_{n+1}}$$

it can be seen that a wavelength calibration of the spectrograph is necessary. Then at a given wavelength the fringe displacement expressed as a fraction of the order distance gives the change in thickness. As $\lambda n = 2t$ for normal incidence, then $dn = 2d\nu t$ and the order separation is linear in terms of wave numbers, and if $d\nu$ is small for $dn = 1$, a change of one order, it is practically

linear in terms of wavelengths. Thus the fringe displacement as a fraction of the order distance can be evaluated.

The fringe sharpness is increased by increasing the magnification due to the projecting lens, and the apparent wedge angle of the interferometer gap depends on the orientation of the wedge apex with respect to the spectrograph slit, but neither of these factors influences the measured change in thickness of the interferometer gap.

In both two beam and multiple beam systems when applied to the study of moving surfaces there is one important inherent disadvantage. The motion revealed is that normal to the surface. Small motions along directions in the plane of the surface cannot be seen. Even at high magnifications the lateral resolving power in either system is limited by the use of parallel light which effectively halves the resolving power of any objective used.

The use of multiple beam fringes to study vibratory motion following publications by Tolansky and Bardsley (1948) has interested other authors.

Holden (1949) has suggested that the transmission like fringes produced in reflection with suitable interferometric coatings could be used for the

study of vibrating metal surfaces. The half width of these fringes is however only 1/5 of the distance between orders.

Bruce (1951) has mentioned the production of transmission like fringes by cutting out some of the beams in the reflected system and their application to topographical and vibrational studies. Bruce, Macinante and Kelly (1951) have described the application of these fringes with both continuous and stroboscopic illumination to the calibration of the amplitude of vibration of a tuning fork in terms of wavelengths of light.

Tolansky has pointed out (1951) in a criticism of these last two papers that the principle of converting reflection into transmission fringes by cutting out beams is not new and was first discussed by Lummer (1900, 1907). He also observes that the method is severly limited, so that its use is confined to low magnifications, and suggests that Bruce's appreciation of the use of the reflected system is not critical.

In the absence of experimental detail it is not possible to discuss this work more completely.

All the multiple beam systems so far considered have used metallic films to produce the necessary reflecting coefficients. The films are good conductors on polished surfaces and this may restrict their application, under

certain circumstances, to piezoelectric crystals. Of interest therefore is the work of Jacquinot and Dufour (1950) who have produced high reflecting coefficients with thin films of dielectrics. The dielectrics are evaporated to form multiple layers and with alternate layers of cryolite and zinc sulphide films of reflecting coefficients of up to 0,90 with low absorption characteristics can be prepared. For higher reflectivities it seems necessary to use alternate metal dielectric layers . These films have not yet been applied to topographical or vibrational studies.

PART III

EXPERIMENTAL TECHNIQUES

CHAPTER I

THE EVAPORATION PROCESS

As indicated in Part II, chapter 2 the practice of multiple beam interferometry requires the use of thin metal films of high reflecting power and low absorption deposited on suitable surfaces or substrates. This is conveniently done by thermal evaporation of the metal in a vacuum. The process may also be used to produce metallic coatings which can act as electrodes.

The technique has been described by Tolansky (1947, 1948), Strong (1946) and others. There follows a brief account of the technique and the apparatus used to produce the coatings of silver for the experiments described in this thesis.

The evaporation process is carried out in a commercial plant type E3 built by Edwards and Co., of Sydenham.

It consists essentially of a vacuum chamber, a large pyrex bell jar some 60 cm. high and 40 cm. diameter which can be evacuated by a three stage silicon oil diffusion pump which is backed by a rotary oil pump. The bell jar rests on a large alloy steel base plate, a vacuum seal between the two being made by an L section neoprene gasket on the rim of the bell jar. A flap valve

set into the base plate connects the vacuum chamber to the diffusion pump. The pressure in the chamber is measured by a Philips type ionisation gauge. The size of the vacuum chamber and the speed of the pumping is such that a complete cycle of evaporation may be completed in half an hour.

The necessary electrodes are brought through insulating vacuum seals in the base plate. Resting on the base plate is a duralumin stage some 50 cm. high the top of which forms a platform for mounting the specimens. On the legs of the stage are two circular electrodes between which about 3,500 volts is available for passing high tension discharge. Just above the base plate are the filament electrodes between which approximately 150 amps of current may be passed. The filaments used for the evaporation of the silver are molybdenum strips 7 cm. x 1 cm. x 0.03 cm., in the centre of which a small circular depression is punched to take a charge of silver. This is supplied in the form of spectroscopically pure silver wire of about 3 mm. diameter which is cut up, for convenience, into 3 mm. lengths.

The general form of the plant is seen in Fig.III,1 the bell jar being clean so that the arrangement of the components on the base plate is visible.

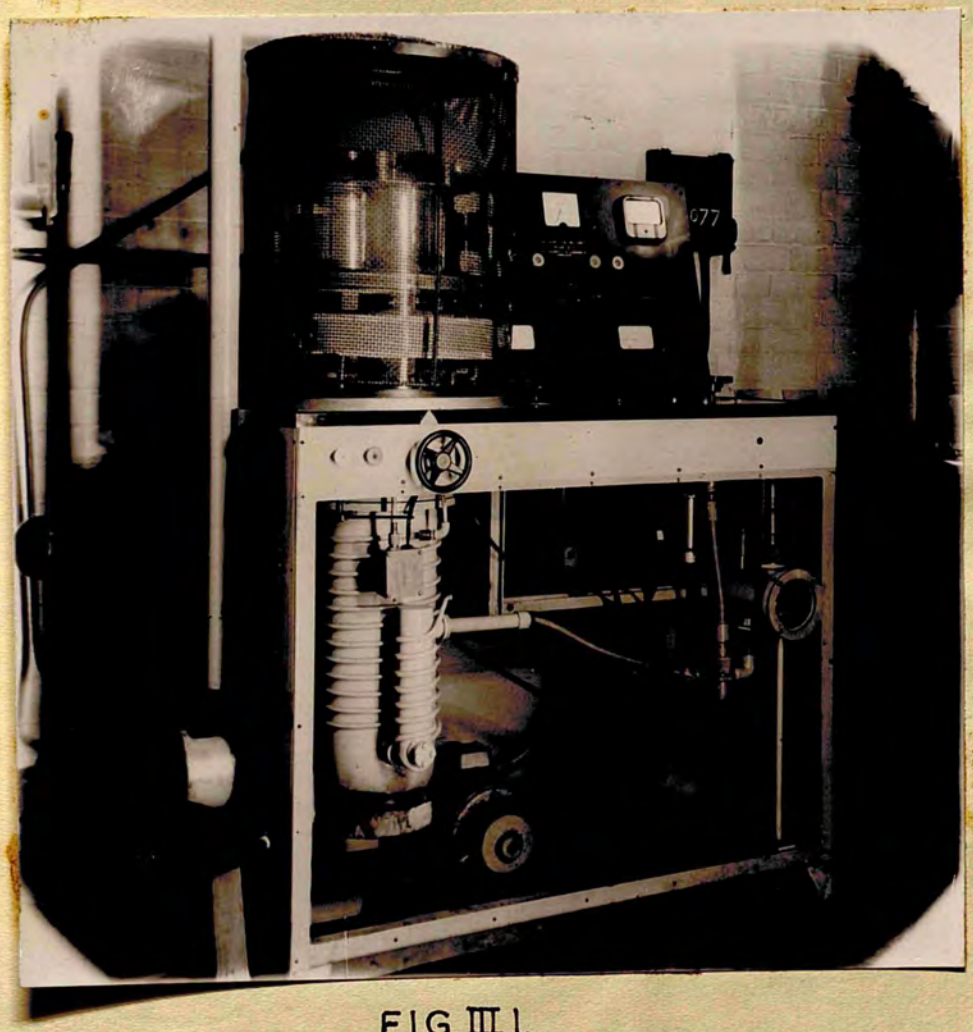

FIG III.1.

A necessary prelimimary to the evaporation process is the cleaning of the surface,of substrate, on which the metal film is to be deposited. The light absorption of evaporated metal films is critically dependent on the cleanliness of the substrate prior to the evaporation. Optical flats of glass are first cleaned with Teepol and water which removes any gross contamination of a greasy nature. They are then rubbed with a solution of hydrogen peroxide (20 vol. strength) applied on a clean pad of surgical cotton wool. Hydrogen peroxide is an excellent solvent for many organic compounds but will not harm the glass. It also dissolves any previous silver coating. The surface is dried with clean cotton wool and rubbed with further pieces until the 'breath figure',formed by breathing gently on to the surface,is a uniform grey in appearance and disappears in about one second or less. For quartz vibrators,after the cleaning with Teepol, concentrated nitric acid applied on a cotton wool pad rapidly cleans the surface and does not attack the quartz. It also rapidly removes any silver coating. This initial cleaning process is designed to produce a certain minimum amount of surface contamination which can be removed easily just before the actual evaporation of th e metal.

The substrate is th en mounted on the platform near the top of the vacuum chamber and the bell jar

evacuated. At a pressure of about I mm. of mercury the high voltage discharge is struck. The discharge completes the final cleaning of the substrate by ionic bombardment, the intensity and duration of the discharge being suited to the nature of the substrate.

When the pressure in the chamber is reduced to less than 10^{-4} mm. of mercury the silver can be evaporated by heating the molybdenum filament. While the silver is fusing a moveable shutter is swung over the filament to protect the substrate from possible contamination.

The thickness of the coating and hence the reflectivity is judged by observing the transmission of light from the filament through the evaporated film on the substrate (or the glass monitor if the substrate is not transparent). In this way reflectivities may be estimated to within a few per cent. The filament-specimen distance is calculated to give less than I per cent variation in density of deposit over a circle I0 cm. diameter at the level of the substrate. For the evaporation of metal electrodes on to quartz vibrators, the filament arrangement can be modified when necessary, as for example when coating the two cylindrical surfaces of a ring vibrator. The thickness of the deposit required to give a low resistance coating (4-5 ohms across the electrode) depends on the nature of the

substrate. A polished surface needs only a thin coating similar to an interferometric coating while an etched or ground glass surface requires a much heavier deposit.

Care has to be taken to remove any silver which may find its way to surfaces other than the one being coated. Such thin films show selective absorption of light and also may form a high resistance connection between electrode coatings.

CHAPTER 2

OPTICAL SYSTEM

The optical system used for the experiments described in this thesis has undergone continuous development as the experiments have proceeded. It owes a great deal to the design of the Cooke Troughton and Sims Projection Microscope.

It consists of three parts. The optical system producing a beam of parallel light, the interferometer system and the mirror system for producing the reflected or the transmitted system of multiple beam interference fringes, and the camera system. It is shown diagrammatically in Fig.III.2. and is photographed in Fig.III.3. with some of the associated electronic equipment.

The first part of the system is mounted on an optical bench I. A light source S is focussed by a condensing lens L_1 on to an iris aperture A. Filters may be inserted at F. The aperture A is in the back focal plane of a well corrected lens L_2 (F 2.9 focal length 8 ins) which thus emits a beam of parallel light.

The interferometer system I is mounted on bench III together with mirrors M_1, M_4 and M_5. On bench II are mounted mirrors M_2 and M_3. M_1, M_2 M_3 and M_5 are front surface aluminium mirrors. M_4 is plain glass.

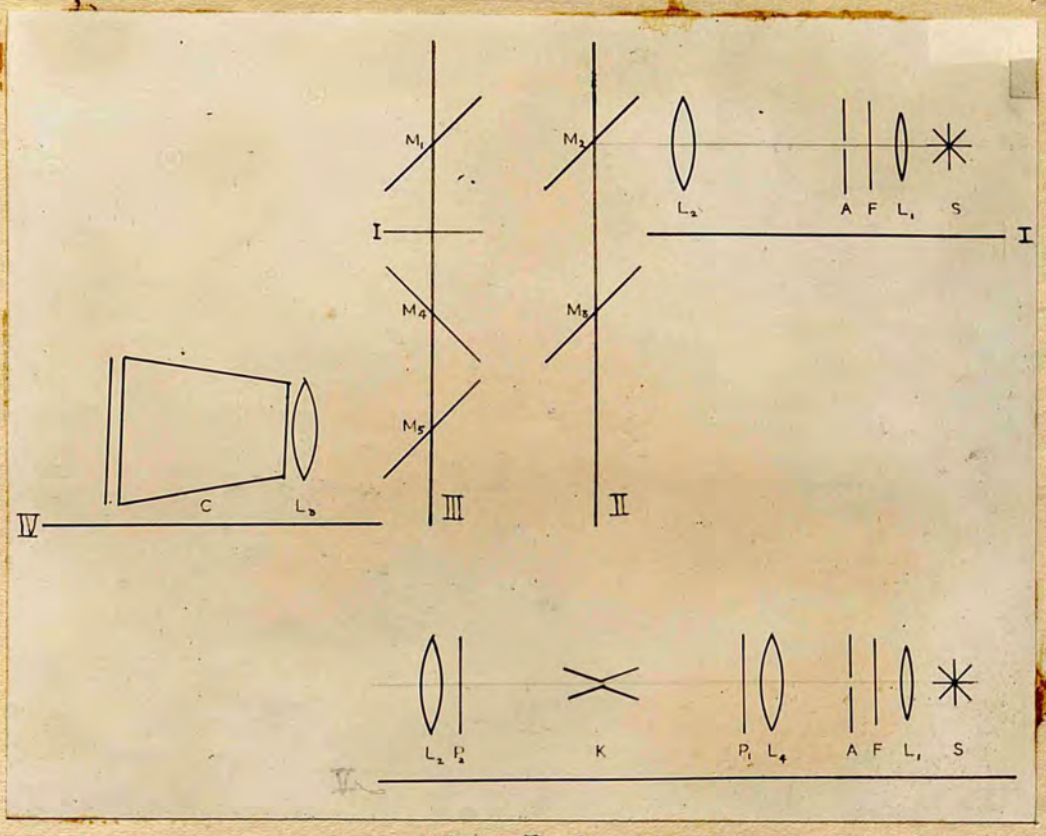

FIG. III.2.

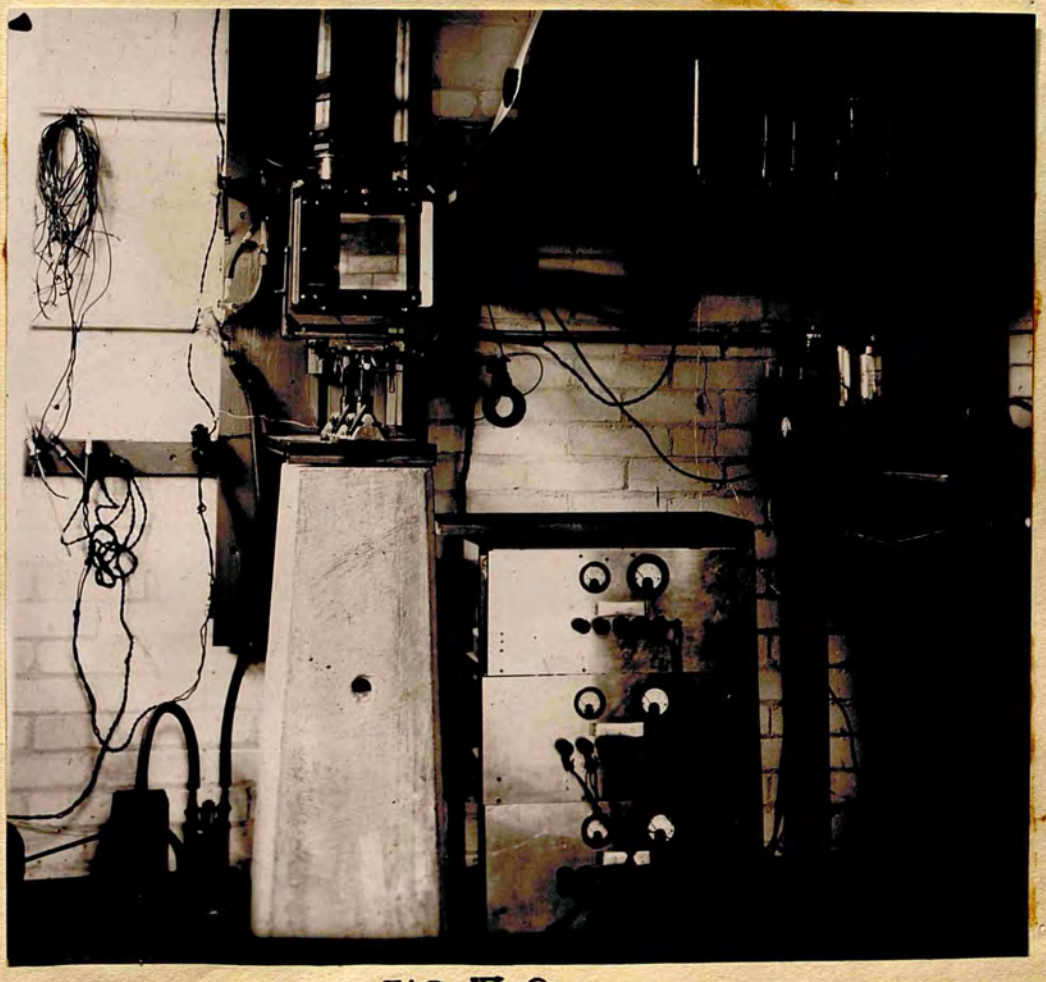

FIG. III.3.

54A

A camera body C is mounted on bench IV. The camera lens L_3 is a well corrected lens chosen to give a range of suitable magnifications. The three lenses used in the experiments were as follows:- (F 4.5, focal length 7 ins.), (F 4, focal length 5 ins.), (F 4.5, focal length 2 ins.). The camera, adapted from an ex-R.A.F. copying camera with an extendable bellows body (up to 18 ins.) is modified to take a half plate holder and a ground glass focussing screen. The optical benches are all electrically earthed.

With a monochromatic light source at S and using mirrors M_1 and M_2 the transmitted multiple beam Fizeau system can be observed, whilst with mirrors M_2, M_3, M_4 and M_5 the reflected system can be observed, the mirrors not required in each case being moved out of the system. With a white light source at S and a spectrograph mounted in place of the camera, multiple beam fringes of equal chromatic order can be observed in transmission and in reflection. The lens L_3 then serves to focus the interference system on to the slit of the spectrograph. The optical arrangement is such that the image of the interferometer system seen on the focussing screen is reversed left to right and is erect top and bottom.

Monochromatic illumination for the multiple beam Fizeau system of small interferometric gap is provided

with a 125 watt 230 volt Mercra high pressure mercury lamp. The lamp is run from the A.C. mains in series with a Mazda lux MRG 506 stabilizing choke and a 300 ohm 1 ampere variable resistor, the latter permitting the lamp to be underrun and affording some control over the intensity of the lamp and the line width of the radiation. For large interferometric gaps (greater than 0.5 mm.) the Mercra lamp is replaced by a low pressure mercury vapour arc of the type described by Tolansky (1947) run from 110v D.C. in series with a stabilising choke and a variable resistor. A Wratten 77A filter is used to isolate the green (5461 A) line of mercury. The white light source for the multiple beam fringes of equal chromatic order is a carbon arc, or more conveniently an Ediswan 50 candle power 230v. A.C. Point-O-lite lamp.

Stroboscopic illumination is provided either by a Geisler tube filled with mercury vapour or a nitrobenzene Kerr cell arrangement. The Geisler tube is fitted immediately behind the iris diaphragm A with the capilliary tube horizontal and normal to the direction of the optical bench. With the Kerr cell, the optical train on bench I is rearranged as on bench V in Fig.III.2. The Kerr cell is of the diverging plate type with minimum separation between the plates of about 1½ mm. Lens L_4, an achromat of focal length 3.5 ins. provides a converging beam of

suitable angle for the Kerr cell plates. Lens L_2 is arranged to give a parallelbeam as before. Polaroids are mounted at P_1 and P_2. The circuits used to drive both the Geisler tube and the Kerr cell are described in Part III chapter 3.

In all cases, the collimating lens L_2 must emit a parallel beam of sufficient diameter to illuminate the whole aperture of the interferometer. The lens used gives a 2½ inch diameter beam which is adequate for the interferometric systems used and, having an internal iris, the diameter of the beam can be reduced if necessary. The camera or projecting lens L_3 has an aperture large enough to collect all the direct and multiply reflected beams coming from the interferometer.

The observations are recorded on suitable photographic plates such as Kodak P.1200 for those cases when little light is available and Kodak P.300 when adequate light is available, the exposure times varying from a few seconds up to some fifteen minutes.

The jig forming the interferometric mounting depends on the particular experiment and many different types have been employed. They are conveniently referred to in the appropiate sections of Part IV.

CHAPTER 3

ELECTRONICS

In general the electronic circuits described in this chapter are orthodox. They consist of power supplies, valve oscillators, circuits for driving the stroboscopic devices, frequency measuring instruments and general service equipment.

The power supplies are in the form of four power packs and may be seen in Fig.III.3. They are constructed from Government surplus equipment. They run from the 230 volt A.C. mains and supply a convenient range of voltages listed in table III 1. The circuits are not described as they follow conventional practice.

Three valve oscillators are used to drive the vibrators. They are respectively a Pierce oscillator, a bridge oscillator and a Hartley oscillator.

The Pierce oscillator is of standard design and is described in the circuit diagram in Fig.III.4.

The bridge oscillator is of modified Post Office design and is shown schematically in Fig.III.5. It consists of a Wheatstone bridge in one arm of which is the quartz vibrator. A two stage maintaining amplifier tuned to the resonant frequency of the vibrator is connected across the

Table III.1

Power Pack Voltages

	Voltage	Current	Service
A.C	110 v	5 a	American equipment
	6 v	10 a	heater voltage
	4 v	10 a	heater voltage
D.C.	500 v	120 ma	high tension
	350 v	120 ma	high tension
	250 v	120 ma	high tension
	5000 v	1.5 ma	extra high tension

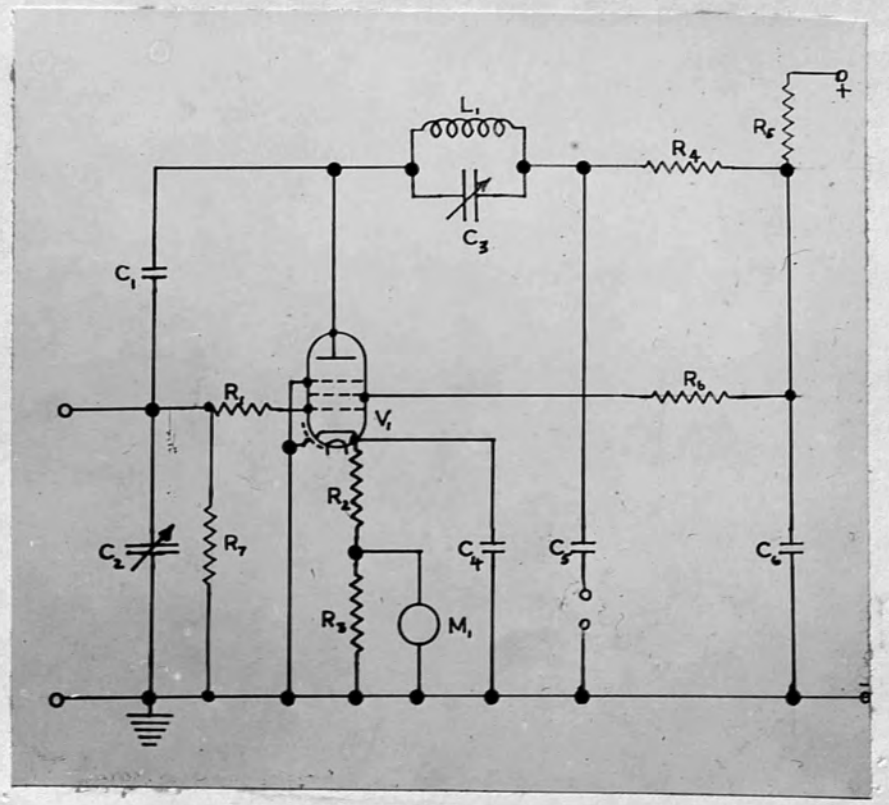

FIG. III. 4.

R_1 150 Ω	C_1 2.2 pf
R_2 180 Ω	C_2 25 pf
R_3 75 Ω	C_3 0.0035 (× 2) μf
R_4 500 Ω	C_4 0.1 μf
R_5 10K Ω	C_5 0.1 μf
R_6 47K Ω	C_6 0.1 μf
R_7 2.2M Ω	M 0–5 m.a.

L_1 to tune C_3

V_1 SP. 61.

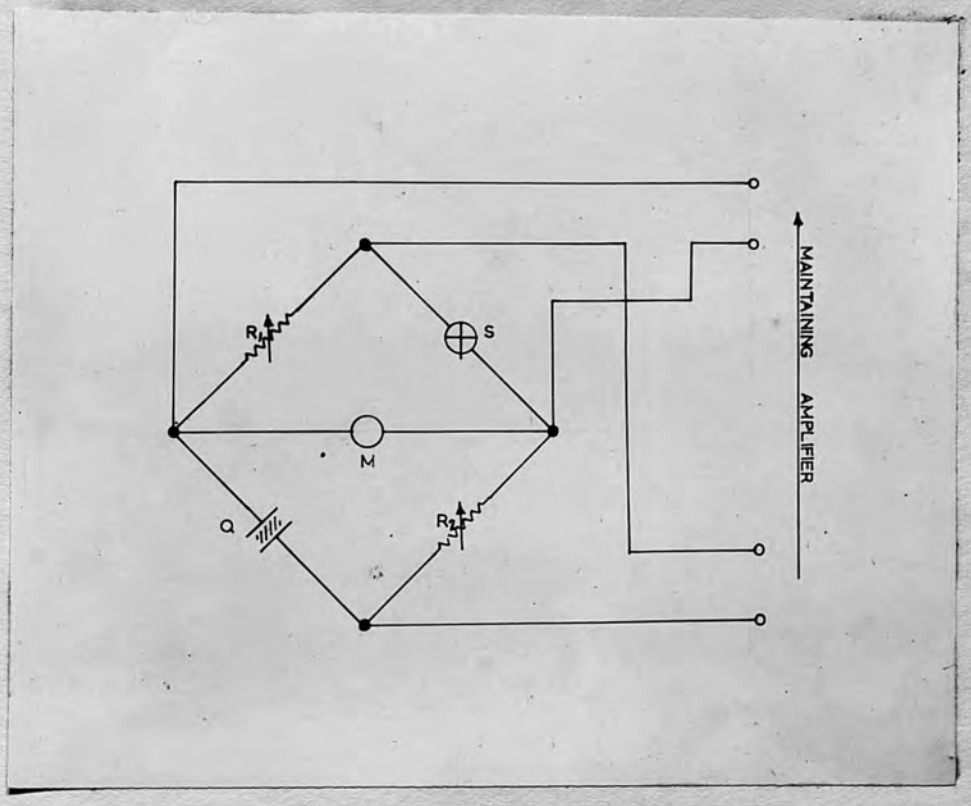

FIG. III .5.

R_1 1, 10, ... 100Ω, 10Ω steps.

R_2 1KΩ.... 11KΩ 1KΩ steps
100Ω... 1000Ω, 100Ω steps
10Ω... 100Ω, 10Ω steps all in series

Q 100 Kc/s xtal

S 6 volt lamp M v.t. m.a.

bridge, and when the phase change and attenuation across the bridge are balanced by the phase change and gain across the amplifier, the vibrator is maintained in oscillation at series resonance. The current through the vibrator can be varied by changing the values of R_1 and R_2 and, with a knowledge of the resistance of the crystal and the applied voltage across this resistance and R_2 in series, the value of the current can be calculated. The crystal resistance can be obtained from calibration curves of crystal resistance against applied voltage for certain values of R_1 and R_2. The applied voltage is measured by a radio frequency (r.f.) thermocouple instrument.

Both the bridge oscillator and the Pierce oscillator shown in Fig.III.10a. were learned by the Post Office research station, Dollis Hill.

The Hartley oscillator was designed to provide an oscillator of high stability, good wave shape and sufficient power to resonate quartz vibrators under conditions of high damping and at the same time drive the stroboscope circuits. It is shown in Fig.III.10b.

The circuit diagram is shown in Fig.III.6. It consists basically of a push-pull circuit of Hartley design with an auxiliary control circuit to keep the r.f. voltage across the tuned circuit of the oscillatorsection at constant amplitude.

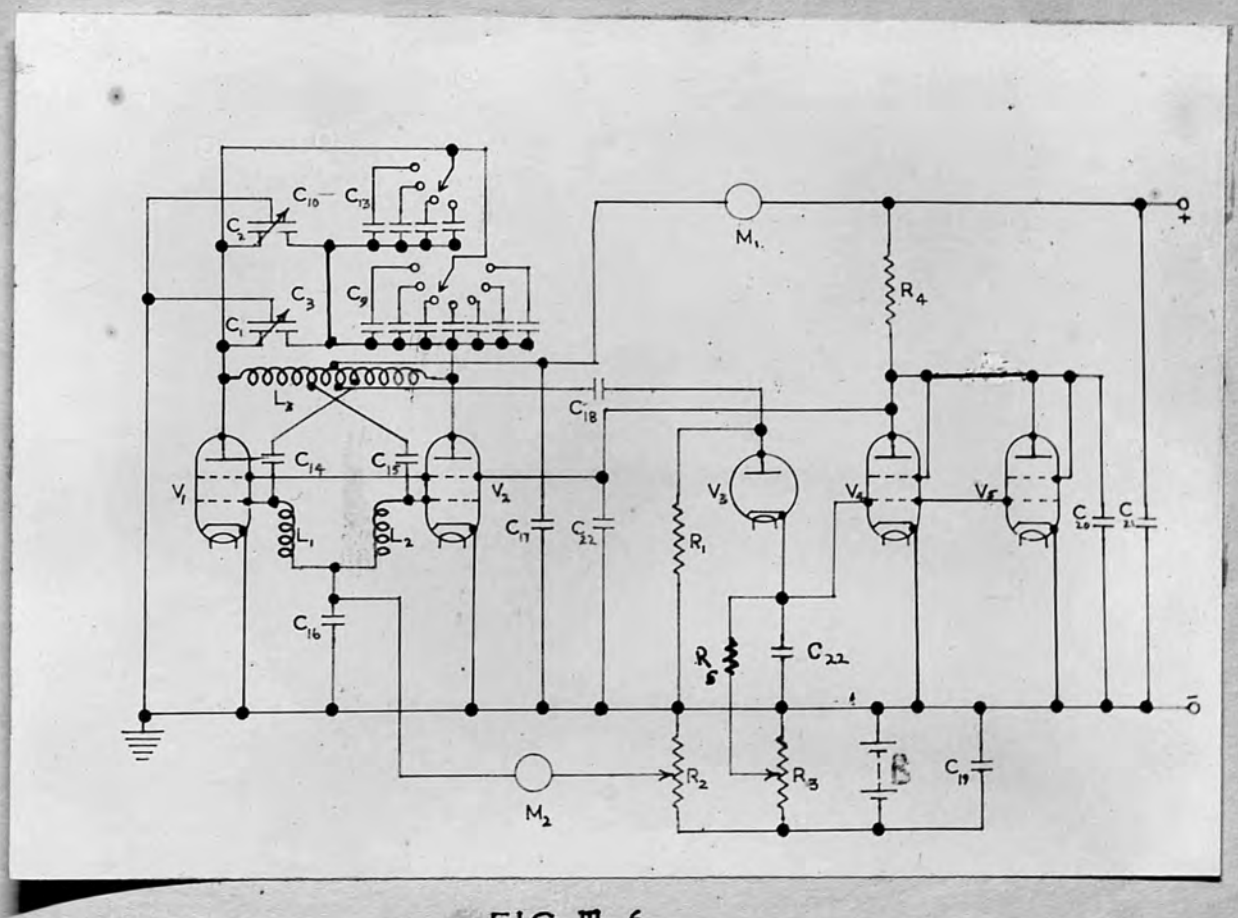

FIG. III. 6.

R_1	500 KΩ	C_1	100pf	C_{14}	·005μF	V_1	6L6G
R_2	10K Ω	C_2	10 pf.	C_{15}	·005μF	V_2	6L6G
R_3	10K Ω	C_3	50pf	C_{16}	1μF	V_3	6H6
R_4	5 K Ω	C_4	100pf	C_{17}	1μF	V_4	6L6G
R_5	500K Ω	C_5	150pf	C_{18}	·002μF	V_5	6L6G
		C_6	200pf	C_{19}	1μF		
		C_7	250pf	C_{20}	0·1μF		
L_1	r.f. choke	C_8	300pf	C_{21}	1μF	B	120v. H.T.
L_2	r.f. choke	C_9	350pf	C_{22}	1μF		
L_3	65 turns C_1	C_{10}	400pf				
		C_{11}	750pf	M_1	0-75ma		
		C_{12}	1000pf	M_2	0-25ma		
		C_{13}	1250pf				

The main tuning capacitor C_1 is of the split stator type with .04 in. electrode spacing. In parallel with it is a smaller split stator capacitor C_2 which provides a fine tuning device. A series of silvered mica condensers C_3-C_{13} can be switched in parallel with C_1 and C_2. The inductor L_3 is one of a series of four plug-in coils, single layer close wound with double cotton covered copper wire 28 gauge on Tufnol formers of various diameters. The frequency of the tuned circuit can thus be smoothly varied over a considerable range. It covers a frequency band of 45 Kc/s to 2000Kc/s. The oscillator valves V_1, V_2 are a pair of beam tetrodes. A variable bias from R_2 affords some control over the wave shape generated.

The amplitude control works as follows. A small amount of r.f. energy is tapped off from the tuning coil, rectified by a diode V_3 and fed on to the signal grids of a pair of beam tetrodes V_4, V_5 running in parallel. This rectified signal varies the anode current of V_4, V_5 and modifies the voltage drop produced by this current in a high wattage resistor R_4. The voltage at the anode end of R_4 is taken back to the screen grids of V_1 and V_2. A variable bias on V_3 from R_3 controls the level of the feedback voltage. The component values are chosen so that a change in voltage across the tuned circuit will produce a change in the screen grid voltage on V_1 and V_2

which is sufficient to counteract the original change.

The two methods of achieving stroboscopic illumination, the Geissler tube and the Kerr cell, are mentioned in Part III, chapter 2.

The circuit used to drive the Geissler tube is shown in Fig.III.8 and is similar to the circuit described by Dye (1932). A simple tuned circuit L C in series with a D.C. voltage is connected through two resistors R_1 and R_2 to the discharge tube. It is inductively coupled to the Hartley tuning circuit and tuned to the same frequency. The coupling is varied so that an A.C. voltage of some 300 volts peak to peak and equal to the D.C. voltage is induced in the circuit. This gives a voltage which varies from 0-600 volts each cycle, and produces one flash per cycle in the discharge tube.

The Geissler tube has been used up to I Mc/s, the rapid deionisation of the discharge necessary at this frequency no doubt being caused by the glass walls of the capillary tube. To overcome this frequency limit a Kerr cell was successfully used to provide stroboscopic illumination. The Kerr cell has been used up to a frequency of over 300 Mc/s (Miers 1936) but few details could be found in the literature describing the use of a cell in this manner. Valuable operating data however may be found in Miers book. The particular cell used was built

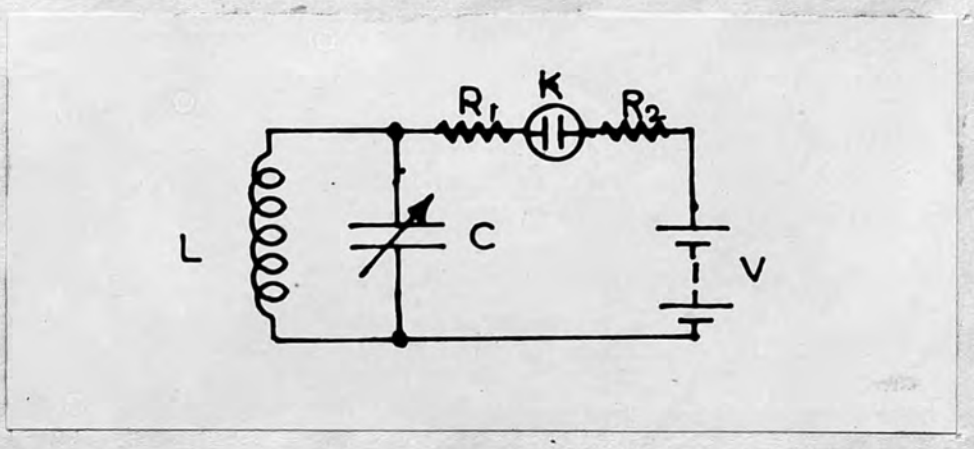

FIG. III.8.

L_1C_1 6 turns

R_1 R_2 10 KΩ.

V 300 v. H.T.

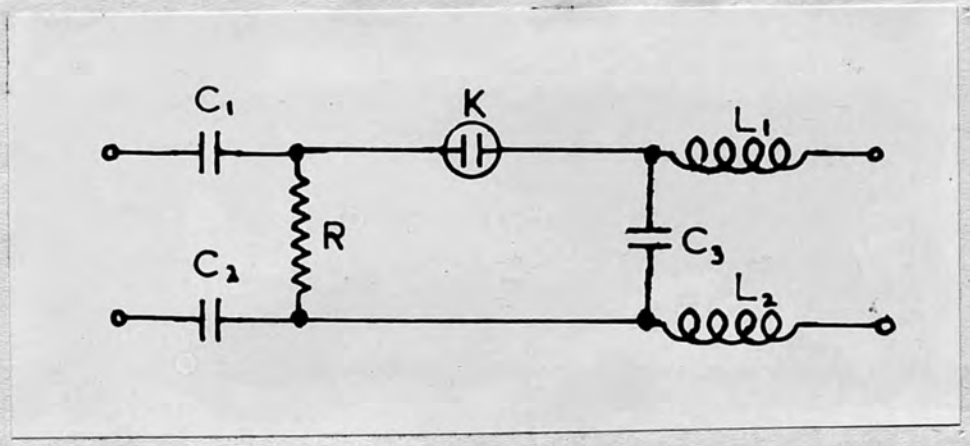

FIG. III.9.

C_1 5000pf

C_2 5000pf

C_3 5000pf

R 1 MΩ

L_1 L_2 r.f. chokes

by T.R.E.Malvern had a breakdown potential of 3½ Kv and required some 2½ Kv to produce a 90° rotation of a beam of plane polarised light passing through it. The first attempts to drive the cell at 100 Kc/s were based on pulse techniques familiar in radar work. A sine wave of a few volts is taken from the oscillator, squared and differentiated to give a sharp pulse. This pulse is then amplified using wide band coupling and ringing chokes. It was found however that at this frequency it was not possible to amplify the pulse beyond some seventy volts and at the same time keep the pulse width less than a microsecond. At higher frequencies the difficulties increased.

Finally, the same principle of using a biased sine wave as in the drive for a Geissler tube was used. The circuit is shown in Fig.III.9. An r.f. voltage of some 800 volts peak to peak taken from across the tuning circuit of the Hartley oscillator is fed through capacitors C_1, C_2 and C_3 to the Kerr cell K. A bias voltage of 1.7 Kv is taken from the E.H.T. power pack and fed through r.f. chokes L_1 and L_2 and a resistor R to the Kerr cell. Thus the path is provided for both the r.f. and the D.C. voltages. The arrangement for the Kerr cell has been used up to 2 Mc/s.

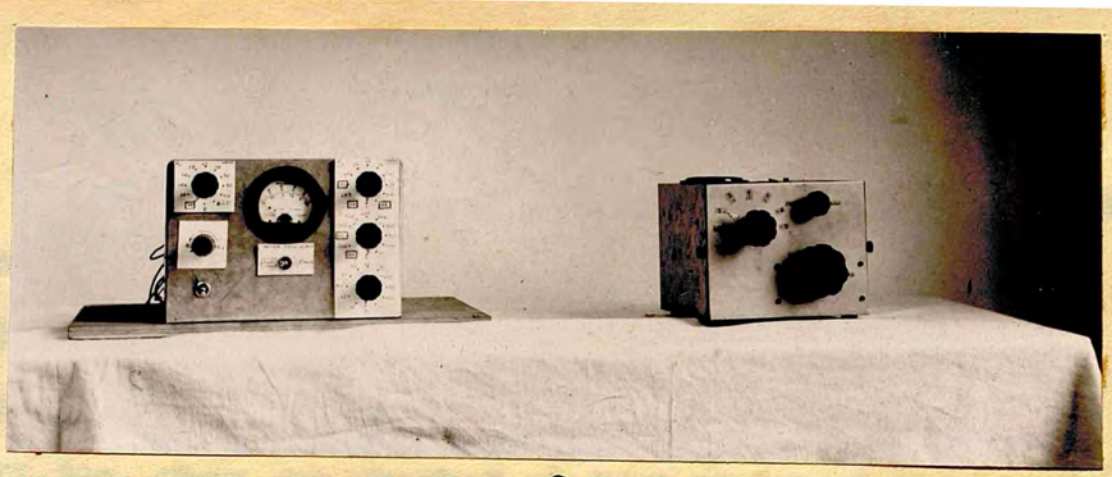

a

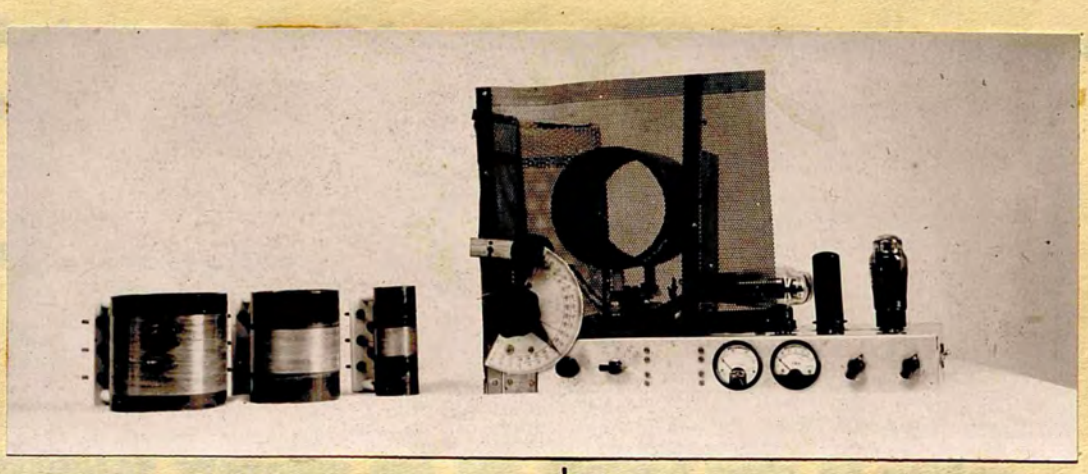

b

FIG. III.10.

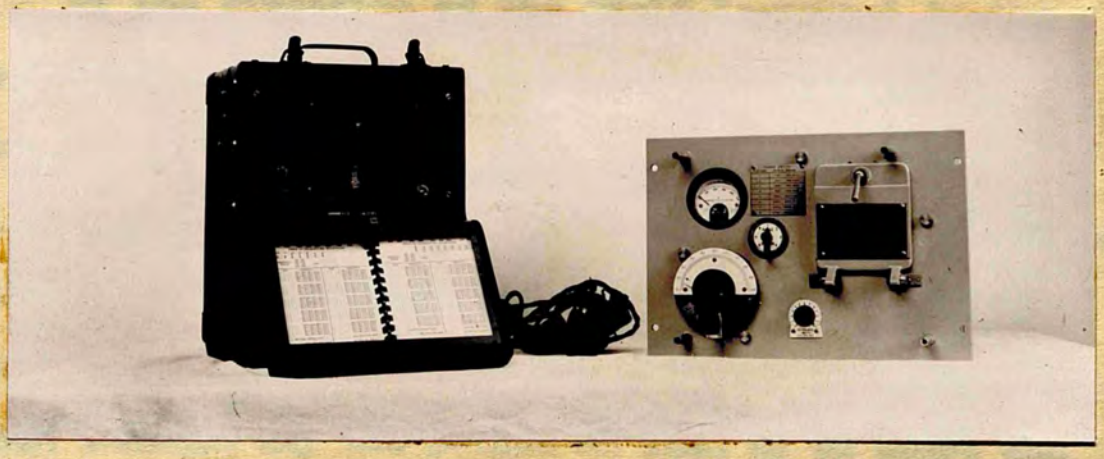

c

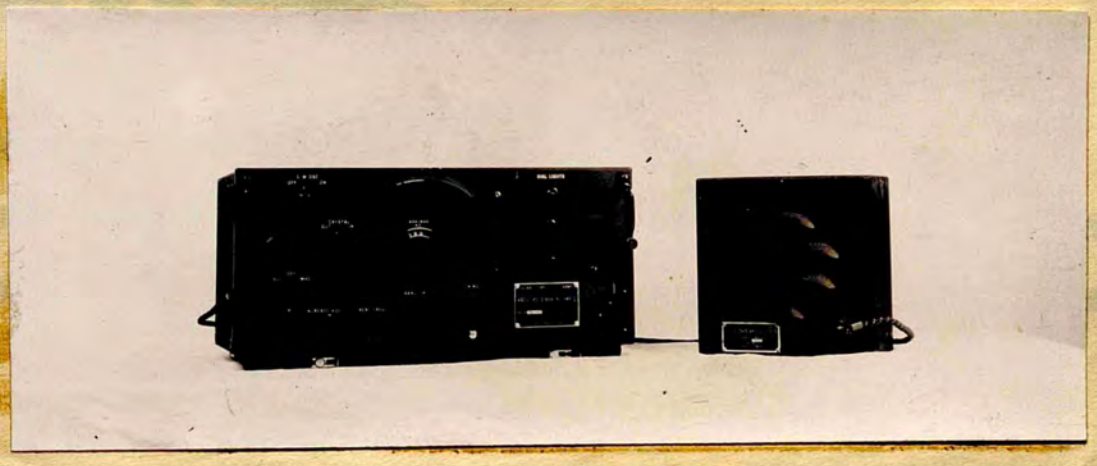

d

The fundamental frequency of any of the oscillators is identified by an absorption wavemeter of Admiralty pattern (Marconi) and the frequency measured by a crystal controlled heterodyne wavemeter of U.S. Army pattern Fig.III.IOc. They are checked against standard frequency transmissions and the B.B.C. transmissions with a communications receiver of U.S. Army pattern (Fig.III.IOd.) These three pieces of equipment were government surplus and had to be overhauled thoroughly before use.

The electrode system used of course depends on the particular vibrator and the desired mode of motion.

If the direction of the field is normal to the surface under examination, then the electrodes must be effectively transparent. They may then take the form of small strips of metal or wire grids or thin silver films. Fortunately an interferometric coating on a polished surface has a resistance of only a few ohms (perhaps 4-5 ohms) between any two points an inch or so apart and so can act as an electrode.

If the field is in other directions than this opaque electrodes such as metal plates, opaque coatings of silver etc. may be used. The r.f. voltage needed to drive the vibrator depends on the external damping of the vibrator.

Varying the distance of one of the electrodes from the vibrator affords some control over the amplitude of the vibrator in initial experiments. The particular electrode systems used will be described in the appropriate sections of Part IV.

CHAPTER 4

THE POLISHING PROCESS

As indicated in Part II Chapter 2 the surface under investigation by multiple beam interferometry must have an approximately plane surface with a high degree of polish.

While natural quartz crystals may posess a high degree of natural polish on many surfaces the quartz vibrators are cut from the natural crystal with diamond impregnated saws, ground to the correct dimensions with abrasive materials and finally etched in hydrofluoric acid. They thus posess a mat surface in the finished state. In order to examine any surface of a vibrator by multiple beam interferometry it must therefore be optically polished.

The polishing process described in this chapter enables almost any quartz vibrator to be given plane poli shed surfaces, flat to at least one wave length of light (usually 5461 A) and when necessary to a twentieth of a wave length. Normally a trade secret, the technique is soon acquired and perfected with practice.

The process of polishing has been discussed by Strong (1946), Twyman (1942) and recen tly in a

comprehensive treatise published by the Revue D'Optique (1949). The method described here was developed to suit the particular problem of polishing finished quartz vibrators with the aid of Mr Menage of the Technical Optics department of Imperial College, London.

Essentially it consists of grinding the surface of the vibrator with a suitable abrasive on a very flat surface, gradually reducing the size of the abrasive, then polishing away the abrasive marks with a polishing medium on a pitch surface.

The flat grinding surface is a circular cast iron lap of either 3 in. or 6 in. diameter with a boss threaded to fit a standard $\frac{1}{2}$ in. Whitworth thread (supplied by Optical MeasuringTools Ltd. Slough). The abrasives are Carborundum and Alexite powders supplied by the Carborundum Manufacturing Co. Manchester. The abrasives are carefully graded in particle size and referred to by numbers as shown in TableIII2. The polishing surface is formed by Brown Swedish Pitch and the polishing medium is Cerium Oxide both supplied by Hopkin and Williams Ltd. London.

The polishing machine on which the laps are mounted is a metallurgical polishing machine made by Cooke, Troughton and Sims of York and is shown in Fig III.II,

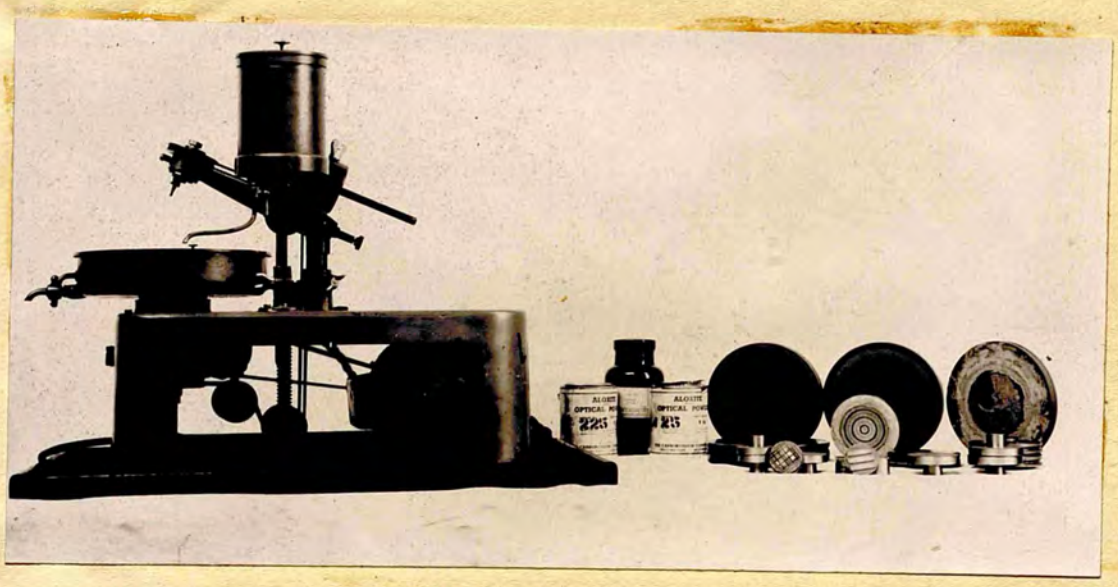

FIG. III.11.

Table III.2

Aloxite and Carborundum Grit

Number	Particle Size
240	50-70 microns
600	9-13 microns

Aloxite Optical Powder

Number	Particle Size
225	22.5 microns
125	12.5 microns
50	5.0 microns

A synchronous motor drives the lap spindle through a reduction gear box by a belt and pulleys. This driving system is modified so that the spindle will run at speeds from 25-250 r.p.m. An 'automatic polishing head' provides an eccentric motion at half lap speed from the lap spindle. This head is only used when large amounts of material have to be removed by rough grinding. A small water tank with a drip feed is provided.

To manipulate the vibrator plates during the process it is necessary to mount them on 'runners'. These are flat brass laps similar to the cast iron laps and made in suitable sizes with diameters ranging in half inch steps from I in. to 4 ins.

The laps and the runners are trued to flatness by grinding three of the same diameter, in pairs, one on the other in cycle rotation. Thus if the three are labelled A, B and C, A is ground on B, then B on C, then C on A and so on. This procedure allows for the fact that the top lap tends to become concave and the bottom one convex during the grinding. The bottom lap is mounted on the machine spindle driven at about 100 r.p.m. and the top lap given a diametral stroke by hand as in Fig. III.12A. A suitable abrasive is 240 carborundum for rough grinding and 600 carborundum for finishing. The resultant surface can be tested for flatness quite accurately by using

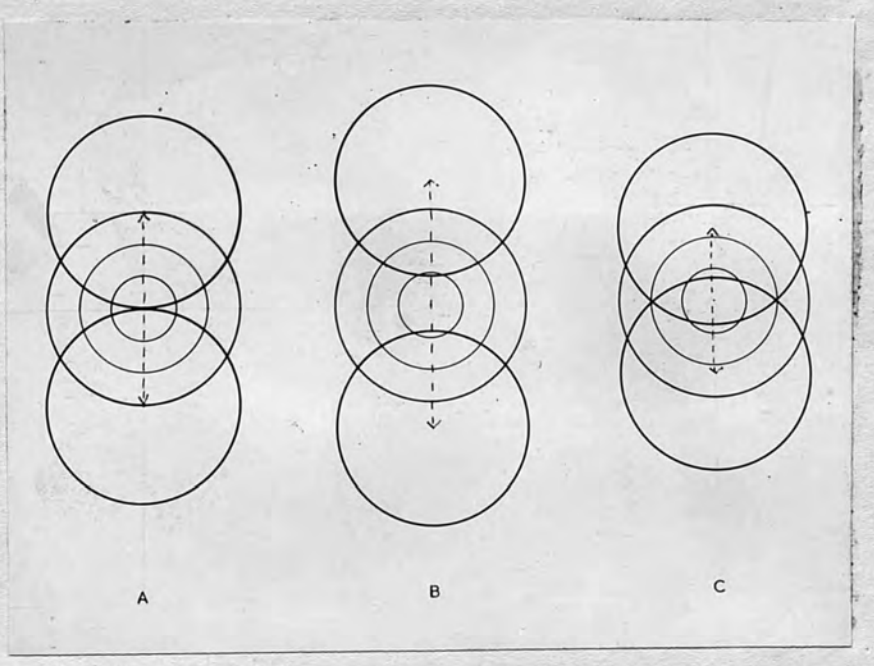

FIG. III.12.

'mechanics blue',a grease base blue dye. The 'blue' is thinly smeared on the surface of one lap,then one of the other laps is rubbed against it,the dye is rubbed off the first lap on to the high spots of the second lap.

The vibrator is fastened down on to the runner with paraffin wax. The wax is melted on to the warm surface of the runner,the vibrator is gently bedded down with the fingers and the whole assembly allowed to cool when the wax sets and hardens. Paraffin wax is very suitable for this purpose because of its high resistance to shear strains and its low melting point. It is necessary for the runner to have a flat surface or the quartz will spring when released after the polishing is completed and lose its figure or flatness.

The grinding of the vibrator is started with 225 Aloxite in water on one of the laps,this grade being suitable for surfacing the usual etched finish of the vibrator. As soon as the surface has a uniform appearance, i t is washed clean of the abrasive,the lap is washed, and the next abrasive 125 Aloxite is used. Grinding with this abrasive continues until the coarser grinding marks of the 225 grade are removed. The gradual change in the surface pitting being visible in the colour of the white light reflected from the surface at grazing

incidence, the colour changing from a reddish hue to white as the pits become smaller. The process is repeated with the final grade 50 Aloxite. Care must be taken with this grade as the particle size is comparable with that of many dust particles which may fall on the lap surface and scratch the surface of the quartz. Cleanliness is essential and no trace of the previous abrasive must be present in the following stage.

The next part of the process is that of the polishing. Whereas the grinding process may be considered to be a controlled fracturing of the surface of the specimen by sharp hard grains of abrasive on a tough substrate, the polishing process is one of planing away the rough surface by the sharp edges of an abrasive which is uniformly distributed in a firm but yielding medium.

The pitch plays an essential part in the polishing process. As the viscosity of the pitch changes very rapidly with temperature it must be correctly tempered. First of all the pitch is warmed and filtered through several layers of fine cheese cloth to remove any foreign bodies. A little is chilled to room temperature on one of the laps and then gently crushed between the teeth. If the pitch flows first then splinters, the temper is

correct. If it only flows, it is too soft, while if it only splinters it is too hard. Soft pitch is hardened by boiling; hard pitch is softened by adding black wax or turpentine. When tempered the pitch is poured into a dish lined with brown paper and allowed to set.

To prepare a pitch pad, pieces of pitch are chipped out of the dish with a knife and laid on the surface of a brass runner which is then gently warmed until the pitch begins to flow. It can then be formed into a pad which should be about ½ inch thick and equal in diameter to the surface of the specimen. The surface of the pitch is then flattened by warming the lap and pressing a flat piece of plate glass against the pitch. A paste of cerium oxide and water is used to stop the pitch sticking to the glass. Second and third warmings and pressings using cerium oxide and water between the pitch and the glass will give a nice flat prepared surface. When the edges are trimmed with a knife the pad is ready for use.

The runner carrying the pitch pad is then mounted on the polishing spindle which is rotated at a speed of some 40 r.p.m. Three equidistant circular grooves are cut in the surface of the pitch with a sharp pointed knife, a process known as ringing. The specimen is then manually given a diametral stroke across the lap as in Fig.III.12.

using cerium oxide and water as the polishing medium.

The pad gradually assumes the figure of the ground surface and begins to polish it. In about an hour , a partial polish appears on the quartz and a fine network of cracks known as the 'undergrey'can be seen. As the polishing proceeds the operater can feel the specimen contacting the pad more and more closely,the specimen running smoothly over the surface of the pitch,heat from the friction between the two surfaces keeping the top layer of the pitch soft. If the spindle speed is too fast,contact is less intimate the pitch hardens, and the specimen runs roughly over the pitch surface, the precise lap speed depending on the effective diameter of the specimen.

The figure of the quartz can now be tested against a reference glass flat using standard reflection Fizeau fringes. The three rings and the regular stroke produce a 'regular figure'. That is ,the surface will be either convex or concave about the centre of the specimen. A convex surface is corrected by ringing the outside of the pad and increasing the length of the stroke as in Fig.III.12B. A concave surface by ringing the centre of the pad and decreasing the stroke Fig.III.12C. The rings gradually fill up as the pitch flows during the polishing process.

The polishing continues until the surface of the

quartz has a high lustre and is as flat as is required. The whole process of polishing the ground surface takes some eight hours since quartz is so hard, but the figuring of the surface is made relatively easy by the good thermal conductivity of the quartz.

The ease with which a vibrator can be flattened depends on its size and shape. Circular and square plates are relatively easy, while rectangular plates are more difficult. If they are 'blocked' by mounting scrap pieces of similar thickness around them, then edges and corners which normally tend to wear down will be protected. The thickness of the vibrator should not be less than about I mm. and not less than about I/I5 of the other dimensions for convenience.

In some of the experiments described in Part IV it was necessary to have small holes drilled in the optical flat. Holes from 0.050 in. to 0.I in. can be speedily drilled in glass by the following technique. A copper tube of size slightly less than that of the finished hole is turned in the lath so that a sharp edge is formed at one end. It is then used as a drill using I20 grit crushed diamond bort in turpentine oil to do the cutting.

PART IV

EXPERIMENTAL RESULTS

CHAPTER I

MULTIPLE BEAM FIZEAU FRINGES

The original experiments with multiple beam Fizeau fringes on the surface of quartz vibrators were carried out on four rectangular X cut bars of form shown in Fig.IV.IA. The two major surfaces of each bar had been polished and examined for any possible surface structure with the multiple beam fringes as it had been conjectured at the time that the frequency ageing phenomenon may be due to a surface change of some nature. No large scale structure had however been observed on any of the polished surfaces.

An attempt was made to observe the surface of the vibrator with the multiple beam fringes whilst it was vibrating at some suitable frequency.

The surface observed was given an interferometric silver coating with a reflecting coefficient of about 90 per cent. A very light silvering was then evaporated on to the opposite face of the vibrator. The high reflecting face was then placed resting in contact with a similarly coated optical flat. Electrical connection was made to the lightly silvered surface by spring contact and to the silver layer on the optical flat in the same way. Thus the silver films provided the electrode system, the field

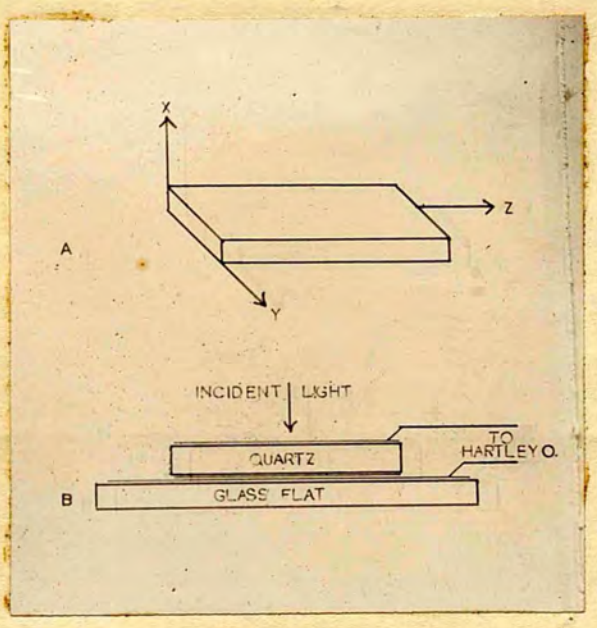

FIG. IV.1.

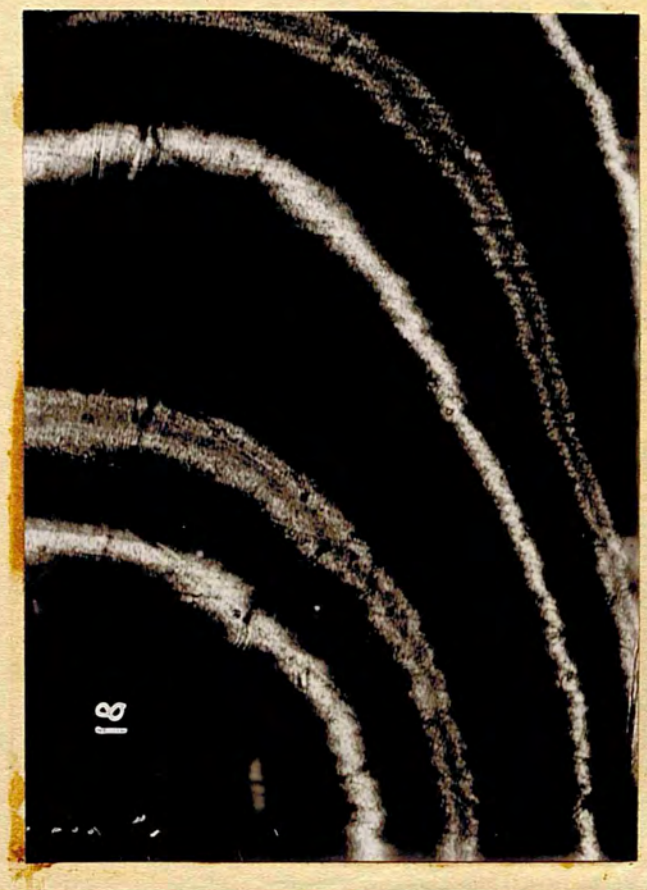

1

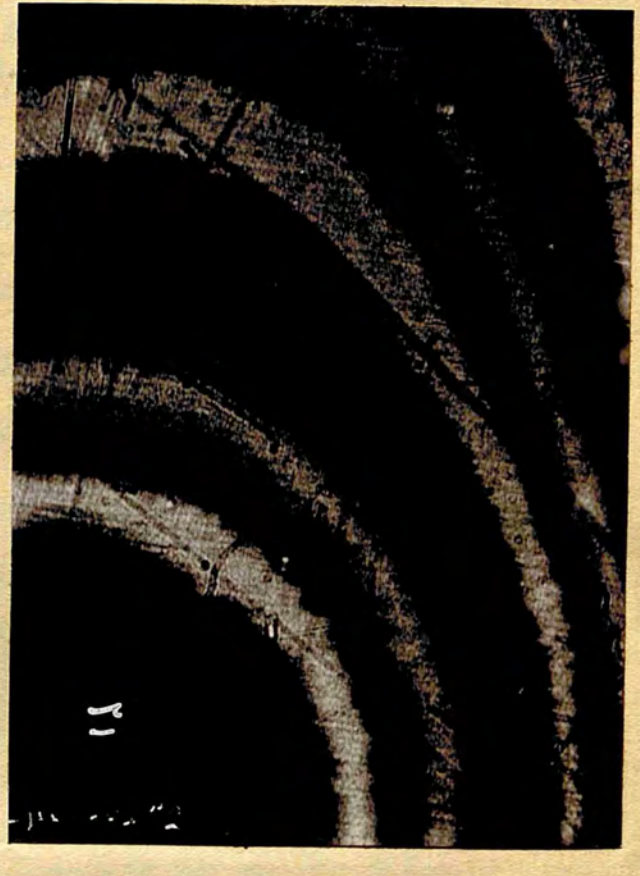

2

being along the X axis of the bar.

Leads were taken from the electrodes to a conventional Hartley oscillator with some 300 volts on the anode of the valve, the vibrator being connected in parallel with the tuning circuit. Fig.IV.IB shows the experimental arrangement.

When illuminated under the correct conditions, sharp multiple beam Fizeau fringes were formed in the air gap between the two interferometric coatings, the shape of the fringes depending on the figure on the polished surface of the vibrator and on the particular fringe dispersion obtained. The air gap could be adjusted by light manual pressure on the vibrator to give a suitable fringe dispersion.

Two of the first pictures taken are shown in Plates I and 2 (x I5). These show the fringes produced by th e filtered green and yellow radiation of a mercury arc. In Plate I the vibrator, and hence the fringes, are at rest. As the frequency of the Hartley oscillator was smoothly varied, the vibrator was resonated at some frequency, and the fringes broadened as in Plate 2. Normally the least motion in the multiple beam system will disturb the fringes and so when it was seen that the oscillatory motion of the vibrator only broadened the existing fringe pattern locally it was realised that

the oscillating fringes may well form a new pattern characteristic of the motion of the whole vibrator.

The magnification was reduced and in Plate 3 (x 7) the rest fringes of the green and yellow mercury lines on the stationary vibrator are seen, the ends of the vibrator being cut off by the particular microscope stage used. In Plate 4 oscillating fringes over the surface of the resonating vibrator are seen. The local broadening of the fringes can be seen clearly. Plate 5 shows the vibrator resonating at a different frequency the fringes, this time formed by just the green line, take a form reminiscent of that taken by the vibrating string in the classical experiment of Melde, revealing nodes and antinodes along their length. The local amplitudes vary from zero to a maximum of some 750 Angstroms. The extreme sharpness of the fringes at their nodes is remarkable and even with the relatively imperfect surfaces used an amplitude of about $\frac{1}{100}$, or some 56 Anstroms, can be detected. Scratches on the surface of the quartz may be seen in the pictures as fine black lines running across the fringes. The broader white lines seen on Plate 5 are scratches on the silver produced while the dispersion was being adjusted.

Further experiment showed the remarkable

3

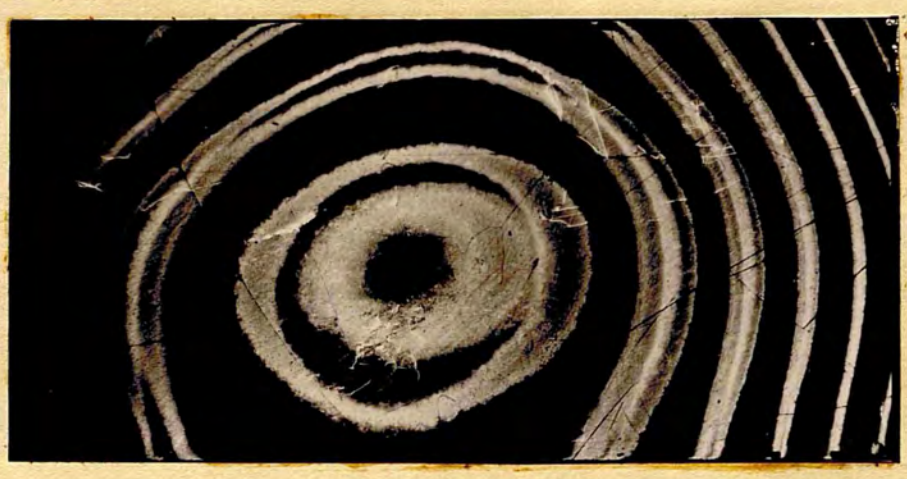

4

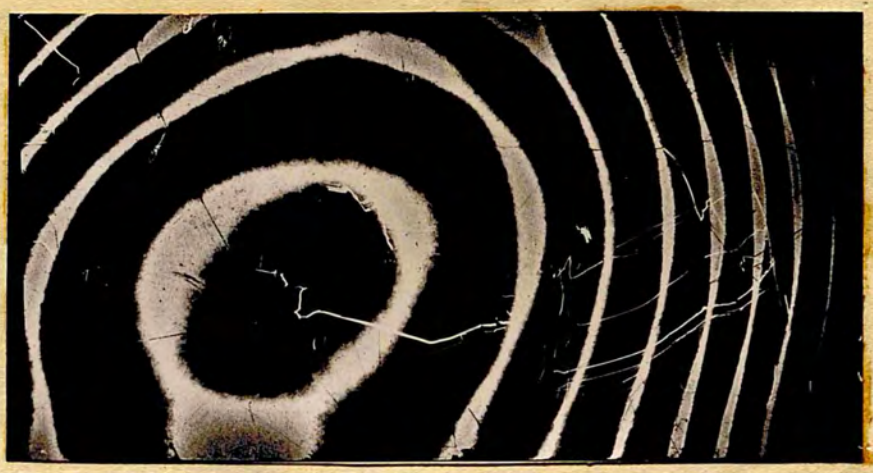

5

adaptability of these fringes to the study of a vibrating surface. Plates 6,7 and 8 show different fringe dispersions over the same surface of the same vibrator for one resonant frequency, the dispersion increasing from Plate 6 to Plate 8. Here the top silver film electrode was dispensed with and a strip of tinfoil, visible on some of the pictures was used instead. It was found that if the top silver film electrode was thick enough not to be too fragile, it scattered the parallel beam incident on the interferometer and reduced the fringe sharpness. It can be seen that the low dispersion of Plate 8 provides a much more complete picture of the surface deformation, i.e. of the nodal and anti nodal regions, than do the higher dispersions although the latter are more sensitive.

In Plate 9 the amplitude of vibration is sufficiently large to cause overlapping of adjacent fringes and it can be seen that the bright edge of the fringe appears to retain its identity even in this case. Plate 10 shows a crossed fringe picture produced by a double exposure, the fringe dispersion in one exposure being at right angles to that in the other. This crossing gives a fuller picture of the surface deformation and the nodal regions than a single

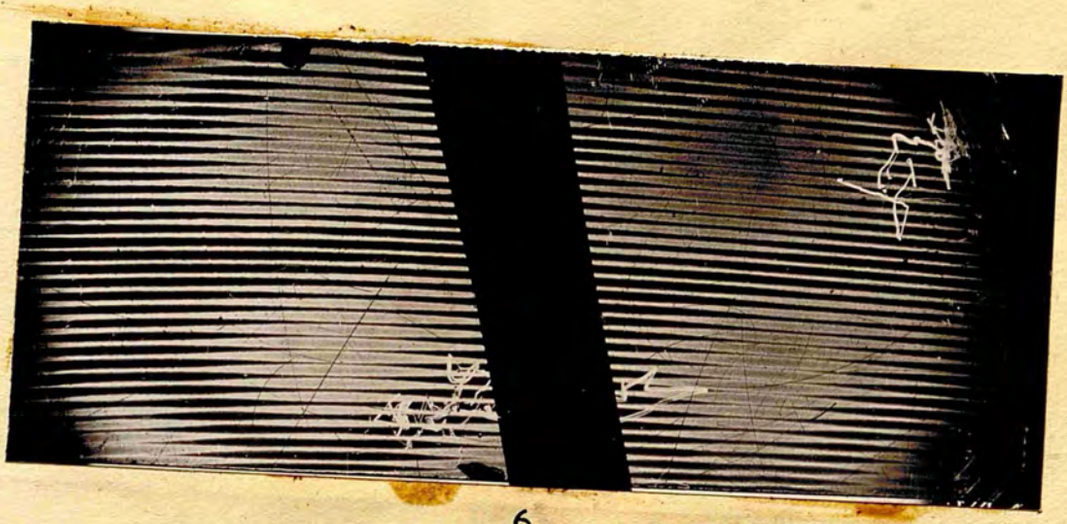

6

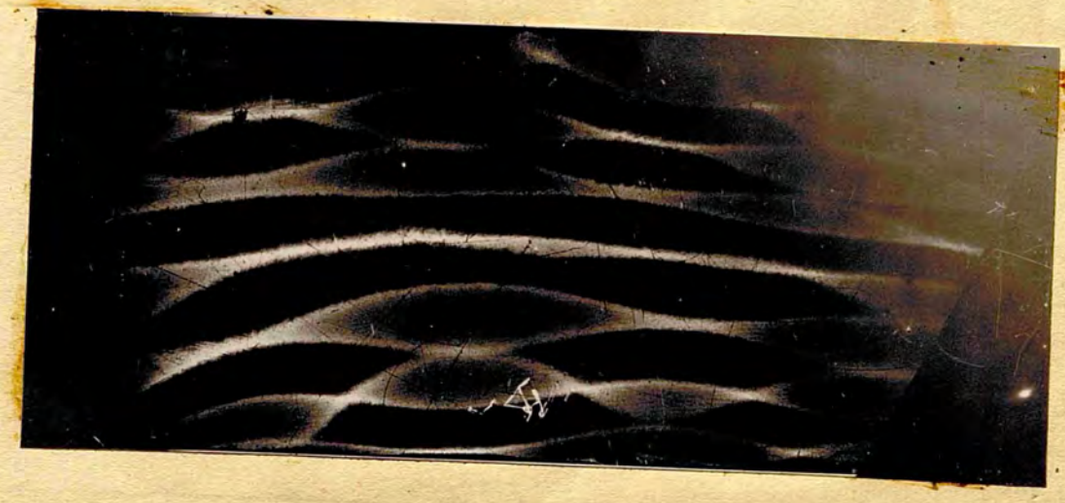

7

8

9

10

dispersion, as well as providing visual evidence that the oscillation pattern does not depend on the direction of the fringe dispersion.

About this time a survey of the literature had revealed the earlier interferometric and other work on the motion of quartz vibrators. It was seen that the advantages possessed by the multiple beam methods over the two beam methods lay in the sharpness of the multiple beam fringes as discussed in Part II Chapter 2.

In Plate II (x 7) are shown the oscillating multiple beam fringes under optimum conditions. The vibrator was a rectangular GT cut crystal designed to run at 100 Kc/s, the dimensions being 32.9 x 30.5 x 1.2 mm. (illustrated in Fig.I.2.). It was fully polished on both major surfaces by a commercial firm one side being flat to a wavelength of green light, the other side only being flat to about ten wavelengths and being approximately parallel to the first side. The flattest face was coated with a silver film of high reflecting coefficient, about 95 per cent, and matched against a similarly coated optical flat. The top electrode was a rather coarse wire grid which can be seen running across the picture. The frequency was about 3 Mc/s and the mode of vibration appears to be a flexural type. However at this time no

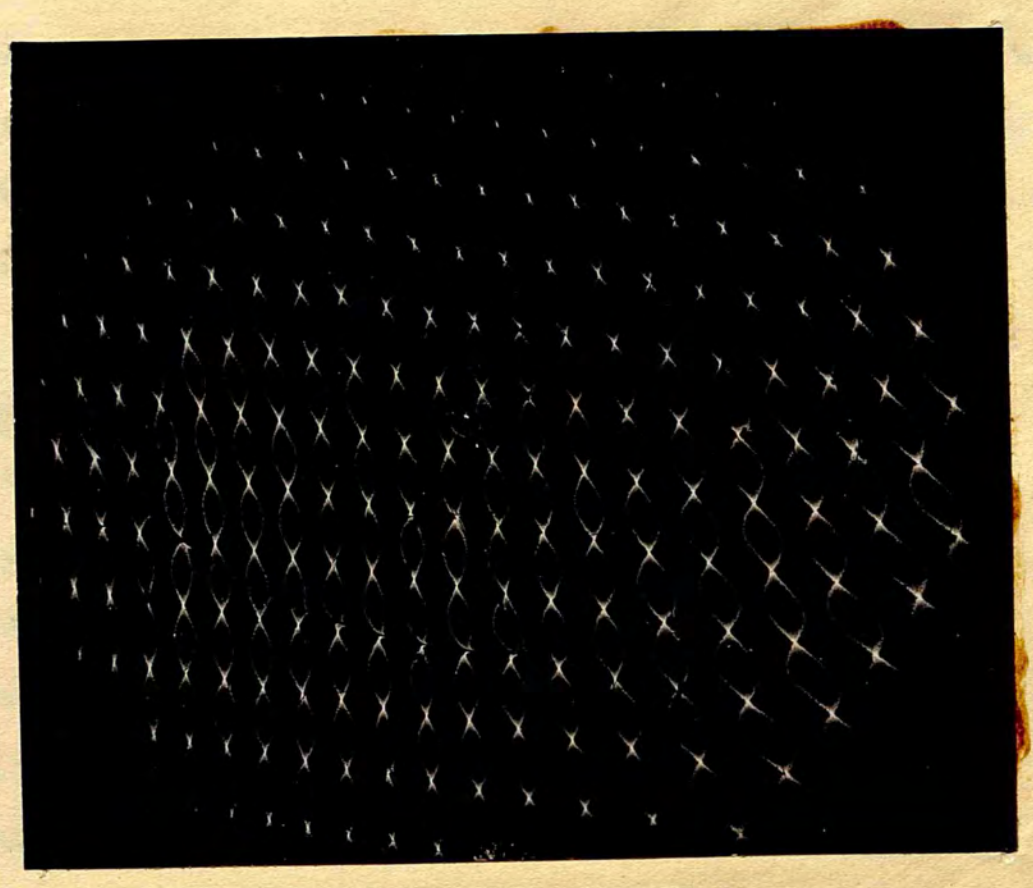

11

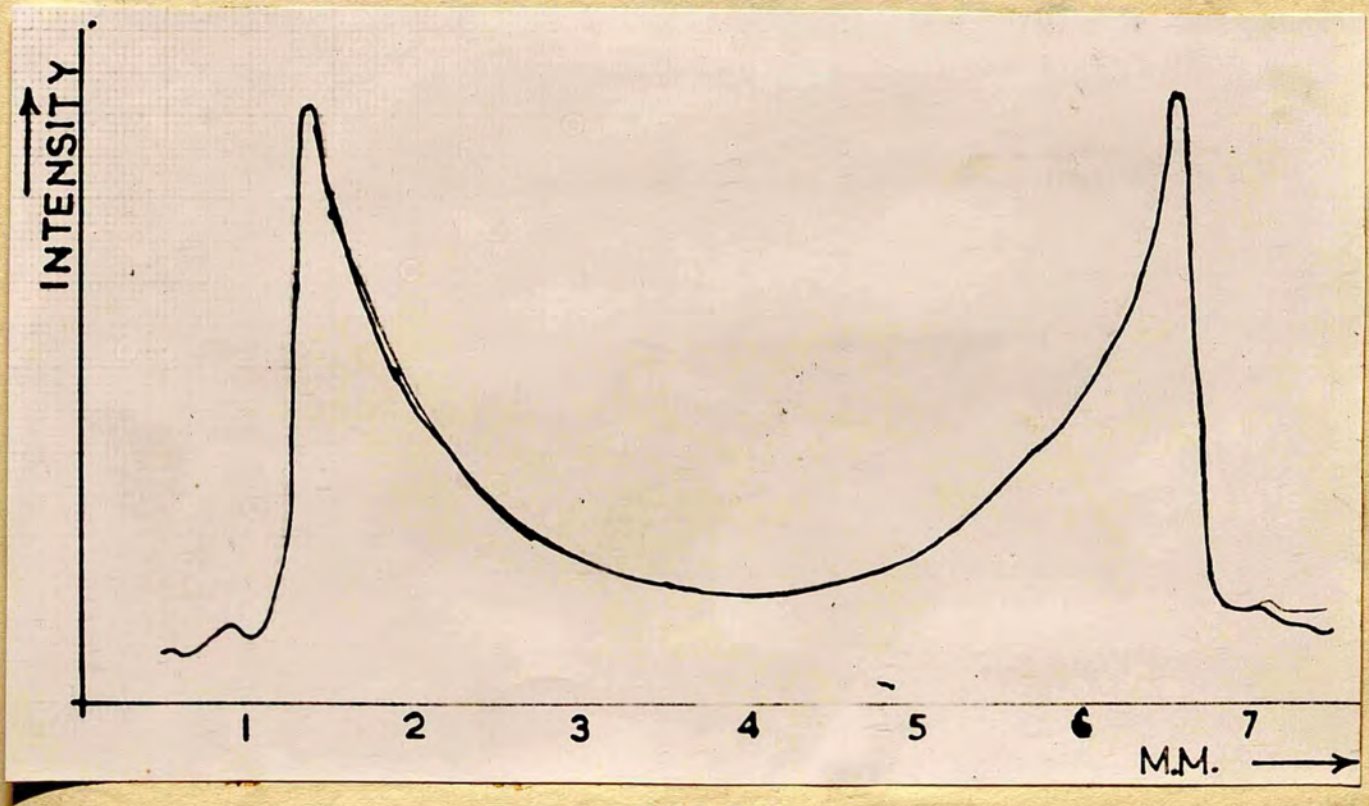

FIG. V. 2.

frequency measuring equipment was available and the waveform of the Hartley oscillator was so poor that no reliable information on the frequency or mode of vibration could be obtained.

A typical microphotometer trace taken across one of the fringe loops is shown in Fig.IV.2. The steep drop of intensity from the peaks and the assymetry of each peak can be seen. It was found that the peaks decreased in sharpness as the reflecting coeff icient decreased, but owing to the difficulty of making accurate microphotometer measurements a precise investigation of this point was not made.

In the reflected system the fringes given with reflecting coefficients of 90 per cent or greater disappear when the vibrator is resonated with an amplitude similar to that in any of the previous plates. The reason for this has been discussed in Part II Chapter 2. The reflecting coefficient of the interferometric coatings was therefore reduced and at a reflecting coefficient of 70 per cent on both surfaces the fringes could still be seen when oscillating. After the publication of Holden's results an experiment was made under opti mum conditions with silver films of low absorption and a

reflecting coefficient of 80 per cent. Plate I2 shows the rest fringes and Plate I3 shows the oscillating fringes when the surface was given a piston like motion of small amplitude. The fringe sharpness, about I/IO of an order, and the visibility are both quite good. Their inten sity distribution is similar but opposite to that of the transmitted system in that the oscillating fringes have a dark edge which may be observed to retain its identity when the amplitude of vibration is large enough to cause overlapping of adjacent fringes. These fringes have been used in the laboratory to examine opaque bodies such as metal crystals in vibration.

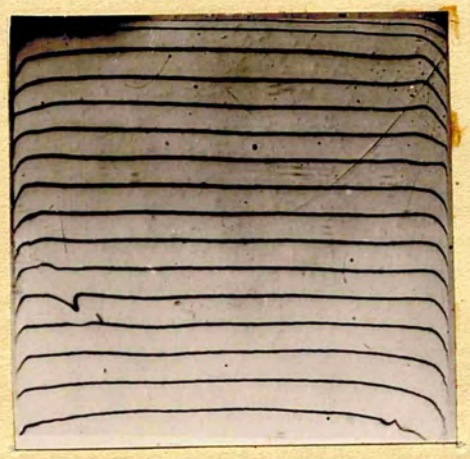

12

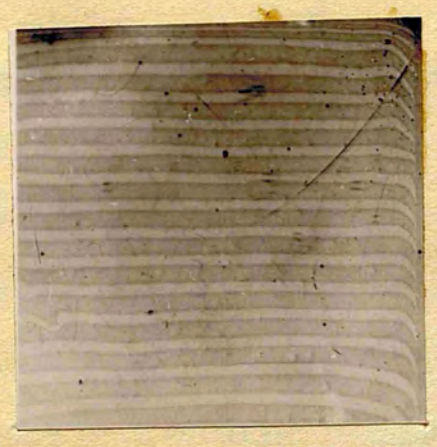

13

CHAPTER 2

MULTIPLE BEAM FRINGES OF EQUAL CHROMATIC ORDER

When the multiple beam fringes of equal chromatic order are used to examine a vibrating surface they behave in a similar manner to the multiple beam Fizeau fringes.

The vibrator used was the X cut bar shown in the previous plates arranged as in Fig.IV.I. and the mode of vibration was that shown in Plate 6. Illumination was by a carbon arc, the magnification on the spectrograph slit was (x 7) and the spectrograph used was a constant deviation instrument with a dispersion of 60 Angstroms/mm at the photographic plate. The figures are enlarged (x 3½) from the plate.

Plate I4 shows the transmitted fringe system at rest and Plate I5 shows the appearance of the system when the vibrator was resonated. It can be seen that the fringes broaden out where the slit crosses those parts of the surface which are vibrating. These fringes show the amplitude along the particular line section chosen for examination as discussed in Part II Chapter 2.

The reflected fringe system is shown, in Plate I6 at rest and in Plate I7 oscillating. The reflected

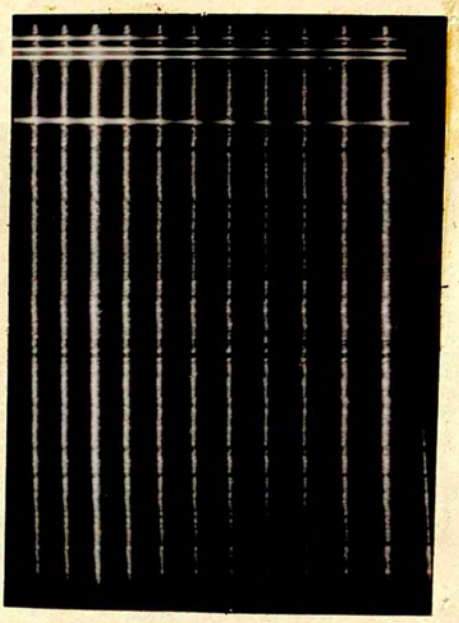

14

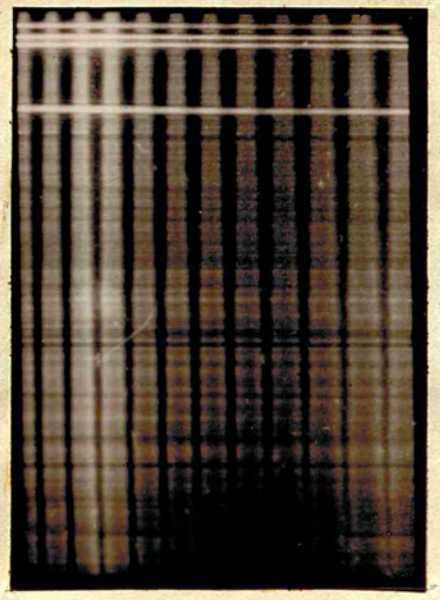

15

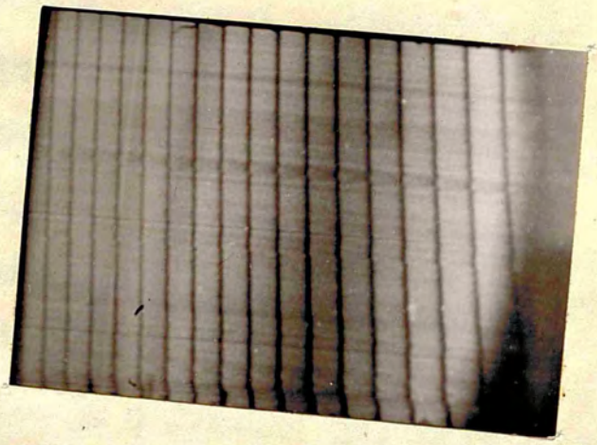

16

17

system was produced with the same silverings as were used for the transmitted system,i.e. about 90 per cent, and consequently the visibility of the reflected system in oscillation is rather poor. From a practical point of view the fringes of equal chromatic order are not suitable for mapping out the motion of a whole surface and are best reserved for examining small amplitudes at chosen points eg. near a nodal line.

The horizontal marks on both sets of plates are due to dirt on the spectrograph slit. The variation of exposure across th e fringes due to the non uniform chromatic response of the photographic plate,etc.,has been corrected in the printing process.

CHAPTER 3

MULTIPLE BEAM FRINGES WITH LARGE INTERFEROMETRIC GAPS

The extension of the technique to large interferometric gaps was then attempted. The quartz vibrator used was the GT cut crystal of Plate II. The vibrator was clamped at a nodal region in the centre by two pairs of spring loaded phosphor bronze pins as shown in Fig.IV.3. This is the usual form of support when the crystal is driven in the fundamental face shear mode of 100 Kc/s. A circular opaque spot of silver 5 mm. in diameter was evaporated on to the centre of each major face, then both faces received an interferometric coating of silver with a reflecting coefficient of 80 per cent. Electrical connection to the interferometric film at the opaque spot was made by the clamping jig.

Multiple beam Fizeau fringes were produced between the two silvered faces of the vibrator. The large interferometric gap caused experimental difficulties. The resolving power of such an interferometer is equivalent to a Fabry Perot interferometer with the same separation and is some 200,00. Consequently the high pressure arc was replaced by the inductance stabilised vacuum arc mentioned in Part III Chapter 2. The collimation was also critical with this large gap.

The vibrator was run as an oscillator at parallel resonance in the Pierce circuit described in Part III Chapter 3. Plate IB shows the rest fringes over just less than one half of the vibrator surface, part of the surface being masked by the support. The fringes are quite sharp and are double due to the natural birefringence of the quartz. Plate I9 shows the oscillating fringes when the vibrator was set into oscillation. The nature of the fringe broadening is quite different from that seen previously in the surface deformation experiments as in Plate II. A typical microphotometer trace across a pair of the fringes is shown in Fig. IV.4. It can be seen that the fringes have a square topped intensity distribution. The broadening is about a third of the distance between orders. It is due not only to a change in interferometric gap but also to a change in the optical constants of the vibrator under stress. Unfortunately the vibrator was shattered by overstressing soon after this experiment so no work on the separation of the effects causing the fringe broadening was done. It was thought that the velocities of the moving surfaces of the vibrator may, by producing a Doppler effect in the frequency of the incident light beam, contribute to the broadening of the fringe. However a calculation showed that

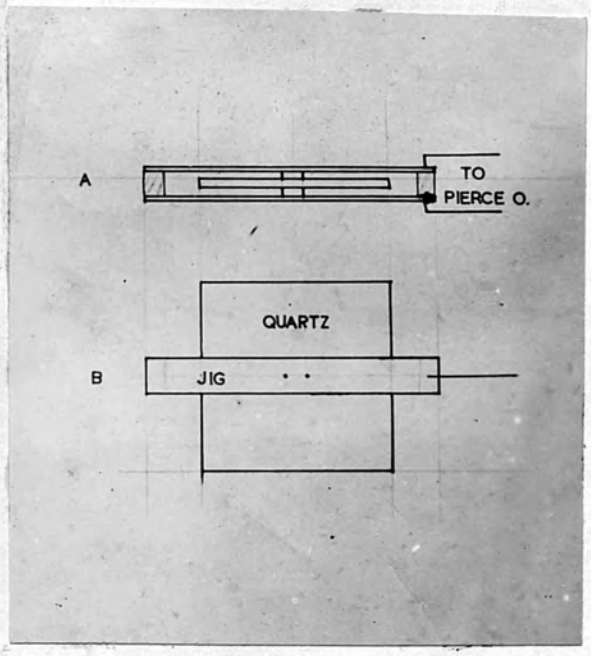

FIG. V. 3.

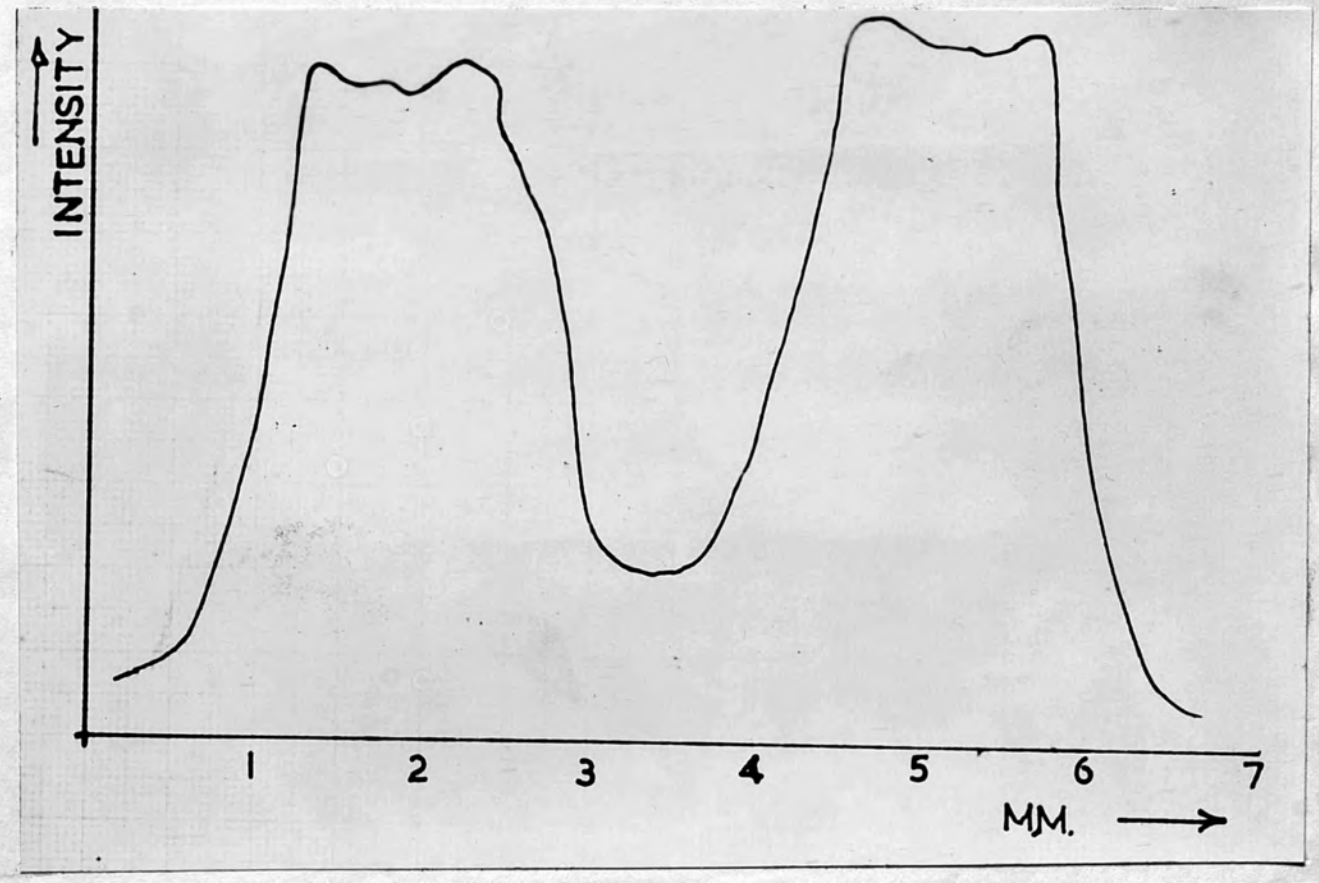

FIG. V. 4.

18

19

at a frequency of 100 Kc/s and a maximum fringe amplitude of two orders, say 5000 A, the velocity of the surface is only about 16 cm/sec. and therefore Doppler effects are ruled out. The acceleration of the surface however reaches remarkably high values. With the above figures the maximum acceleration is about 2×10^{7} cm.sec^{-2}.

A combination of this type of oscillating fringe with the surface type oscillating fringes should provide a useful method of investigating the dynamic optical properties of crystals and their dependence on the stress relations inside the crystal.

Fringes of equal chromatic order cannot be practically used with such large interferometric gaps because of the enormous dispersive power that would be required in the spectrograph.

CHAPTER IV

STROBOSCOPIC PICTURES

The picture of a vibrating surface revealed by multiple beam fringes is thus fairly complete in that the deformation of the surface at any point is clearly seen. Continuous illumination however cannot reveal the relative phase of different regions of a vibrating surface. To examine the phase, the stroboscopic devices described in Part III have been used.

Plate 20 shows an area of the surface of one of the four X cut bars resonating at about 650 Kc/s under normal continuous illumination. The multiple beam fringes were formed in the usual manner and the oscillatory circuit was the push pull Hartley described in Part III. The electrodes were formed by the silver film and a wire grid placed above the vibrator. Plate 21 shows the vibrator under stroboscopic illumination from the Geisler tube (Part III) driven from the Hartley oscillator.

Because of the feeble intensity of illumination from the discharge tube, the interferometric coatings were chosen to have a reflecting coefficient of some 80 per cent the resultant exposure times being of th e order of 30 seconds on the fast plates. The period of illumination was made to coincide with the maximum

20

21

22

deformation of the surface, where the velocity of displacement was a minimum, and so the effect of the finite duration of the light pulse was minimised. However the duration of the light pulse does give the fringe a slight wing.

Plate 22 shows the vibration when the illumination occurs at the opposite extreme of the vibration to that shown in Plate 21. This was done by tuning in the crystal from the other side of the resonance pont.

In spite of the reduction in the reflecting coefficient of the silver film the fringes are quite sharp.

In Plate 23 another fringe dispersion shows the same vibrator under continuous illumination at a different frequency, the amplitude of vibration being greater than in the previous set of plates. The reflecting coefficient of the films was increased to about 90 per cent and the exposures were of the order of 5 mins. on fast plates. Plates 24 and 25 show the strobe fringes at two slightly different amplitudes of vibration. Plate 26 shows the rest fringes and the strobe fringes superimposed by means of a double exposure and reveals the true nodal regions as those where the strobe and rest fringes coincide. In other regions it can be seen that they do

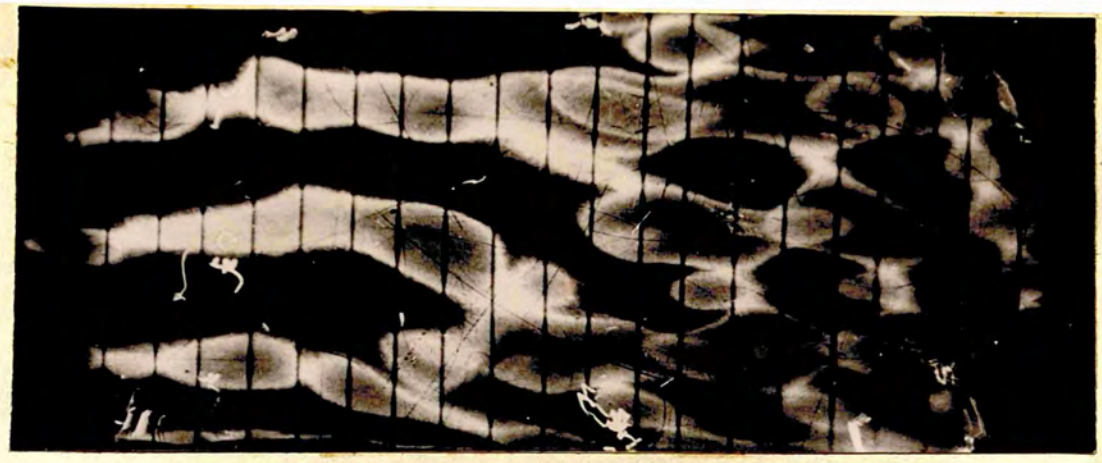

23

24

25

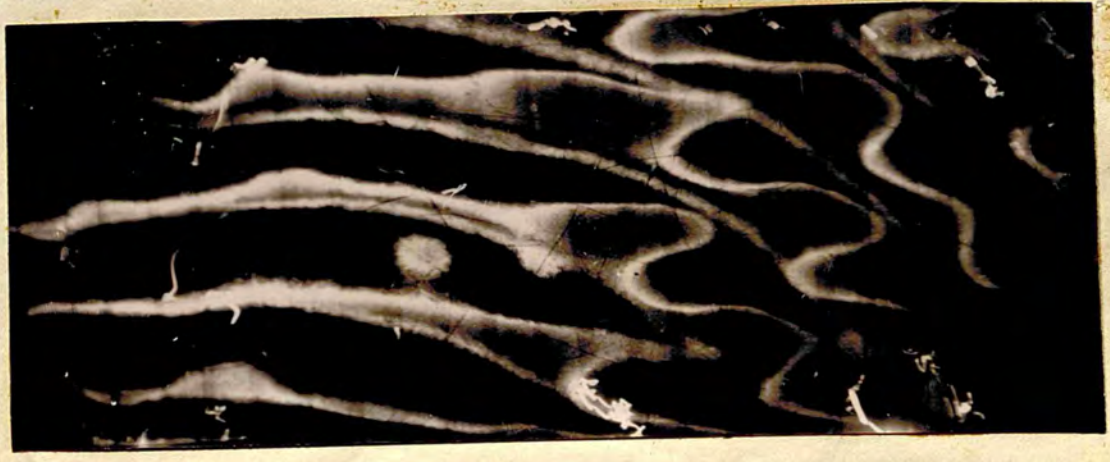

26

not coincide and here there is some small residual motion.

The maximum frequency of operation of the Geisler tube was found to be about I Mc/s. The Kerr cell can be used at much higher frequencies. The strobe fringes produced with its help are similar to those produced with the Geisler tube. With the Kerr cell, the amount of light available is greater as the high pressure arc is used, and the silverings can be heavier. It can thus be used to observe the phase of vibration with the silverings normally used under continuous illumination.

CHAPTER V

DOUBLE INTERFEROMETER

The multiple beam Fizeau system was extended to the simultaneous observation of the displacement of two opposite parallel surfaces of a vibrator.

The vibrator used was one of Dye's original X cut discs loaned by the National Physical Laboratory. The two major surfaces of the disc were optically flat and approximately parallel. They were both given an interferometric coating of silver with a reflecting coefficient of 85 per cent. Two similarly coated optical flats were then matched one against each side of the vibrator as shown in Fig.IV.4. The silver coatings acted as electrodes and the vibrator was resonated with the push pull Hartley oscillator.

Fringes were formed with the mercury green line over the top and the bottom surface of the disc, and the fringe direction of one set arranged to run nearly at right angles to that of the other, the dispersion of each set being similar. Light is then transmitted through the double interferometer only where one set of fringes crosses the other set. Plate 27 shows the fringe system at rest. The camera lens had sufficient depth of focus to image both sets of fringes at once.

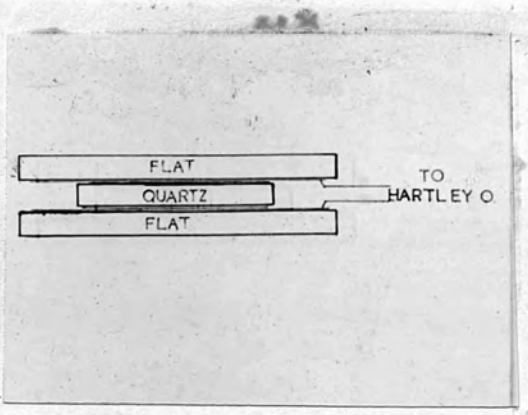

FIG. IV.4.

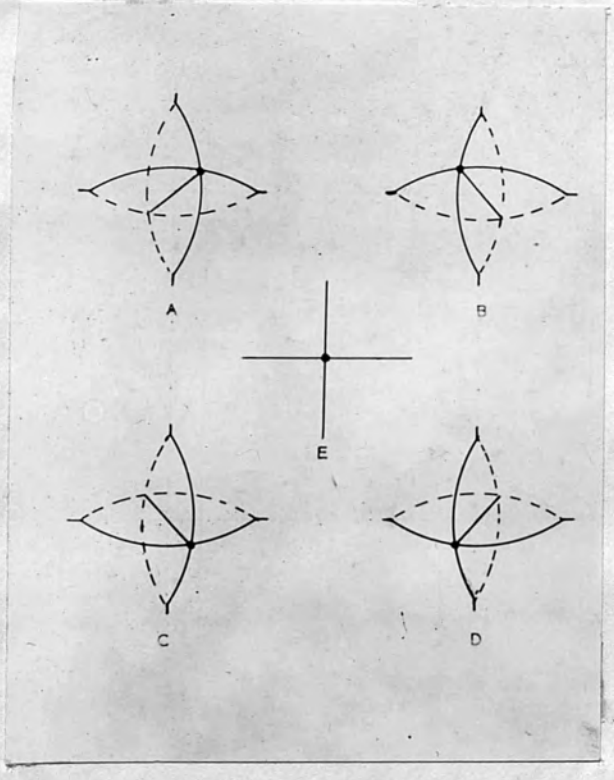

FIG. IV.5.

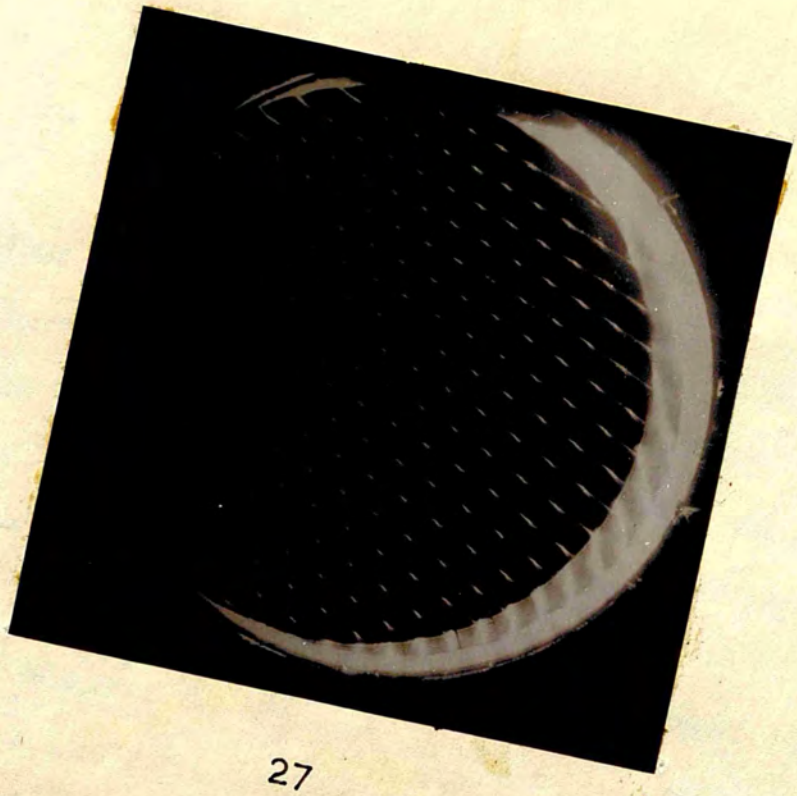

27

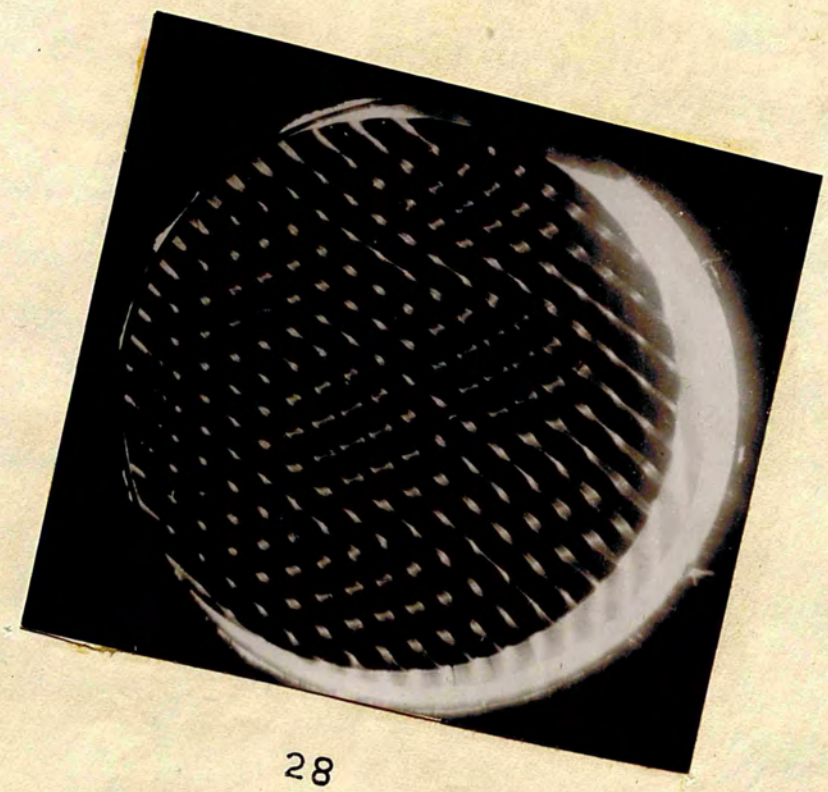

28

88B

The fringes on the interferometer nearer to the camera are visible in between the intersections due to light scattered from the first interferometer. The direction in which the two sets of fringes run is shown by the arrows.

When the vibrator was resonated, the fringes in each interferometer broadened and the bright intersections traced out paths which were not parallel to either set of fringes but fell between these two directions as shown in Plate 28.

The series of drawings in Fig.IV.5 shows that the result is similar to that of the well known Lissajou figures in that the path traced by the intersections of a pair of fringes depends on the relative motion of each fringe.

From the direction of the intersection path and a knowledge of the wedge direction in each interferometer it is possible to determine if the two surfaces are in or out of phase.

Stroboscopic illumination reveals the extreme position of the intersection.

CHAPTER VI

STROBE EFFECT AND STRAIN PICTURES

Some experiments were done at this time to see if the strain patterns observable in polarised light with quartz vibrators could be seen at the same time as the interference system on one of the surfaces. During the experiments a novel effect was observed which will be described first.

The vibrator used for the experiment was the Dye X cut disc of the previous chapter. One face was given an interferometric coating of silver of reflecting coefficient 90 per cent and matched against a similarly coated optical flat in the usual manner to produce multiple beam Fizeau fringes with green mercury light. Then polaroids were placed either side of the interferometric arrangement. The polaroids were crossed, and the Z axis of the vibrator which lies in the plane of the disc was arranged to run at 45° to the direction of the incident plane polarised beam. The vibrator was resonated with the push pull Hartley oscillator at 60.2 Kc/s in the fundamental longitudinal mode along a diameter. Plate 29 shows the oscillating fringes with the analysing polaroid out of the optical system.

As the analyser was rotated it was found

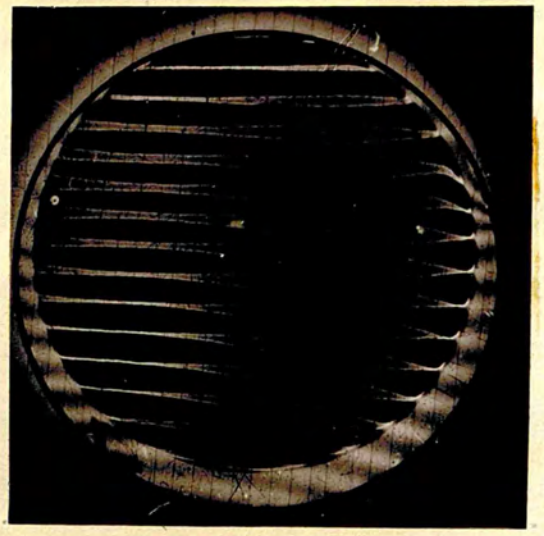

29

30

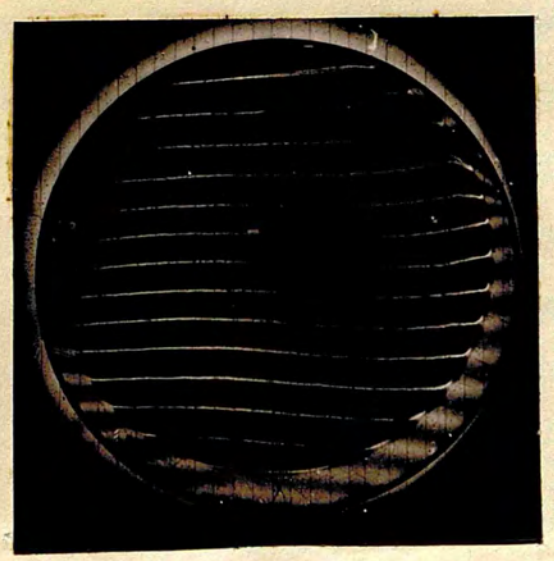

31

possible to cut out each side of the oscillating fringes in turn to give a stroboscopic effect. Thus Plate 30 shows the lower part of the fringes when the polaroids are near the crossed position and Plate 31 shows the upper part of the fringe when the polaroids are near the parallel position. The actual position of the analyser depends on the amplitude of the vibration and the wave length of the illumination.

The effect was observed also for the other fundamental longitudinal mode in the plane of the disc at 97.3 Kc/s, at the third harmonic of 69.2 Kc/s at 206.8 Kc/s, and for a thickness mode at 1850 Kc/s and at some other frequencies in a complex form, fractional sections of the oscillating fringes being cut out.

The effect was not observed in reflection.

Near each position of the analyser, which gave this effect, it is possible to find another position for the analyser where the stress patterns are seen in the crystal for large amplit udes of vibration. Plate 32 shows the vibrator under continuous illumination resonating at a frequency of 217.4 Kc/s. The analyser is adjusted to show a dark strain pattern superimposed on the fringe system.

It is also possible to produce a bright stain

32

pattern superimposed on the fringe system for the other position of the analyser.

Because of the general complexity of the problem of transmission of polarised light through a stressed quartz crystal no further work was done on this problem.

CHAPTER VII

SLIP AND FRACTURE IN QUARTZ

During an experiment with one of the four X cut bars, it was observed that the multiple beam Fizeau fringes running across the surface were not continuous and closer examination revealed abrupt discontinuities in the fringes similar to those seen in Mica (Tolansky 1948) showing that there were steps on the surface of the crystal. These steps can be seen in Plate 33 (x 7) covering part of the bar, the fringes being formed with the green and yellow mercury lines. In Plate 34 (x 20) they are shown enlarged, the fringes being formed with unfiltered mercury radiation and in Plate 35 it can be seen, using a suitable dispersion and the green mercury line, that there are two sets of steps making angles of some 35° and 50° with the length of the plate which is the approximate direction of the Z axis. The steps in each set are nearly parallel in direction and the angles they make with the length of the plate vary by a few degrees. Most step heights are some 500 Angstroms. The other side of this vibrator is shown in Plate 37 (x 7) and is seen to have several deep hollows of irregular shape. There are also a few steps on a much smaller scale than

33

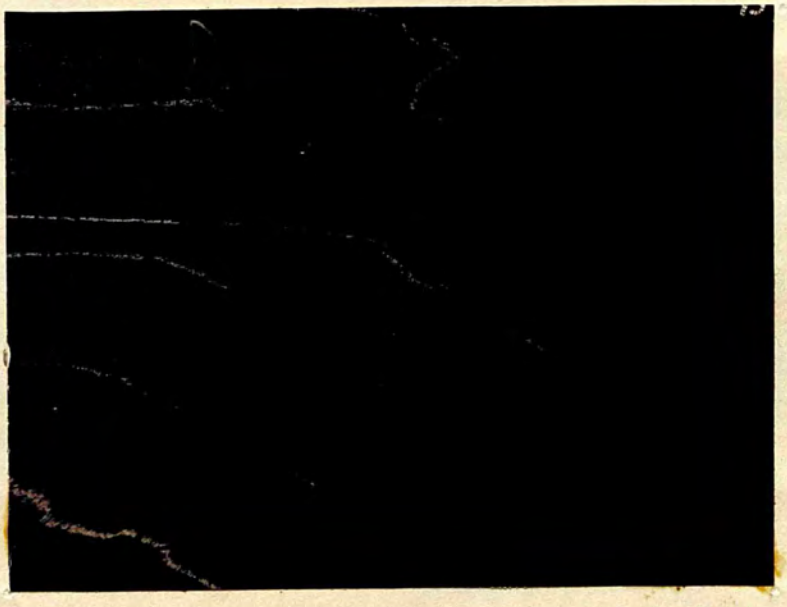

34

35

36

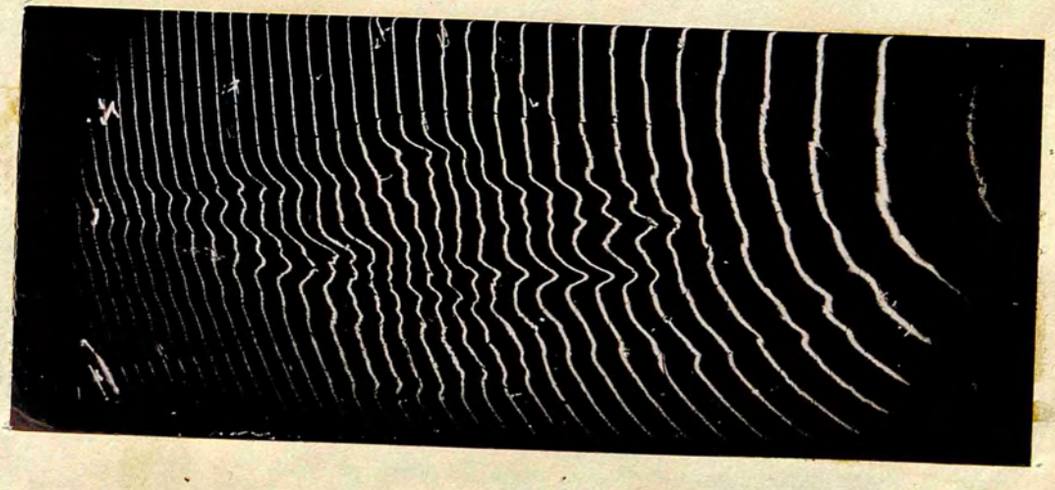

37

those on the opposite face. Plate 36 (x 40) shows some of the steps on the surface of Plate 33 photographed by out of focus microscopy, a technique often used in the laboratory to show up small features under the ordinary microscope.

About the same time one of the other X cut bars was broken by overstressing and it shattered along definite directions similar to those shown by the steps. Plate 38 shows part of the crystal immediately after shattering. The directions of the major fractures are at some 36° to the length of the bar.

The shattering of quartz vibrators due to overstressing is well known and has been mentioned by Booth and Vigoureux (1950) and others. In particular Nomoto (1949) has shown that cracks in X cut quartz plates which have been overstressed run at 38.2° and 36.5° (±2.5°) to the Z axis. These directions correspond, he says, to the projection of the minor rhombohedral surfaces of quartz on to the plane normal to the X axis.

An attempt was made to see if the vibrator with the steps in it would break at the same amplitude that shattered the other vibrator but it did not, and the power available in excess of that value at the time failed to break it.

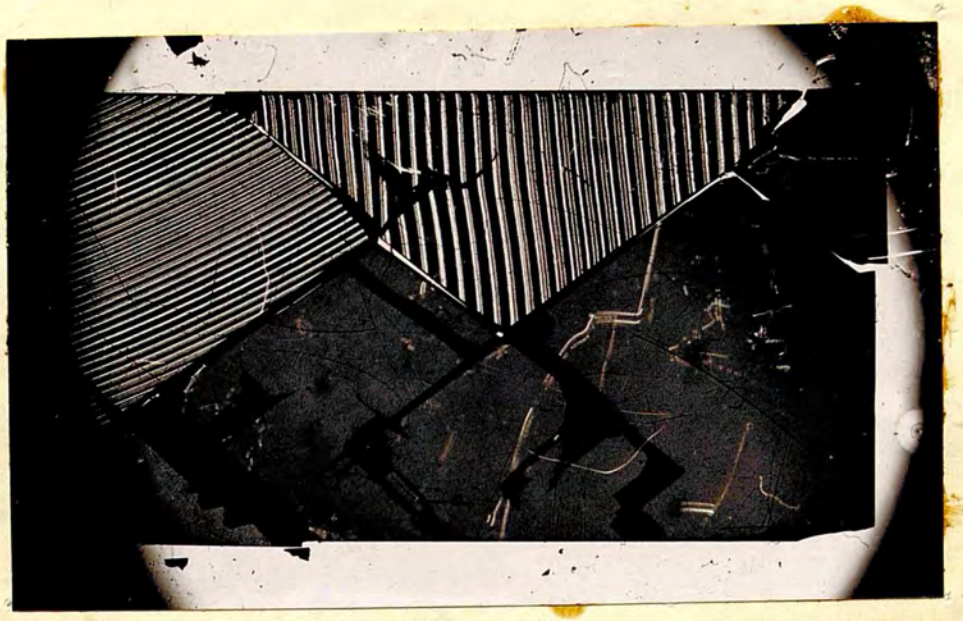

38

39

40

Plate 39 shows the vibrator resonating and it can be seen that the amplitude is less in the step region than elsewhere. This may indicate local damping but of course could have been due to other factors than the presence of steps.

As the four X cut bars were all well polished, although the figure was poor, at the start of the experiments, and had indeed been examined for surface structure, it is thought that the steps may have been produced at some time unobserved during the experiment by vibrational stresses. An explanation is possible in terms of a rearrangement of the macro structure of the crystal following crystallographic slip. The precise nature of the slip mechanism has not yet been revealed and this is the only noticeable example of this effect that has yet occurred. Steps have been seen on one other crystal during a repolishing process but they were only few over a small area of some two or three mm. square. The crystal did not show optical twinning. Tests for electrical twinning would have involved etching the surface and was not thought desirable until further examples occurred.

The appearance of these steps indicated that the mechanism of fracture in overstressed quartz vibrators may be that crystallographic slip occurs first and that

rupture then takes place along the lines of slip. If slip can occur without subsequent rupture it may account for the well known frequency ageing effect in quartz vibrators as a small change in the physical dimensions or the elastic properties could change the frequency by the necessary amount of a few parts in 10^7 or 10^9.

Few experiments have been performed with vibrators running at large amplitudes for they invariably end in the destruction of a carefully polished specimen. When a vibrator is resonated with a small amplitude of vibration (less that 2,000 Angstroms) the oscillating fringes are broadened more or less symmetrically with respect to the rest fringes. An example of this is shown in Plate 40 taken with a double exposure to superimpose the oscillating and the rest fringe.

However in the few experiments in which the quartz vibrator was resonated at a large amplitudes (greater than 20,000 Angstroms), then the fringes moved bodily to show that the surface was bending as a whole. An example of this can be seen at lower amplitudes in the fundamental face shear mode of 100 Kc/s GT vibrators, At even larger amplitudes, the fringes blur and frequently an audio frequency note is heard before the vibrator shatters.

CHAPTER VIII

SOME MODES OF MOTION IN BAR AND RING VIBRATORS AND MEASUREMENT OF THE AMPLITUDE OF VIBRATION

I. A quartz bar has been examined for some of the types of motion associated with quartz vibrators. The bar had its length along the X axis and was of rectangular cross section as illustrated in Fig.I.2. The dimensions were 50mm x 9mm x 9mm. the 9mm edges having a slight bevel.

The face normal to the Y axis was given an interferometric coating of silver with a reflecting coef ficient of about 90 per cent and matched against a similarly coated optical flat.

The electrodes were formed by the silver film and a wire grid supported above the bar,or alternatively by a pair of brass cubes placed one at each end of the bar. Thus the electric field could be directed along the Y axis or the X axis of the bar. Fig.IV.6. shows the jig used to hold the flat and bar,the wire grid being conveniently raised or lowered by means of a screw arrangement affording a measure of control over the amplitude of the vibrator. The electrodes were connected across the circuit of the push pull Hartley oscillator.

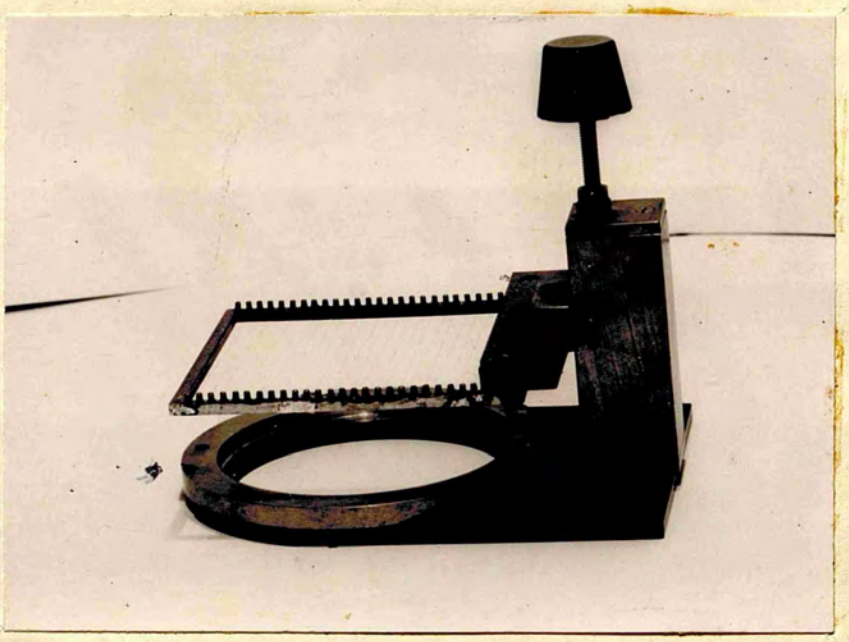

FIG. V.6.

With the field along either the Y axis or the X axis a large number of response patterns were observed. Some of these patterns are presented in this chapter. All the plates in this section are magnified X 2.

With the field along the X axis the flexural modes of even order along the length in the XY plane were easily excited. Plates 43,45, and 47 show the even order modes consisting of the 4th,6th and 8th order modes respectively. Plate 49 shows the 8th order mode of Plate 47 at a larger amplitude. With the field along the Y axis the odd order flexure modes along the length in the XY plane were observed. They are shown in Plates 42,44,46 and 48 comprising the 3rd,5th,7th and 9th order modes respectively.

The frequencies of vibration for each order are given in table IV.1

Table IV.1

Plate No.	42	43	44	45	46	47	48
Frequency Kc/s	60.0	88.5	118.1	148.2	178.1	208.7	239.8

They form an approximately harmonic series and the calculated frequency of vibration 73 Kc/s. of the 3rd order mode,the lowest order observed,is a little above the experimental value of 60 Kc/s. This is to be expected, for as the wavelength of the vibration becomes comparable

with the smaller dimensions of the bar, the waves are no longer purely flexural but become transverse as suggested by Doerffler (1930) and discussed in Meising (1947). Thus the frequencies of vibration of the higher order flexure modes in this bar are proportional to the order of the vibration and not to the square of the order.

Again, with the field along the X axis, the longitudinal modes along the length of the bar were easily excited. Plates 50, 51, 52, 53 and 54 show these modes for the 1st, 3rd, 5th and 7th orders respectively. The frequencies of vibration are given in Table IV.2.

Table IV.2.

Plate No.	50	51	52	53
Frequency Ke/s	50.4	150.3	244.5	311.0

Again they form an approximately harmonic series. The calculated frequency of vibration 50.3 Ke/s agrees well with the observed frequency of 50.4 Ke/s. The frequencies of the higher order modes are a little below the calculated frequencies.

The difference between the two types of motion can be seen clearly. The flexural type is seen by the direct motion and is distinguished by a regularity in amplitude at each antinodal region. The longitudinal

50

51

52

53

type is seen by virtue of the lateral contraction associated with the longitudinal motion, the contraction taking place as expected at the regions of stress and nodes of displacement for the lengthwise motion. The assymetry of the pattern is probably due to the difference between the elastic constants measured in different directions of the vibrator.

The sensitivity of the multiple beam Fizeau fringe system is clearly demonstrated here, for the lateral contraction due to a longitudinal motion is that which Osterburg (1934) was trying to observe when he built his refracting interferometer, the two beam system having failed to show the motion.

The identification of these two types of motion was of value when the ring form of vibrator, described in the next section, was examined.

Several other series of patterns were obtained but their relation to specific modes of motion is not clear. However most of the patterns show a marked symmetry and so are shown in Plates 55-63, the frequencies being listed in Table IV.3.

Table IV.3.

Plate No.	55	56	57	58	59
Frequency Kc/s.	336.8	334.0	336.4	336.4	374.0

55

56

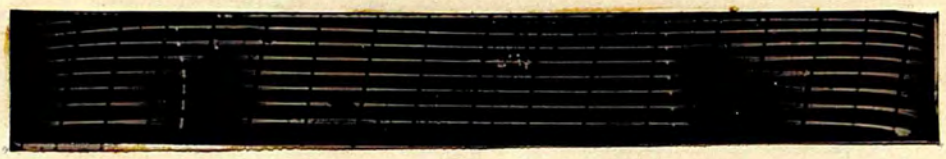

57

59

60

61

62

Table IV.3.(cont.)

Plate No.	60	61	62	63
Frequency Kc/s	377.4	413.5	336.8	354.2

Plate 55 is a high dispersion picture at a large amplitude of the mode seen in Plate 62. Plate 58 illustrates how the oscillating fringes may overlap and yet remain quite distinct. Plate 63 shows many different local amplitudes of vibration.

2. A ring form of vibrator has also been examined. It consists of a hollow cylindrical quartz ring whose axis is in the direction of the Z axis of the quartz crystal as illustrated in Fig.I.2. There are three electric axes, X, in the plane of the ring.

This particular form of ring was designed by Essen (1938) to act as a new form of frequency and time standard. It was designed to run in a longitudinal compressional mode of vibration round the circumference. An alternating electrical field applied to coaxial ring electrodes should produce alternating circumferential strains varying in amplitude round the ring and of opposite sign 60° degrees apart. At the appropriate frequency the quartz resonates and considerations of symmetry indicate that the vibration of the lowest

frequency in the desired mode should be one having nodes at the six regions where the planes containing the Z axis and the three X axes cut the ring. At three of these nodes the ring can be supported. The mean circumference of the ring should remain constant and there should be periodic changes in the cross sectional dimensions of the ring.

Three of the experimental rings were loaned to the laboratory by the National Physical Laboratory. Their dimensions are given in Table IV.4. together with the frequency of the desired mode calculated from the empirical formula given by Essen (1938)

$$f = \frac{2{\cdot}67}{a} \cdot 10^5 \text{ c/sec.}$$

where a = mean radius of ring in cms.

The rings were given an interferometric coating of silver with a reflecting coefficient of some 90 per cent on one of the Z faces and matched against silvered flats in the usual manner. The electrodes were coaxial brass rings of such a diameter as to leave a small air gap between the electrode and the vibrator. Cardboard masks were used to prevent the elctrodes short circuiting across the interferometric coating on the flat. The electrodes were coupled inductively to the push pull Hartley oscillator by a coil of some 500 turns and 2ins. diameter.

Table IV.4

Outside Diameter cms.	Thickness along X cms.	Thickness along Z cms	a cms.	f Kg/s
6.238	0.872	0.706	2.683	99.6
5.800	0.816	1.058	2.492	107.2
5.300	0.514	0.949	1.40	192.8

Plate 64 shows ring I resonating at 99.0 Kc/s. Plates 65 and 66 show ring 2 resonating at 105.0 and 105.9 Kc/s respectively. Plate 67 shows ring 3 resonating at 191 Kc/s. All the plates in this section are at unit magnification. It can be said, to a first approximation, that Ring I shows a fourteen fold symmetry, with some distortion. Ring 2 an eight fold symmetry and a double response (mentioned by Essen) and Ring 3 a twelve fold symmetry. The patterns were similar on both sides of each ring.

As the expected pattern should have possessed a six fold symmetry a series of experiments were carried out to see if the mounting of the ring or the driving circuit was affecting the pattern of the vibration. The rings were each mounted on three ball bearings set at 120° around a circle equal in diameter to, the mean diameter of each ring on a glass plate. Using the Pierce circuit to oscillate each ring, the rings were rotated until minimum damping was obtained when they should have been supported at three of the nodal points. Examination of the top surface of the rings then showed that the pattern was unchanged in each case.

No further work was done on this particular problem until some time later when another ring became

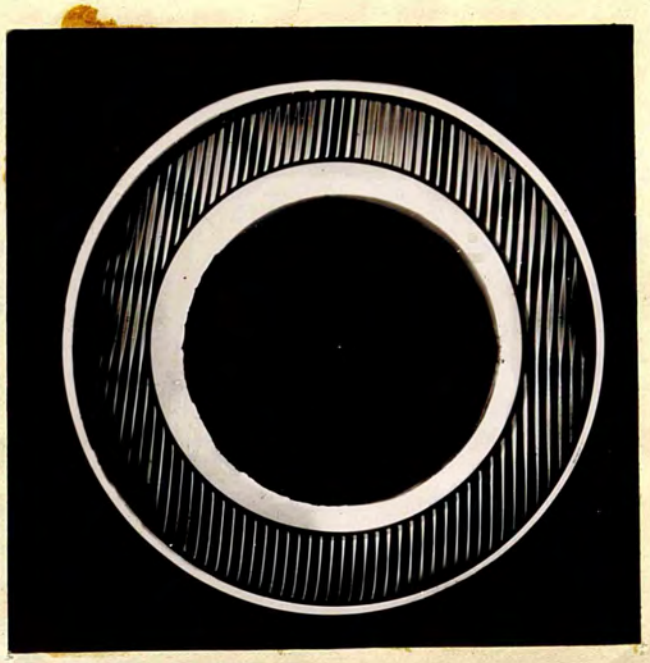

64

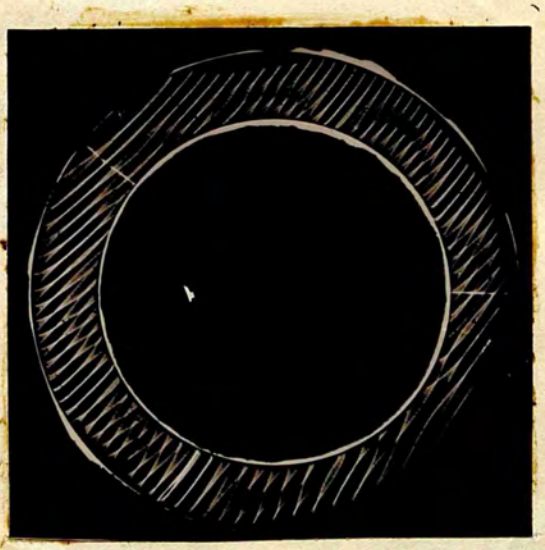

65

66

67

available. This is referred to in the next section on the 100 Kc/s G.P.O. primary frequency standard.

Resonating the rings through the frequency range 50-500 Kc/s it was found that they had a large number of responses, ring 3 for example having about ninety. Several types of pattern were observed. One type reminiscent of the flexure type modes in the bar described previously is shown for ring I in Plates 68,69,70.71 and 72 the number of complete waves round its circumference being 5,6,7,8 and 9 respectively. The frequencies of these modes is given in Table IV.5.

Table IV.5.

Plate No.	68	69	70	71	72
Frequency Kc/s	47.1	65.5	85.5	106.3	127.2

A second type is shown for the same ring in plates 73, 74,75,76,77 and 78 with 4,6,8,10,12 and 14 nodal regions respectively the frequencies being listed in Table IV.6.

Table IV.6

Plate No.	73	74	75	76	77	78
Frequency Kc/s	48.5	60.2	90.7	112.6	133.9	158.6

Both series obey an approximately harmonic progression. Calculations based on the classical expressions of Hoppe (1871),Michell (1889) and Rayleigh (1926) for the

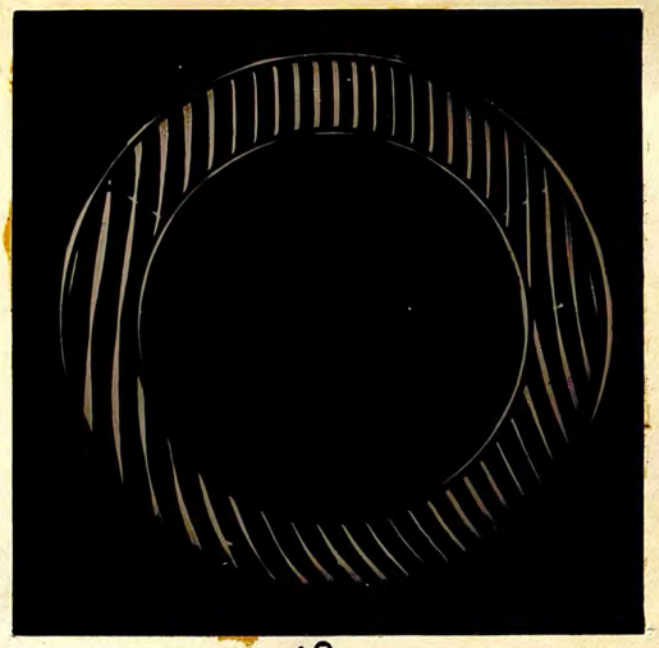

68

69

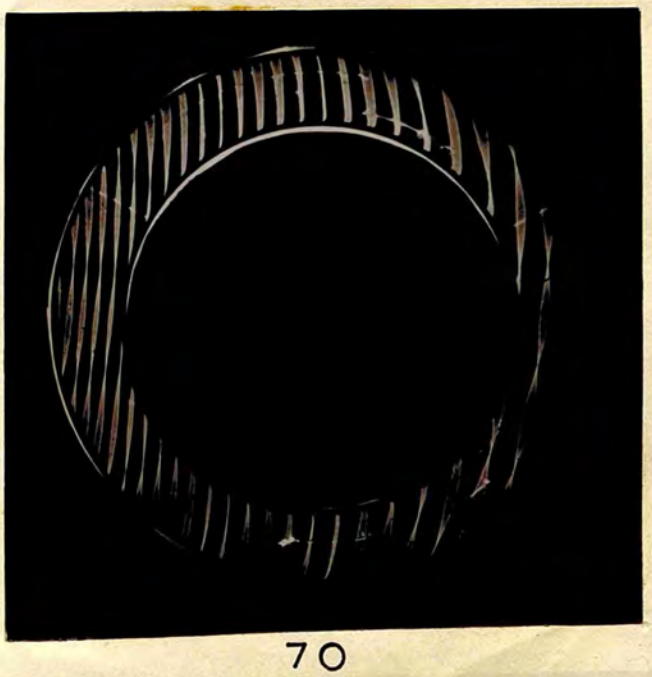

70

71

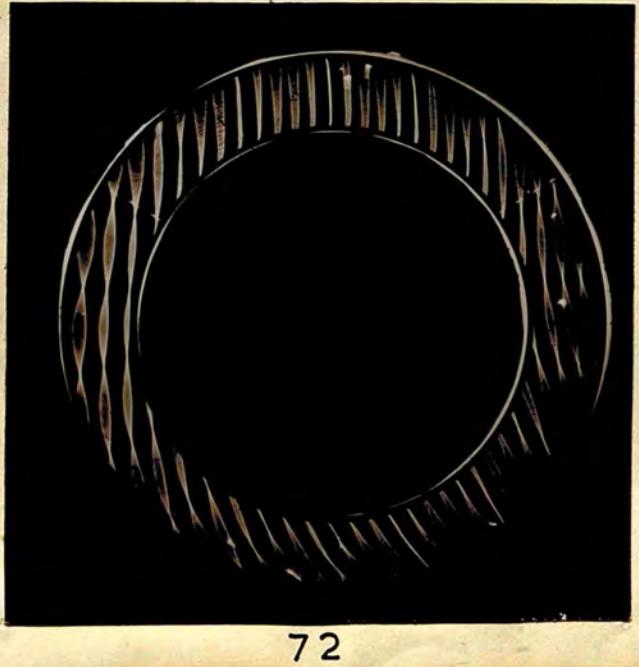

72

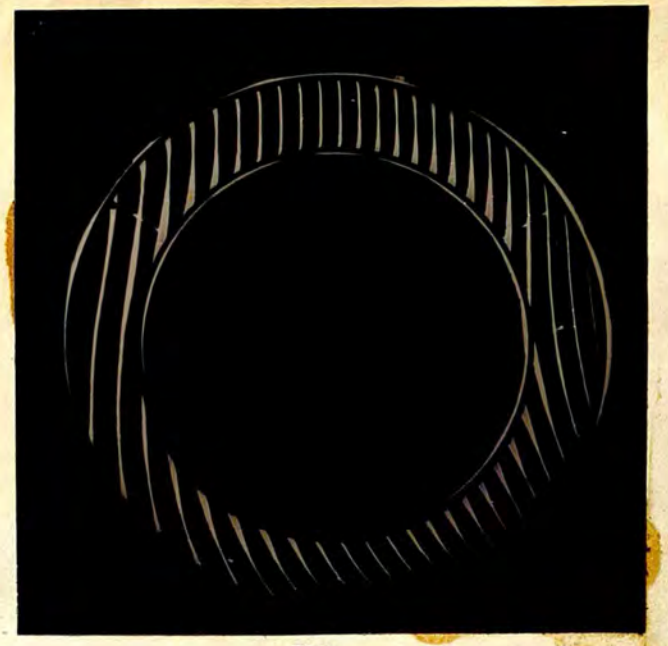

73

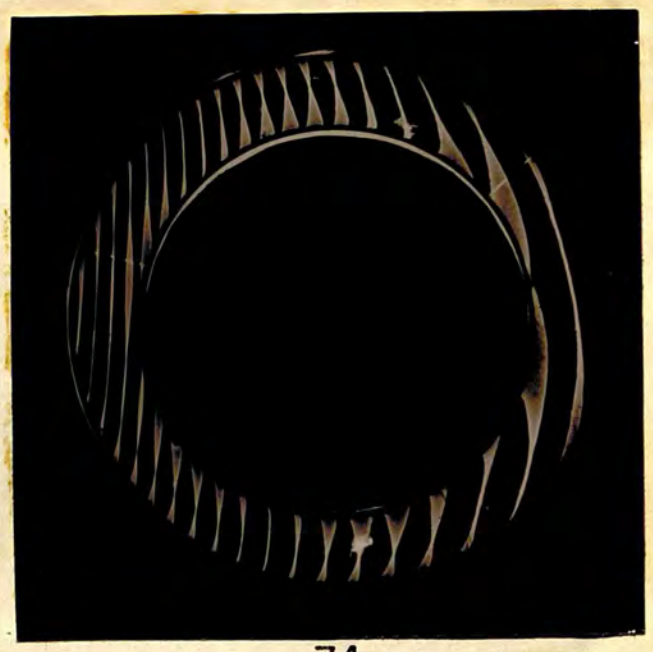

74

75

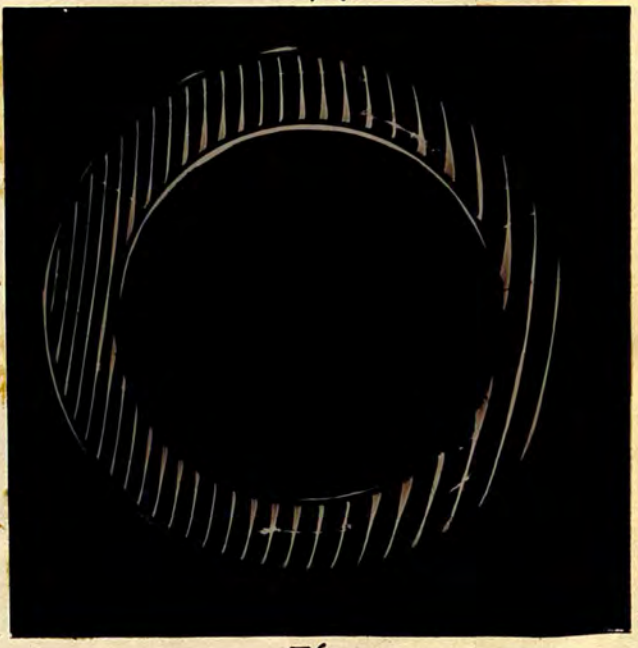

76

77

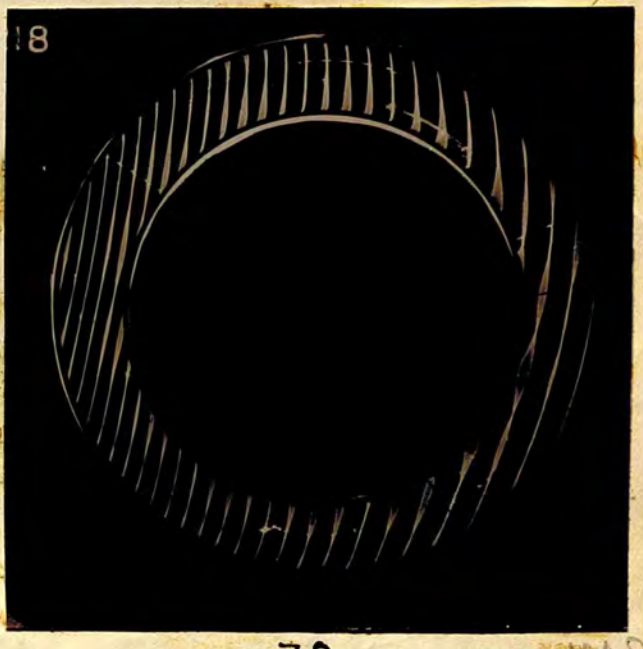

78

frequencies of vibration of various modes of motion in an isotropic ring of circular cross section were not fruitful. No work other than that of Essen (1938) has been published on the vibrations of this type of ring.

Ring 2 displays a type of motion similar to the flexural type as shown in Plate 79 and also shows a second type in Plate 80. which is similar to the second series of ring I. The frequencies are listed in Table IV.7.

Table IV.7.

Plate No.	79	80
Frequency Kc/s	86.9	74.8

Ring 3 shows many symmetrical patterns but they seem to follow no regular series with regard to frequency. Some are shown in Plates 81-92. The frequencies are listed in Table IV.8.

Table IV.8

Plate No.	81	82	83	84	85	86
Frequency Kc/s	62.3	62.3	134.4	207.4	66.4	95.5

Plate No.	87	88	89	90	91	92
Frequency Kc/s	250.3	251.0	245.1	482.8	541.6	546.4

In many of these modes the effects of elastic

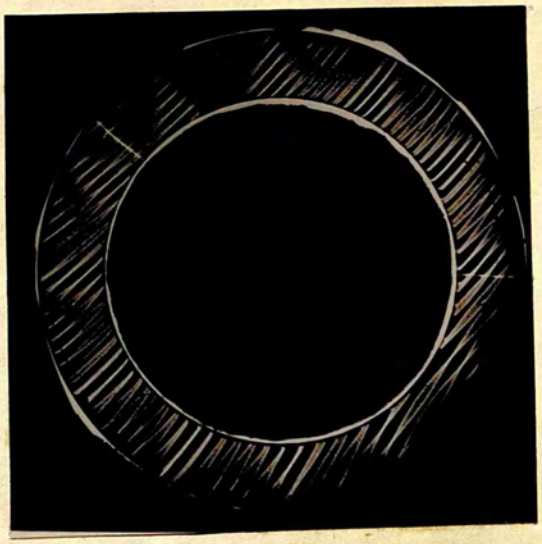

79

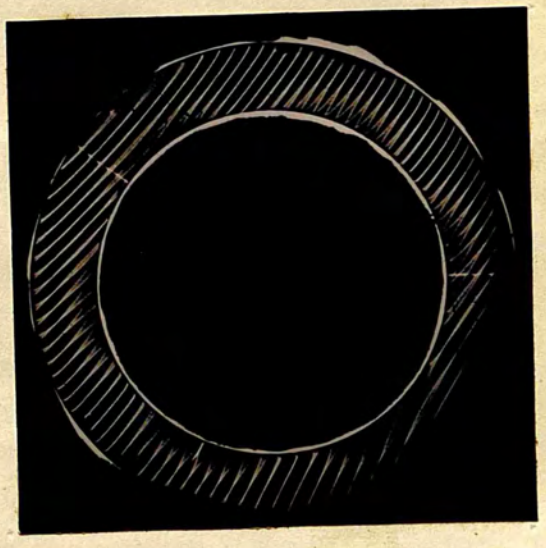

80

81

82

83

84

85

86

87

88

89

90

91

92

105B

coupling between neibouring modes of motion can be seen. Amongst the flexural type modes of ring I are three vibrations shown in Plates 93,94 and 95 , the patterns being rotated successively through some 5° . The frequencies of the three modes are within a few cycles of each other. A similar effect is seen in Plates 96 and 97 for another type of vibration in the same ring. Plates 98 and 99 show the complexity of the patterns in this ring at the higher frequency end of the range. The frequencies are listed in Table IV.9.

Table Iv.9

Plate No.	93	94	95	96	97	98	99
Frequency Kc/s	I27.2	I27.2	I27.2	70.5	70.6	22o.7	345.8

3. Further experiments were made on the longitudinal mode in the Essen type ring vibrator. The ring has been developed by the G.P.O. Research Station, Dollis Hill, to serve as a primary frequency and time standard. In order to reduce the damping on the ring it is carefully suspended at the nodal points. A further investigation of the position of the nodal points by multiple beam techniques was carried out at the request of the G.P.O. and the experiments described in this section were made on one of their rings. The dimensions

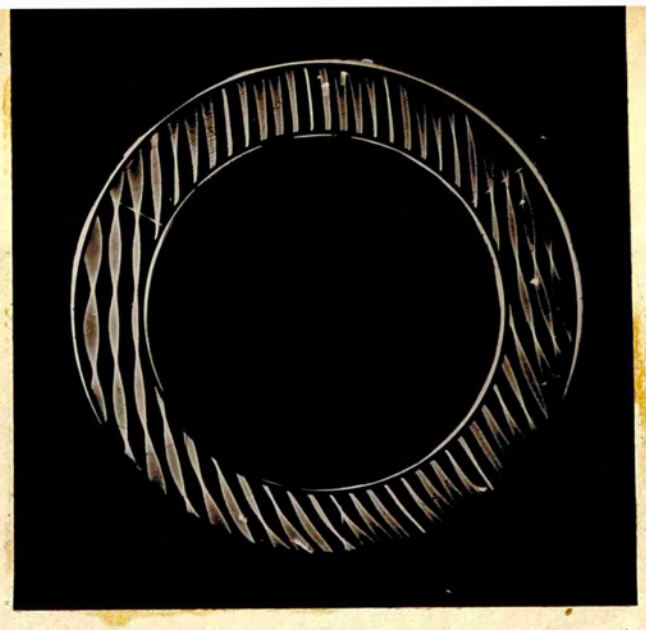

93

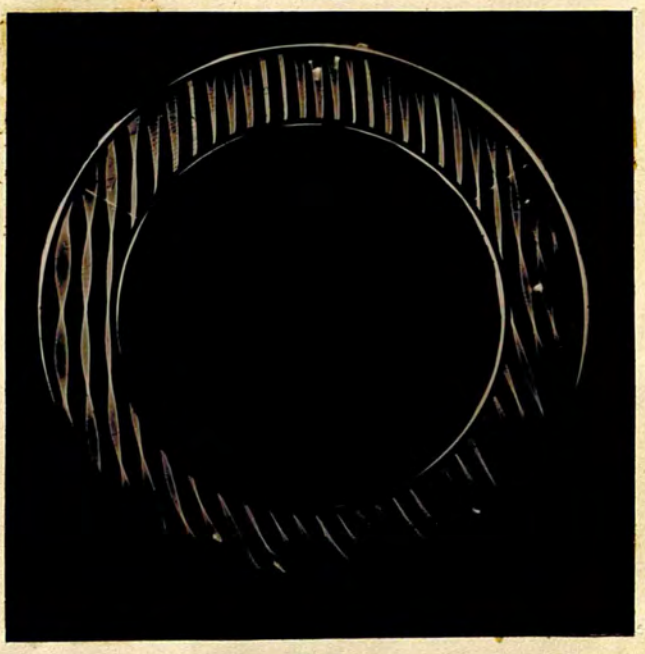

94

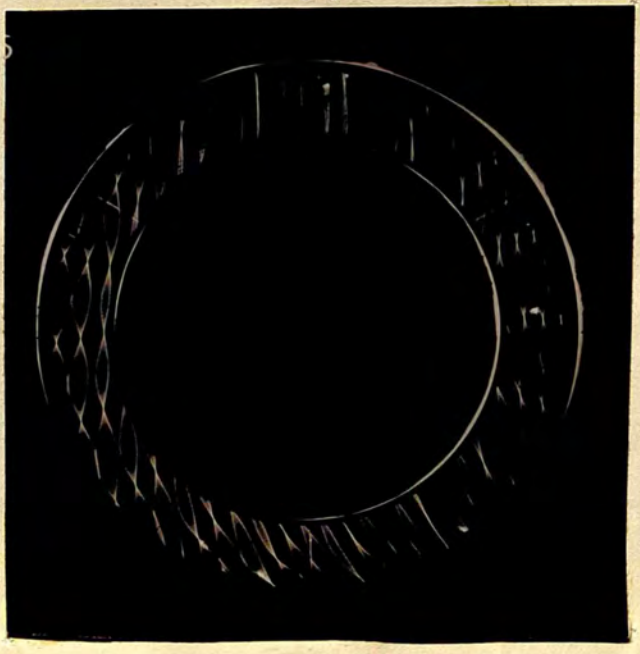

95

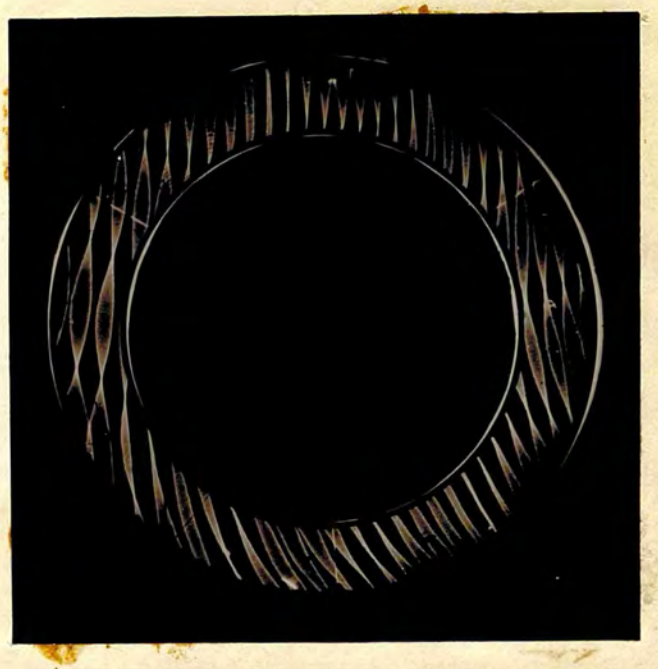

96

97

98

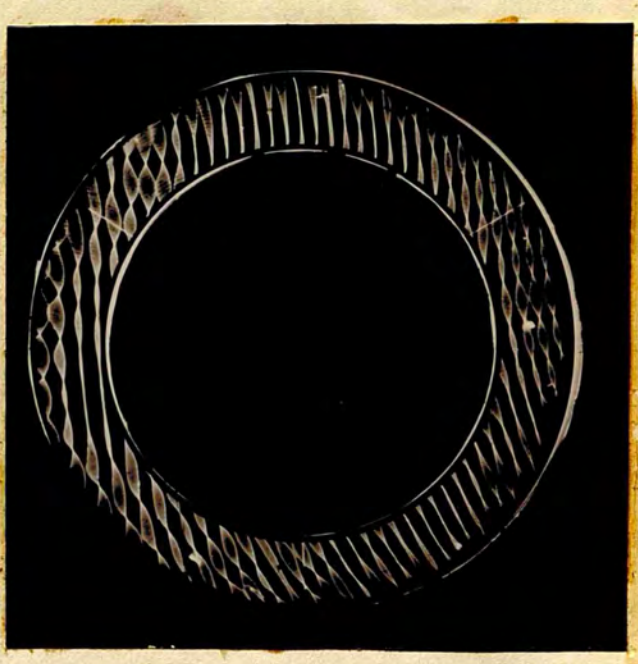

99

of the ring (No.4) are given in Table IV.10. It was cut from high quality crystal and was of proven performance.

The two plane surfaces of the ring were carefully polished and made optically flat. One side was given an interferometric coating of silver with a reflecting coefficient of 90 per cent and matched against a silvered flat in the usual way. The electrodes were coaxial brass rings and the general experimental arrangement was as before and is shown in Fig.IV.7. The electrodes were connected across a parallel tuned circuit of inductance and capacitance coupled inductively to the push pull Hartley oscillator.

The ring was then resonated at 100 Kc/s. The vibration pattern is seen in Plate 100 for one surface and in Plate 101 for the other surface. The two plates are correctly oriented point for point as indicated by the arrows. The threefold symmetry of the pattern can be seen.

It was again thought that the conditions of operation might be affecting the vibration pattern. Normally the ring is run in a vacuum at series resonance in a bridge circuit of Post Office design described in Part III. It is supported at three nodal points disposed

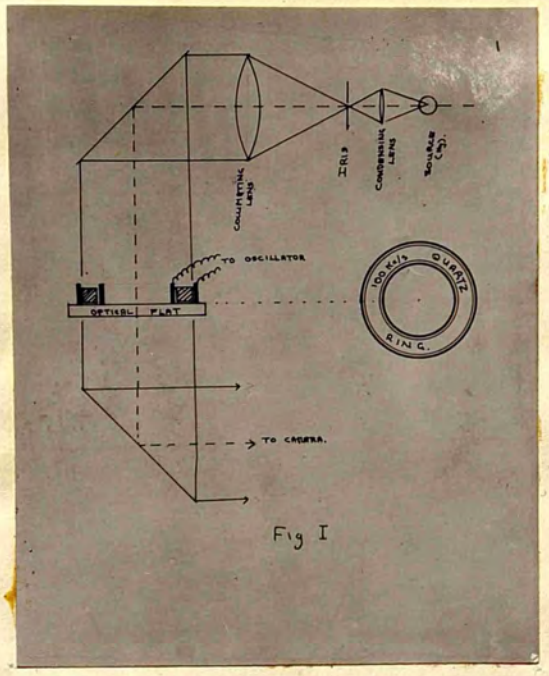

Fig I

FIG. IV.7.

Table IV.10

Outside Diameter cms.	Thickness along X cms.	Thickness along Z cms.
6.118	0.818	1.058

Plane surfaces normal to Z axes within ± 10 secs arc.

Thichness uniform to 0.005 mm.

Beval of 0.5 mm.on all four edges.

Cylindrical surfaces finished 600 carborundum and etched in hydrofluoric acid. Plane surfaces optically polished from etched surface.

at 120° around the circumference. The electrodes are plated on to the cylindrical surfaces and connection is made to them by fine silver wires fused with a silver compound on to each cylindrical surface at a nodal region. It was decided to run the ring under these conditions and to observe the pattern.

The experimental difficulties were solved as follows. The ring was mounted on three copper pins fitting into three projecting arms and radially disposed at 120° ± ½° so as to locate in three radial grooves cut in one of the Z faces of the ring. The pins were 6 mm. in length (a non resonant length) and were tapered in the lath to a fine point. Any burr remaining was removed by rubbing each point once over a few inches of ground glass surface. The pins were then annealed and inserted into holes in the arms. These holes were reamed out to 0.062 ins. and the pins were a push fit in the holes. The jig was constructed so that a glass flat could be brought up close to either the bottom surface or the top surface of the ring. In the first case a fringe dispersion was obtained by screwing down the flat against spring pressure by three 8 BA screws. In the second case, three more screws operated three strips of phosphor bronze which pressed the lower optical flat against three springs. In this case the optical flat had three

0.070in holes drilled to clear the copper pins. The jig is shown dismantled in Fig.IV.8, together with the vibrator and glass flats, and, diagramatically, in Fig.IV.9.

The ring was cleaned in chromic acid and the silver wires were fused on in the G.P.O. laboratories. Then the electrodes were plated by evaporation on to the two cylindrical surfaces, the circular masks used to cover the Z faces slightly reducing the area of the electrode plating as in Fig.IV.II. Then an interferometric coating of silver of 90 per cent reflectivity was evaporated on to one of the Z faces, cylindrical masks being used to protect the electrode coatings. In this way the interferometric coating was prevented from short circuiting the two electrode coatings.

The ring and its mounting were then placed inside the vacuum chamber seen in Fig.III.10 which was then evacuated to a pressure of less than I mm. of mercury by a Hivac rotary oil pump. The ring was oscillated in the bridge circuit at 100 Kc/s and the equivalent series resistance measured and found to be some 70 ohms. The value of the equivalent series capacitance of the ring with the reduced electrode plating was 0.044 $\mu\mu$F and thus the Q of the oscillating ring was over 500,000.

The multiple beam Fizeau fringes were formed

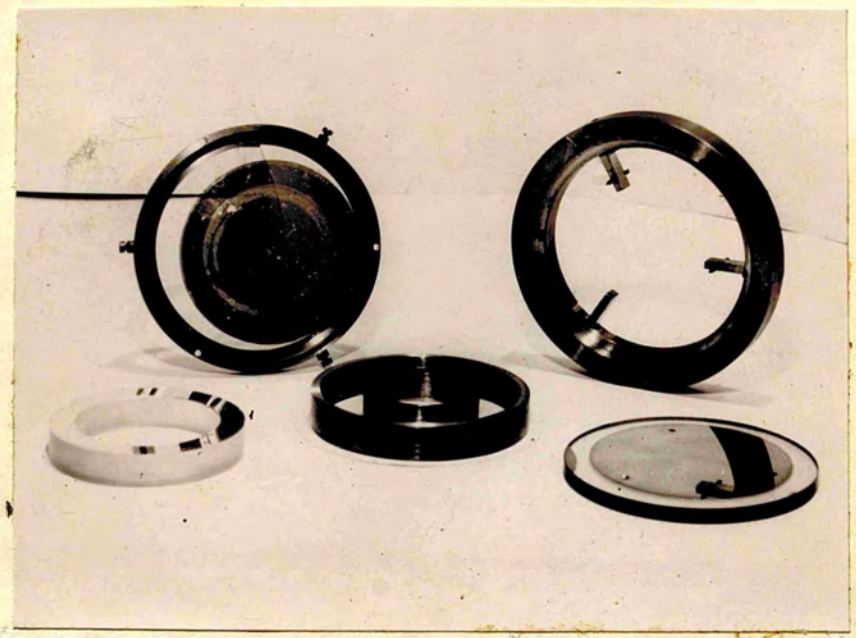

FIG. IV. 8.

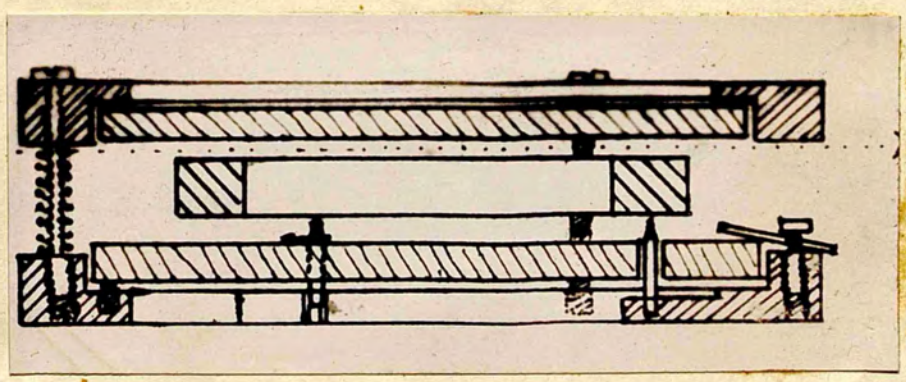

FIG. IV. 9

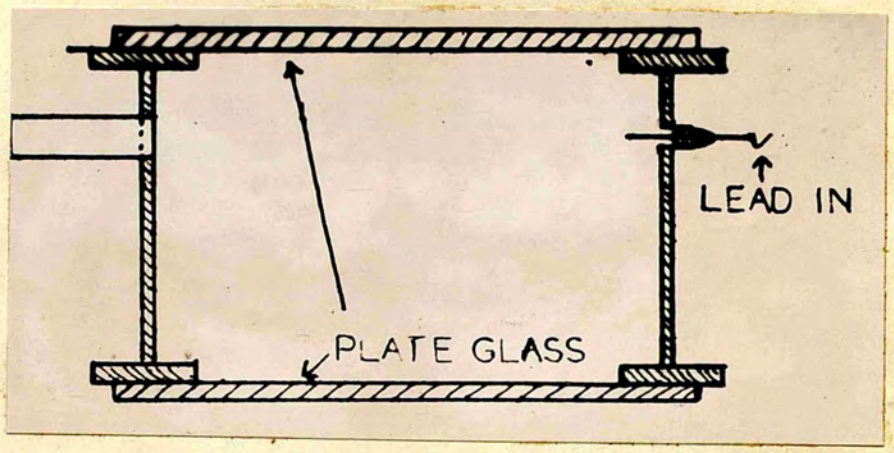

FIG. IV. 10.

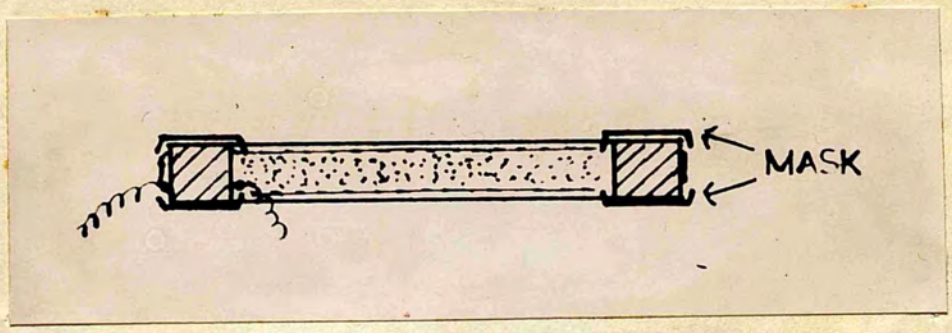

FIG. IV. 11.

in an air gap of about 1/10 mm. in each case, but careful collimation and under-running of the high pressure arc produced serviceable fringes.

Plate 102 and 103 show the two Z faces of the ring running under the above critical conditions and compare with plates 100 and 101 respectively. Comparison shows the distribution of nodes and antinodes to be the same under the two different conditions of observation. This experiment confirms that unless deliberate constraints are applied at antinodal regions the vibrational pattern observed is characteristic of the particular vibrator running in a particular mode, and is independent of the mounting, electrodes and driving circuit in agreement with Schumacher (1937) and Kotlyarevski and Pumper (1941). This means also that the small interferometric gap necessary with the multiple beam techniques does not distort the pattern by virtue of any damping it introduces at the small amplitudes of vibration normally used. The silver film on the Z face was found, experimentally, not to affect the equivalent series resistance of the ring.

The actual pattern is rather complex. It has a threefold symmetry and shows twelve nodal and twelve antinodal regions successively in opposite phase

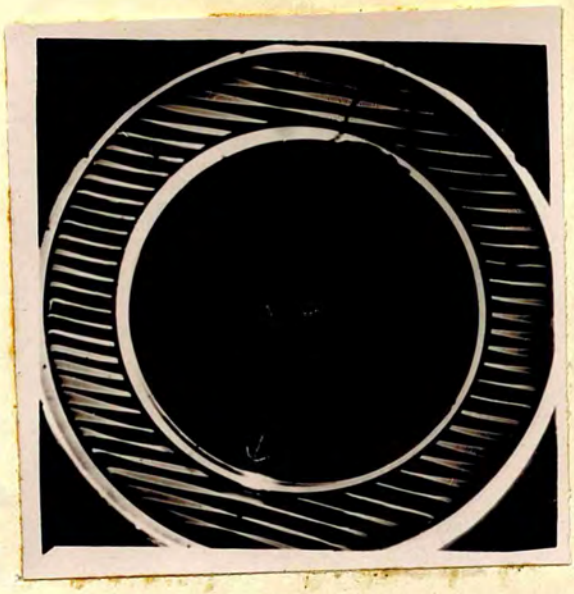

100

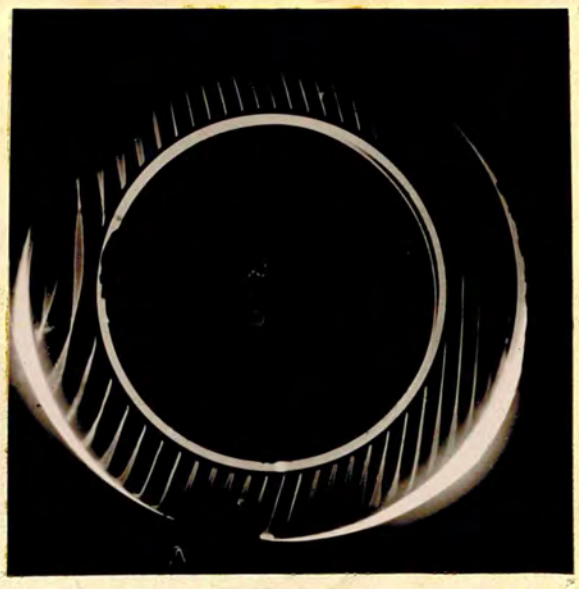

101

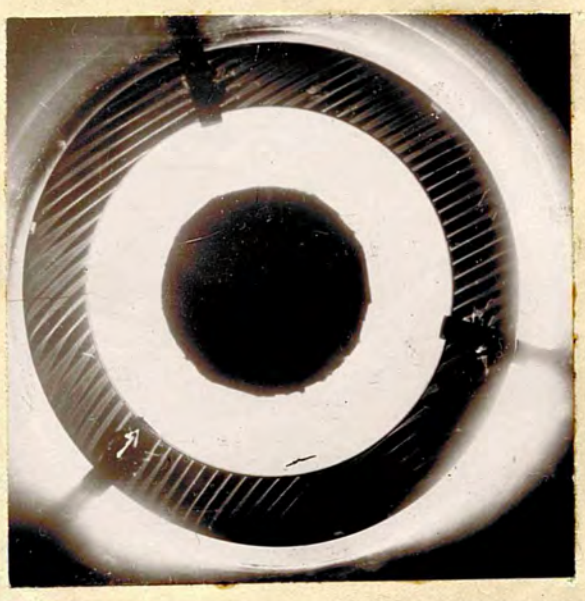

10 2

103

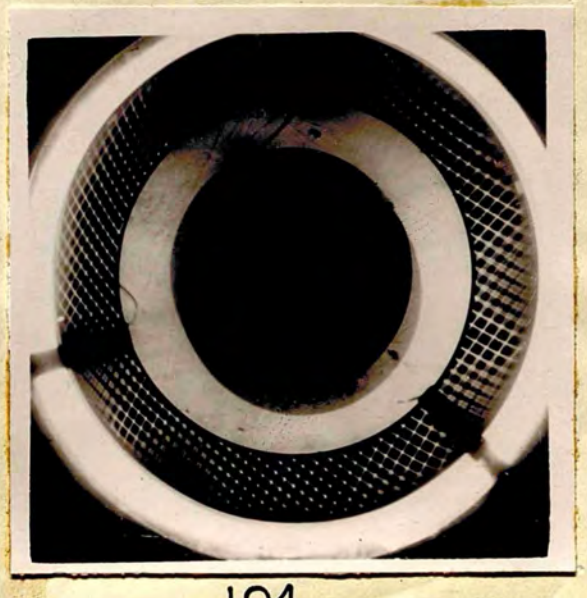

104

as revealed by stroboscopic illumination. Plate I04 shows a crossed fringe dispersion over the top surface of the ring. An analysis of the ring is shown in Plate I05 (x 2). There are three pairs of nodes at the ends of the three diameters A_1, A_2, A_3, which are at 60° to each other, and three pairs of nodes at the end of pairs of radii B_1, B_2, B_3. These latter three pairs are the ones reported by Essen (I938) and do not lie on diameters of the ring. They are related to the nodes on the top surface as shown by Essen, the pattern on the lower surface coinciding with the pattern on the upper surface when one is rotated through an angle of 60 about its centre. Subsequently a second similar ring gave an identical pattern under the same conditions. It was to be expected that the vibrational pattern would be that of the lateral contraction due to the longitudinal motion as seen in the Y cut bar described at the beginning of this chapter and should thus show a sixfold symmetry.

However the type of pattern may be tentatively explained if it is remembered that X cut bars have a second order flexure associated with the fundamental longitudinal mode along the length of the bar. If this third order longitudinal mode in the ring has a sixth order flexure associated with it, then this will account for the nature of the surface displacement. Accordingly a search was made

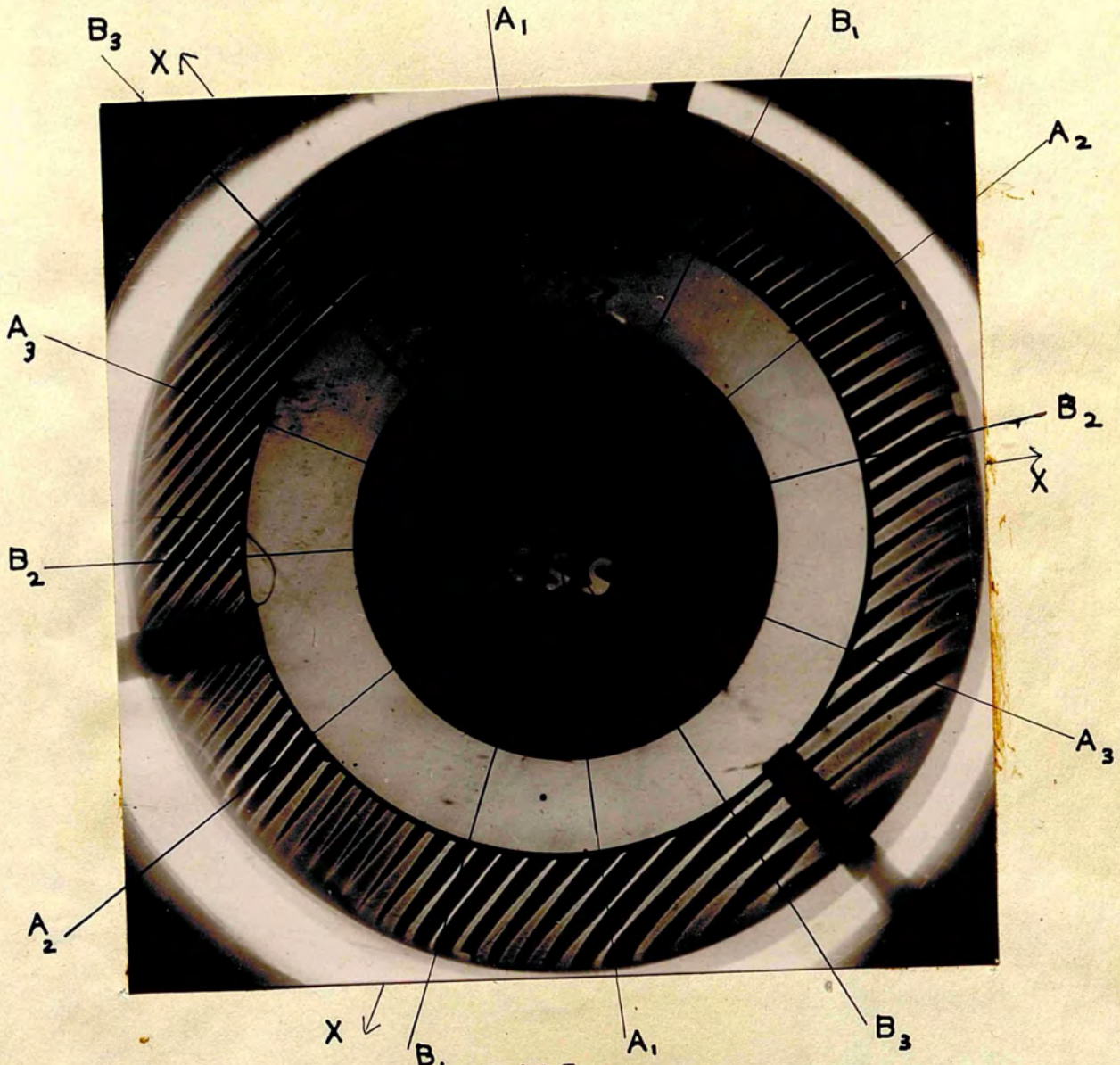

105

for this flexure mode and it was found at 83.9 Kc/s. It is shown in Plate I06 together with the longitudinal mode in Plate I07, the fringe dispersion being the same in each case in order to facilitate comparison.

Referring back to Plates 64, 65, 66 and 67 it can be seen that only Ring 3 (67) is similar in pattern to that in Ring 4. The pattern on Ring I (64) suggests that the motion is coupled to the seventh order flexure and also that the ring is imperfect in some way. The pattern of the double response of Ring 2 (65, 66) is similar to the pattern of Plate 8I given by the same ring and to the series in Plates 74-79 for Ring I. Stroboscopic examination shows that this may be a torsional type of motion.

4. With the bridge oscillator it was possible to vary the current flowing through the ring vibrator and to calculate its value from the bridge constants.

A series of plates was exposed for a series of gradually increasing currents in the range 0-I0 m.a.(r.f.). The same exposure and the same development time was given to each plate. Then the fringe broadening was measured at a particular point on a given fringe at a

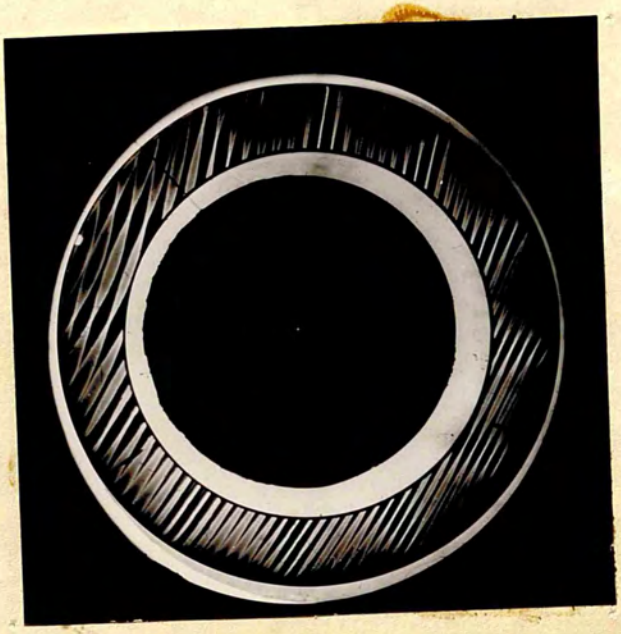

106

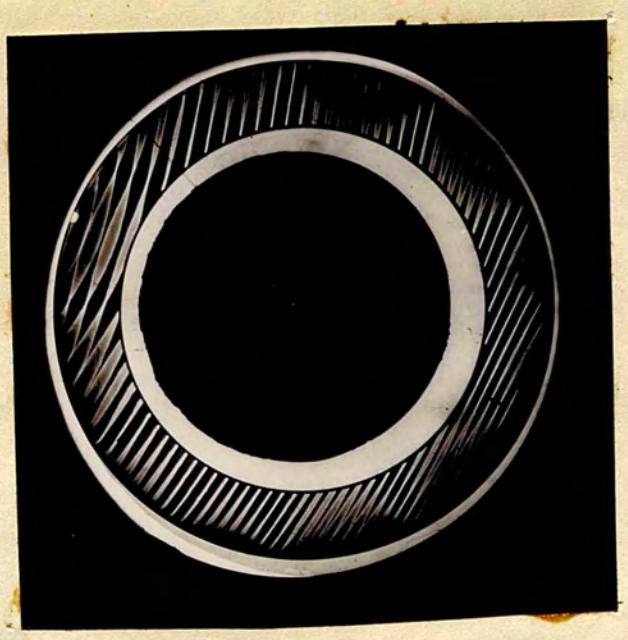

107

position of maximum amplitude in one of the six antinodal regions showing the largest amplitude.

The graph of crystal current versus amplitude is shown in Fig. IV.12 and is seen to be linear in form. The amplitude is given in terms of Angstrom units (total excursion). The normal component of the maximum surface amplitude of the ring vibrator is seen to be proportional to the crystal current. If the damping on the ring changes then its equivalent series resistance, and the voltage needed to produce the same crystal current changes, but the same amplitude will be obtained for the same crystal current. This is found to be true experimentally.

It is believed that this is the first interferometric measurement of the surface amplitude of a quartz vibrator in terms of the crystal current.

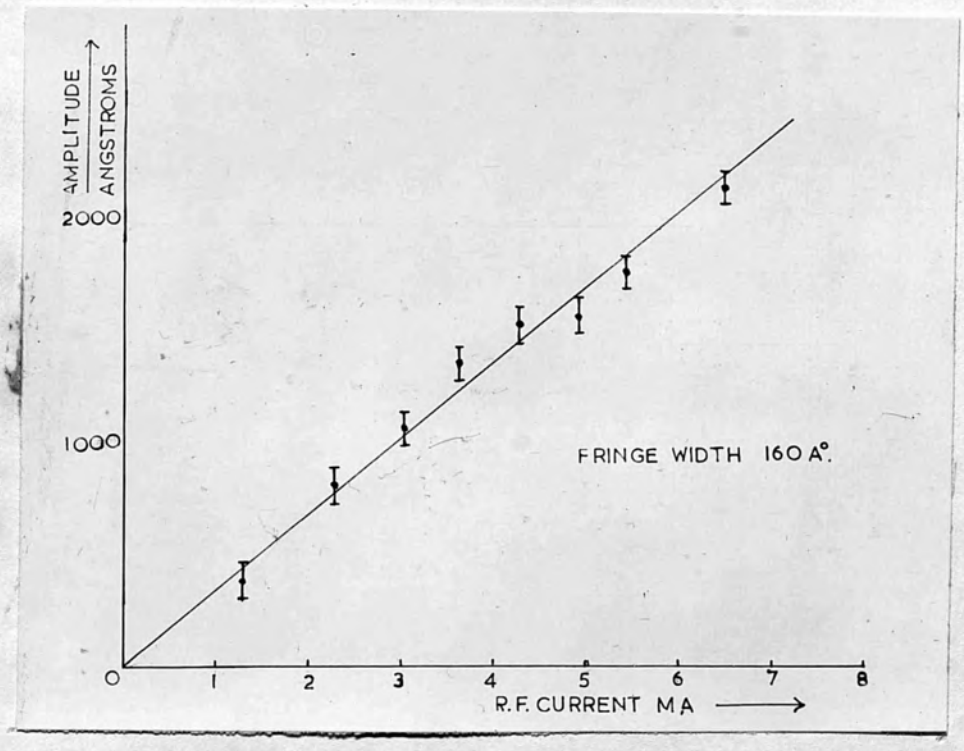
AMPLITUDE
ANGSTROMS
2000
1000
0
1
2
3
4
5
6
7
8
R.F. CURRENT M.A
FRINGE WIDTH 160 A°.

FIG. V. R.

ACKNOWLEDGEMENTS

I wish to thank Professor S.Tolansky for his inspiring supervision and constant encouragement during the progress of this work. I would also like to thank my several colleagues for their assistance in many discussions.

I am grateful to the Ministry of Education and the Ministry of Supply for providing the necessary financial assistance. I am indebted to Dr F.E.Jones of the Telecommunications Research Establishment, Dr L.Essen of the National Physical Laboratory, and the G.P.O. Research Laboratories for the loan of equipment and quarts vibrators and to Mr Menage of Imperial College, London, for teaching me the art of optical polishing. My thanks are due to the workshop staff of the Physics Department, Royal Holloway College for help in constructing some of the apparatus I have used.

Finally I wish to thank my wife for her constant sympathy.

REFERENCES

Airy; 1831, Math. Tracts., p.381.
Avery; 1950, Ph.D. Thesis, Univ. of London.

Bechmann; 1934, Hochfreq. Techn. u. Elekt., 44, 145.
Booth & Vigoreux; 1950, Quartz Vibrators, London, H.M.S.O.
Boulouch; 1906, Journ. de Phys., 5, 789.
Bragg & Gibbs; 1925, Proc. Roy. Soc., 109, 405.
Brossel; 1947, Proc. Phys. Soc. (Lond.) 59, 224.
Bruce; 1951, Nature, 167, 398.
Bruce, Macinante & Kelly; 1951, Nature, 167, 520.

Cady; 1922, Proc. I.R.E., 10, 83.
Cady; 1946, Piezo-electricity, N.Y., London - McGraw Hill.
Chladni; 1802, Die Akustik (2nd Ed. 1830).
Curie, J. & P. Curie; 1880, Bull. Soc. Min. de France, 3, 90.

Doerfler; 1930, Z. für Physik, 63, 30.
Dye; 1926, Proc. Phys. Soc. (Lond.) 38, 399.
Dye; 1932, Proc. Roy. Soc. A. 138, 1.

Essen; 1938, Proc. Phys. Soc. (Lond.) B, 50, 413.

Fabry & Perot; 1897, Ann. de Chemie et de Phys., 12, 459.
Fujimoto; 1927, Thesis, Ohio State Univ.

Giebe & Schiebe; 1925, Z. für Physik, 33, 335.
Gunther; 1932, Ann. der Physik, 13, 783.

Heising; 1947, Quartz Crystals for Electrical Circuits, N.Y., D. Van Nostr. & Co.
Holden; 1949, Proc. Phys. Soc. (Lond.) B, 62, 405.
Hoppe; 1871, J. f. Math., 63, 158.

Jacquinot & Dufour; 1950, J. de Phys. et le Radium; 11, 427.

Kao; 1935, Compte Rendus, 200, 563.
Kotliarevski & Pumper; 1941, Journ. Phys. U.S.S.R., 4, 67.

Love; 1934, A Treatise on the Mathematical Theory of Elasticity, London, C.U.P.
Lummer; 1900, Sitz. Berlin, Akad., 3, 504.
1907, Ann. der Physik, 22, 49.

Mitchell, 1889, Messenger of Mathematics, 19.
Miers; 1936, Television Optics, London, Pitman.
Moens & Verschaffeldt; 1927, Comptes Rendus, 185, 1034.

Nomoto; 1949, Nature, 104, 359.

Oldenburg; 1922, Ann. der Physik, 67, 253.
Osterberg; 1929, Proc. Nat. Acad. Sci., Washington, 15, 892.
" ; 1932, J.O.S.A., 22, 19.
" ; 1933a, Phys. Rev., 43, 819.
" ; 1933b, J.O.S.A., 23, 30.
" ; 1934, Rev. Sci. Instr., 5, 183.

Paasche; 1928, Z. für Tech. Phys., 9, 411.
Petrzilka; 1931, Ann. der Physik, 11, 623.
" ; 1935, " " " , 27, 436.
" & Zachoval; 1934, Z. für Physik, 90, 700.
Pockels; 1890, Neues Jahre Min., 7, 201.
" ; 1894, Abh., Gött., 39, 1.

Rayleigh, Lord; 1926, The Theory of Sound, Vols. I & II, London, MacMillan.
Rayner; 1933, Journ. I.E.E., 72, 519.
Revue d'Optique; 1949, Le Travail de Verres d'Optique de Precision (Paris - Ed. de la Revue d'Opt.).

Schaffs; 1937, Z. für Physik, 105, 576.
Schumacher; 1937, Telef Zeit., 18, 16.
Smith; 1945, Proc. Phys. Soc. (Lond.) 57.

Soaman; 1927, The Properties of Silica (N.Y. Chemical Catalogue Co. Inc.).
Straubel; 1933, Physik Zeit., 34, 894.
" ; 1934, " " , 35, 179.
Strong; 1932, Nature, 129, 59.
" ; 1946, Modern Physical Laboratory Practice, (London), Blackie & Co.
Strong & Dibble; 1940, J.O.S.A., 30, 431.

Tawil; 1926, Comptes Rendus, 183, 1099.
" ; 1928, Bull. Soc. Min. fr. 1298.
" ; 1929, Rev. gen. de l'Elect., 25, 58.
Thomas & Warren; 1928, Phil. Mag., 5, 1125.
Tolansky; 1946, Proc. Phys. Soc. (Lond.) 58, 684.
" ; 1947, High Resolution Spectroscopy, (London) Methuen.
" ; 1948, Multiple-beam Interferometry of Surfaces and Films, (Oxford) Clarendon Press.
" ; 1951, Nature, 167, 815.
" & Bardsley; 1948, Nature, 161, 925.
Tsi Ze; 1928, Journ. de Phys., 9, 13.
" "; 1927, Comptes Rendus, 185, 195.
" " & Taien; 1934, Nature, 134, 214.
" " & " ; 1935, Compte Rendus, 200, 565.
" " , " & Hung; 1936, Proc. I.R.E., 24, 1484.
Twyman; 1942, Prism and Lens Making, (London) Hilger & Watts.

Wachsmuth & Auer; 1928, Z. für Physik, 47, 323.
Waller; 1937, Proc. Phys. Soc. 49, 522.
" ; 1938, " " " 50, 70.
" ; 1939a, Proc. " " 51, 831.
" ; 1939b, Nature, 143, 27.
" ; 1940, Proc. Phys. Soc. 52, 452.
1940, " " " (Lond.) B, 52, 710.
" ; 1941a, Nature, 148, 185.
" ; 1941b, Proc. Phys. Soc. (Lond.) 53, 35.
" ; 1949, Proc. Phys. Soc. (Lond.) B, 62, 277.
" ; 1950, " " " " B, 63, 451.
Volgt; 1910, Lehrbuch der Krystallphysik, (Leipzig, Teubner).